

Radiationless Transitions

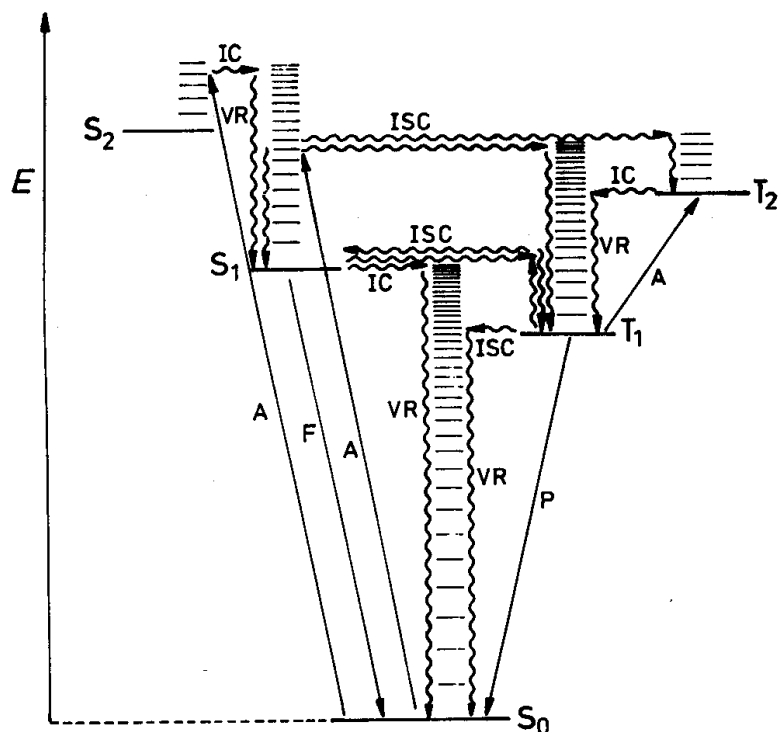
- Spin allowed
- Spin forbidden

Chapters 3 & 5

Principles of Molecular Photochemistry: An Introduction

NJT, VR and JCS

Transition Between States



$S_0 + h\nu \longrightarrow S_1$ spin allowed absorption

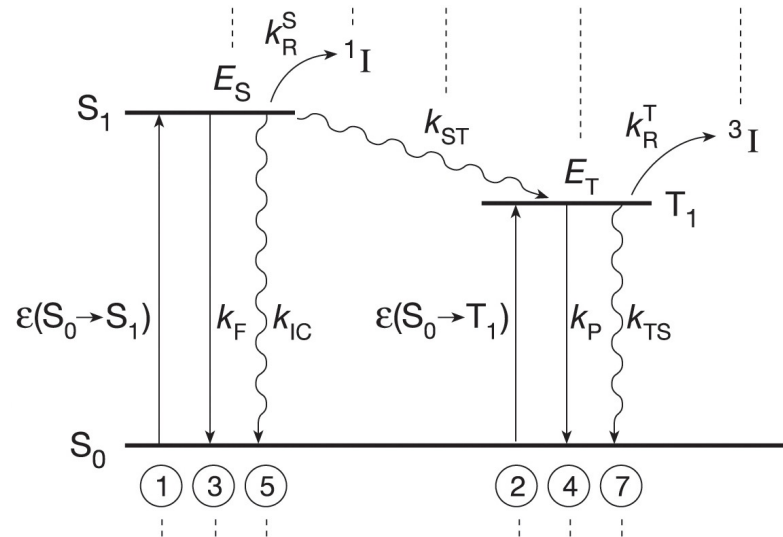
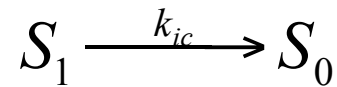
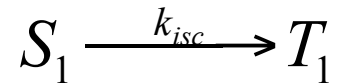
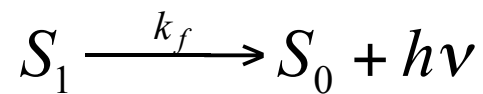
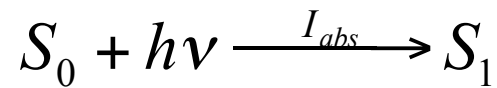
$S_1 \longrightarrow S_0 + h\nu$ spin allowed emission
(fluorescence)

$S_1 \longrightarrow S_0 + \Delta$ spin allowed radiationless
transition
(internal conversion; IC)

$S_1 \longrightarrow T_1 + \Delta$ spin forbidden radiationless
transition
(intersystem crossing; ISC)

Why radiationless transition matters?

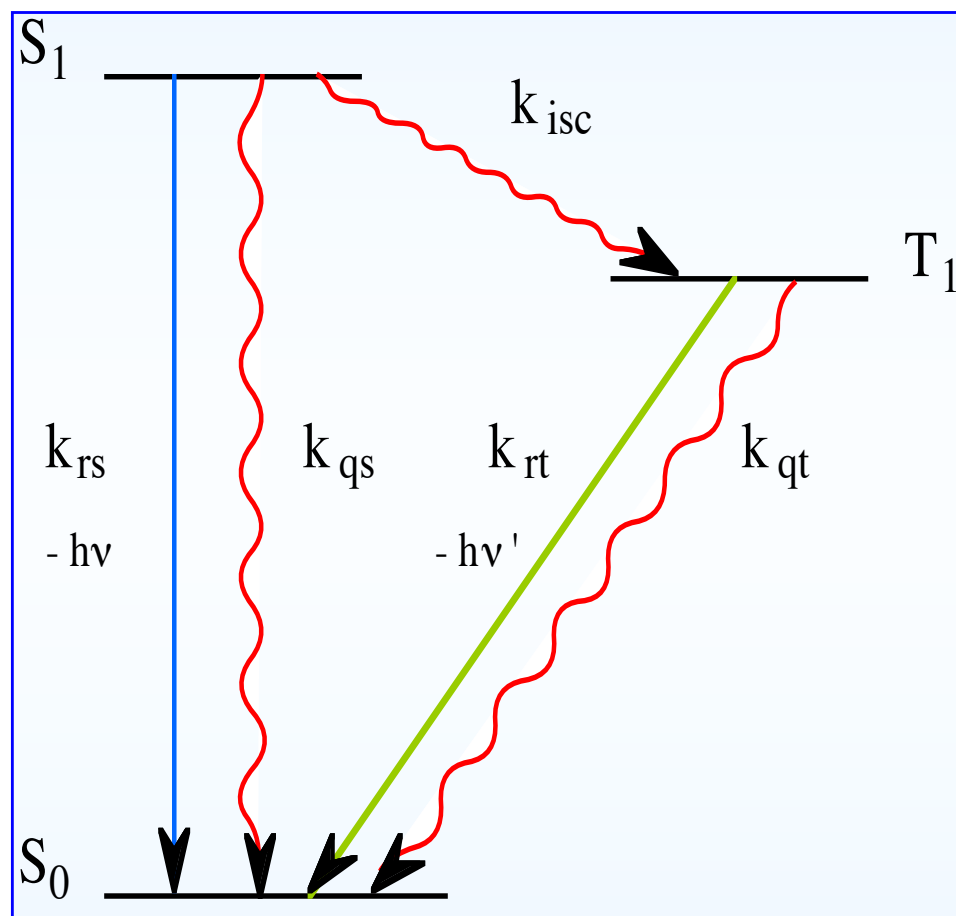
Competes with fluorescence and phosphorescence



$$\phi_f = \frac{k_f [S_1]}{(k_f + k_{isc} + k_{ic} + \dots)[S_1]}$$

Radiationless Transitions

$$(\Phi_1 \cdot \chi_1 \cdot S_1)^*1$$

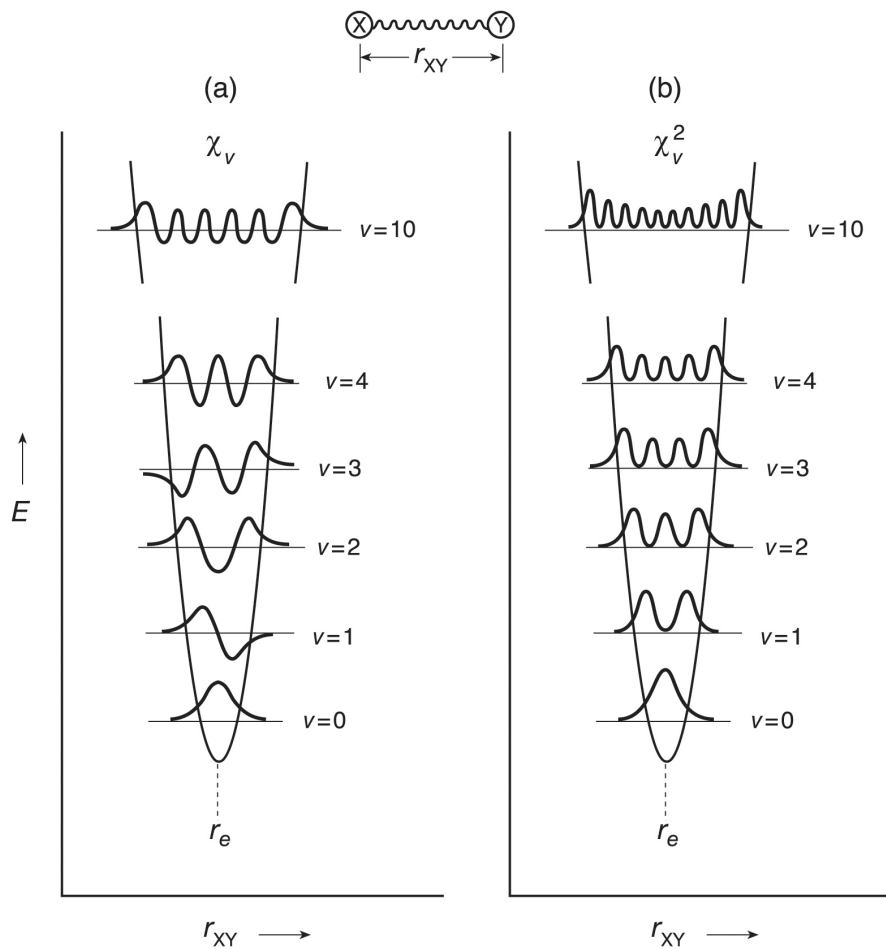


$$(\Phi_2 \cdot \chi_1 \cdot S_1)^*3$$

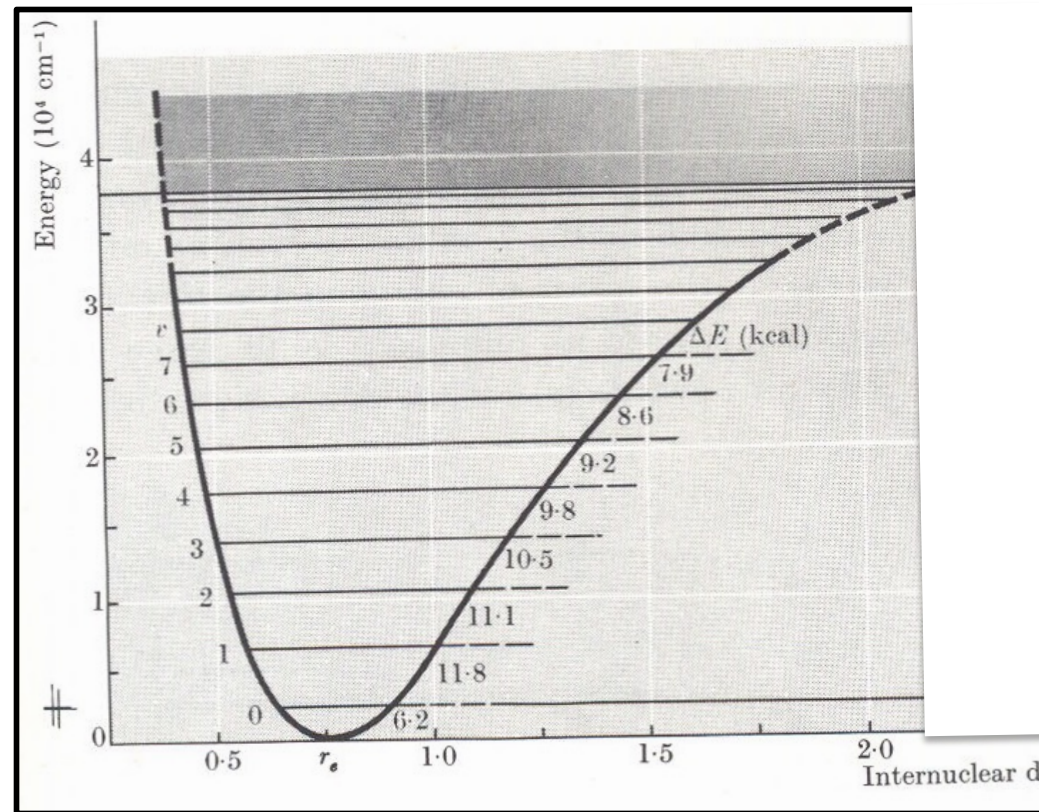
$$\Phi_0 \cdot \chi_0 \cdot S_0$$

- Changes in electronic, vibrational and spin configurations **without the help of a photon**
- Energy redistribution--**electronic to vibrational**

Visualization of vibrational levels within an electronic energy surface

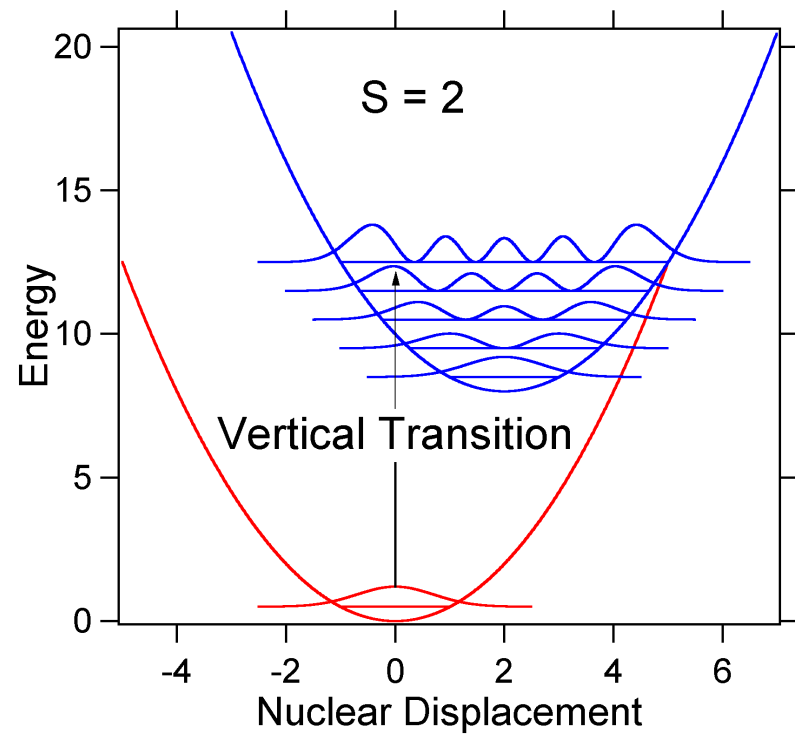
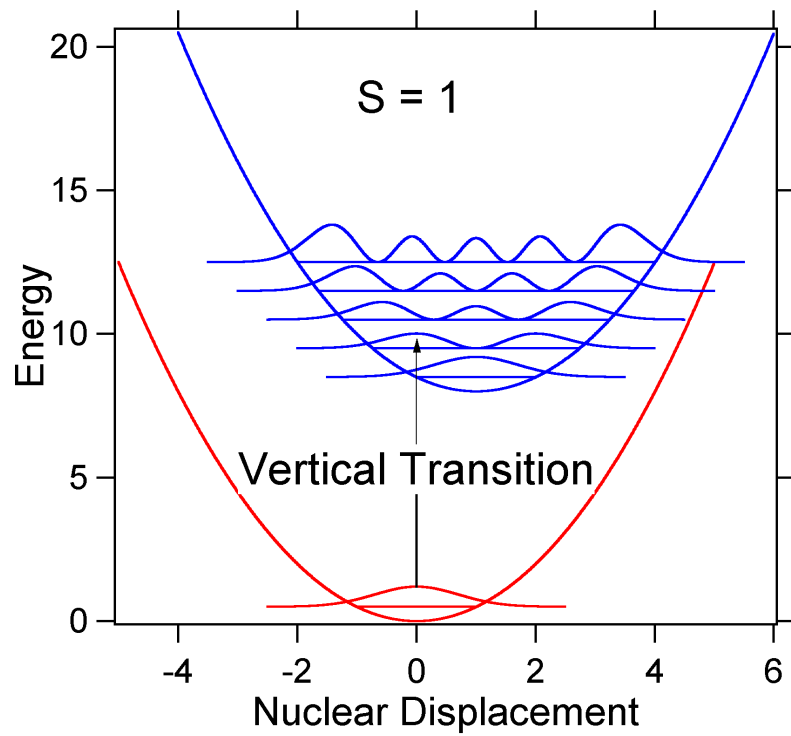


Harmonic

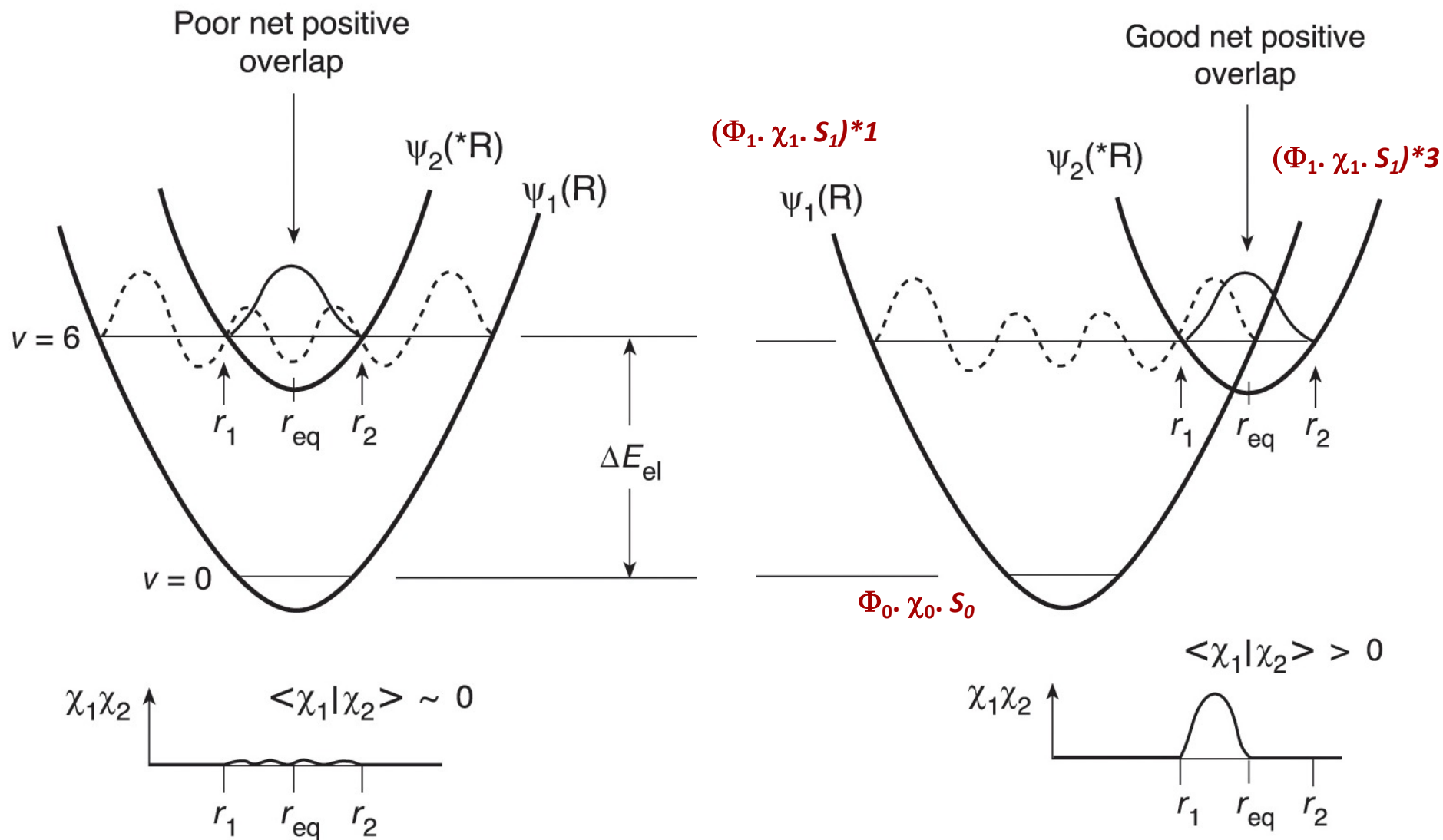


Anharmonic

Relative position of energy surfaces

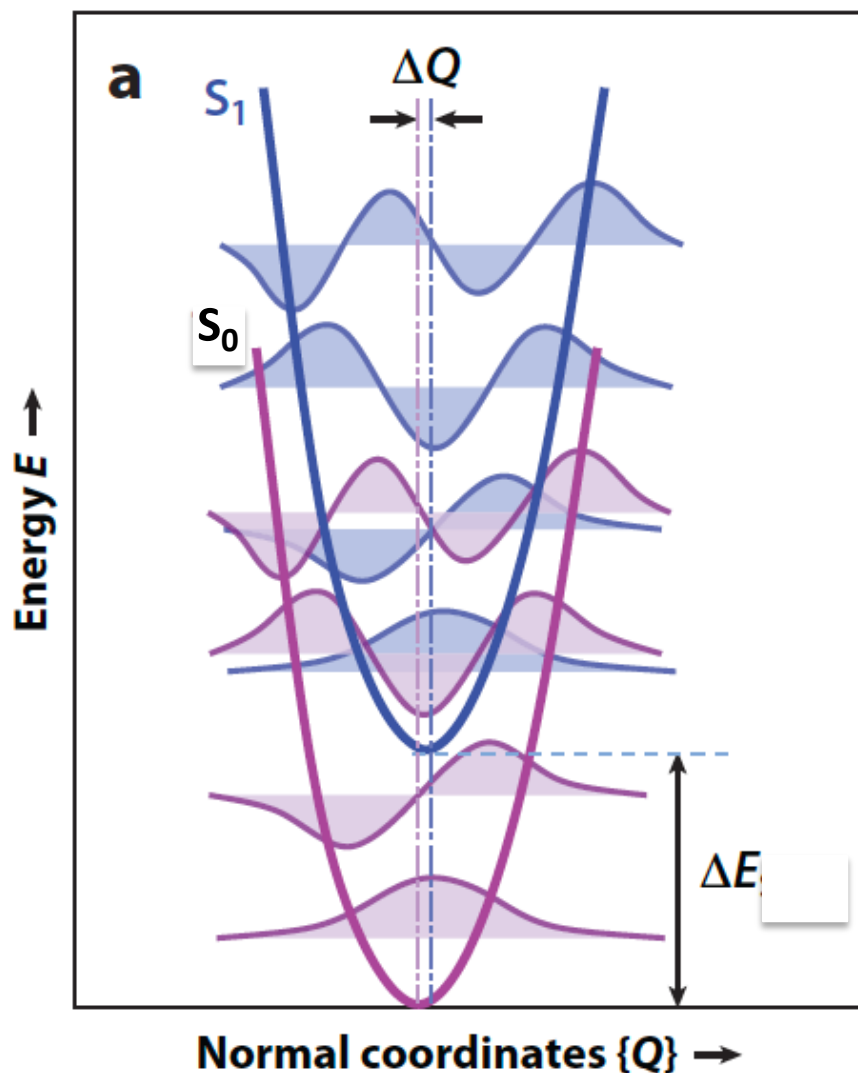


Matching vs. Crossing Surfaces



For the same energy gap the rates are different for the two types of surfaces

Matching surfaces (e.g., polyaromatics)

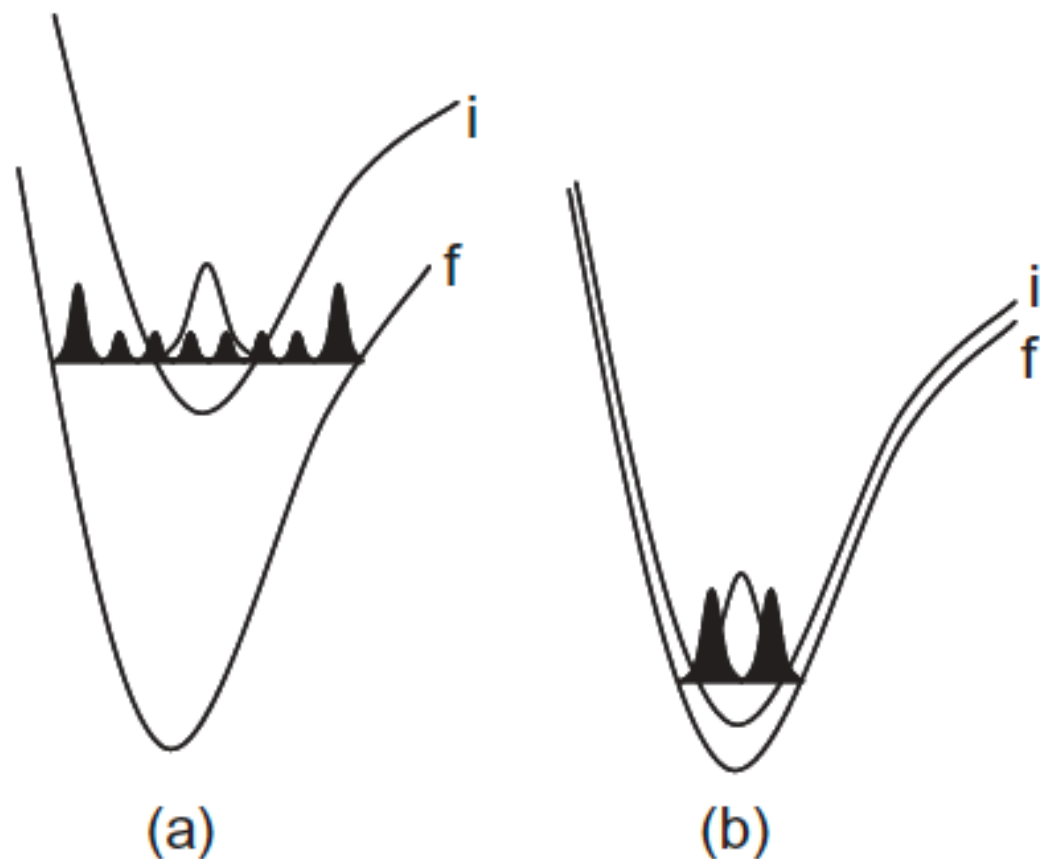


Equilibrium geometries similar

The S_1 and S_0 potentials exhibit small relative displacements. Significant overlaps between their vibrational wave functions are obtained only for small energy separations, $E_{S_1} - E_{S_0}$. The IC probability decreases exponentially with increasing energy gap. This exponential dependence of the transition probability on E is usually dubbed the **Energy Gap Law**.

Basis of energy gap law during radiationless transition in nested surfaces: Vibrational overlap

Nested or matching surfaces:
Extent of vibrational overlap depends on the energy gap



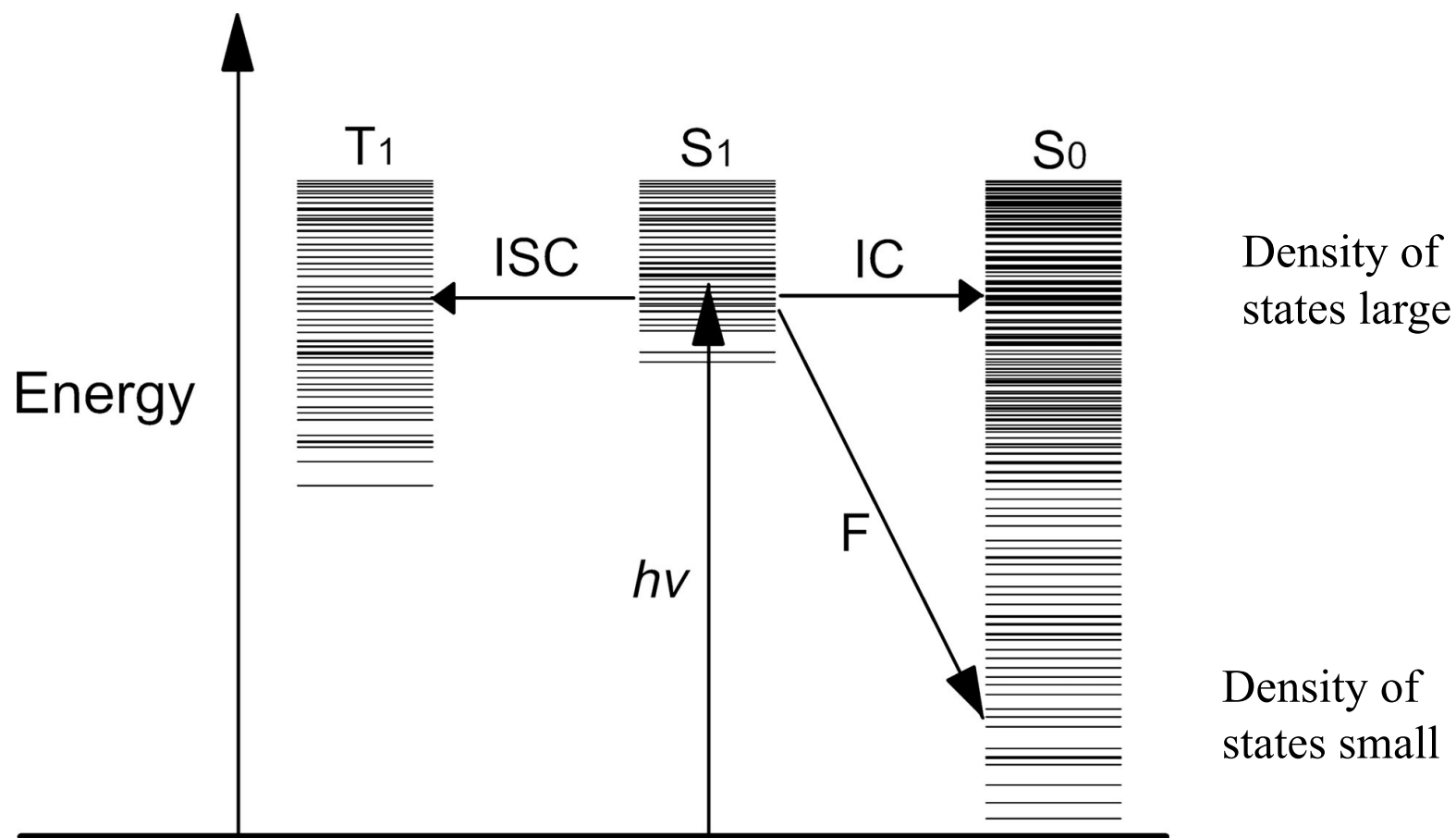
$$f \sim \exp^{-\Delta E}$$

$$k_{IC} \sim 10^{13} f_{\nu}$$

$$k_{IC} \sim 10^{13} \exp^{-\alpha \Delta}$$

Matching (nested) surfaces

Vibrational overlap can be off-set by density of states



Large energy gap favors higher density of states as the vibrational levels that overlap would be in the region with have higher density. Thus energy gap and density of states work in opposite direction.

Dependence of rate of k_{IC} (S_1 to S_0) on energy gap

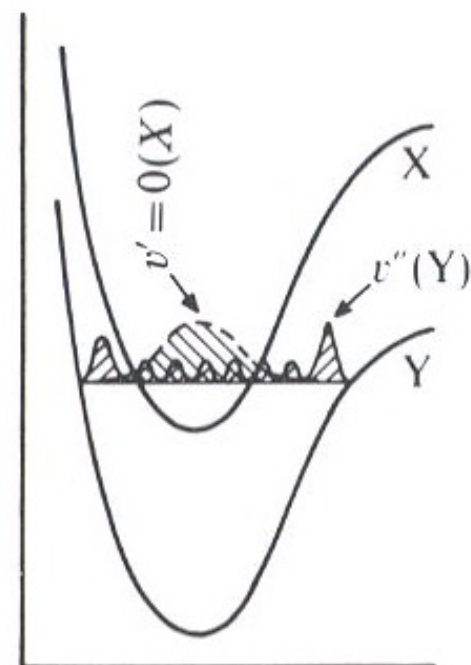
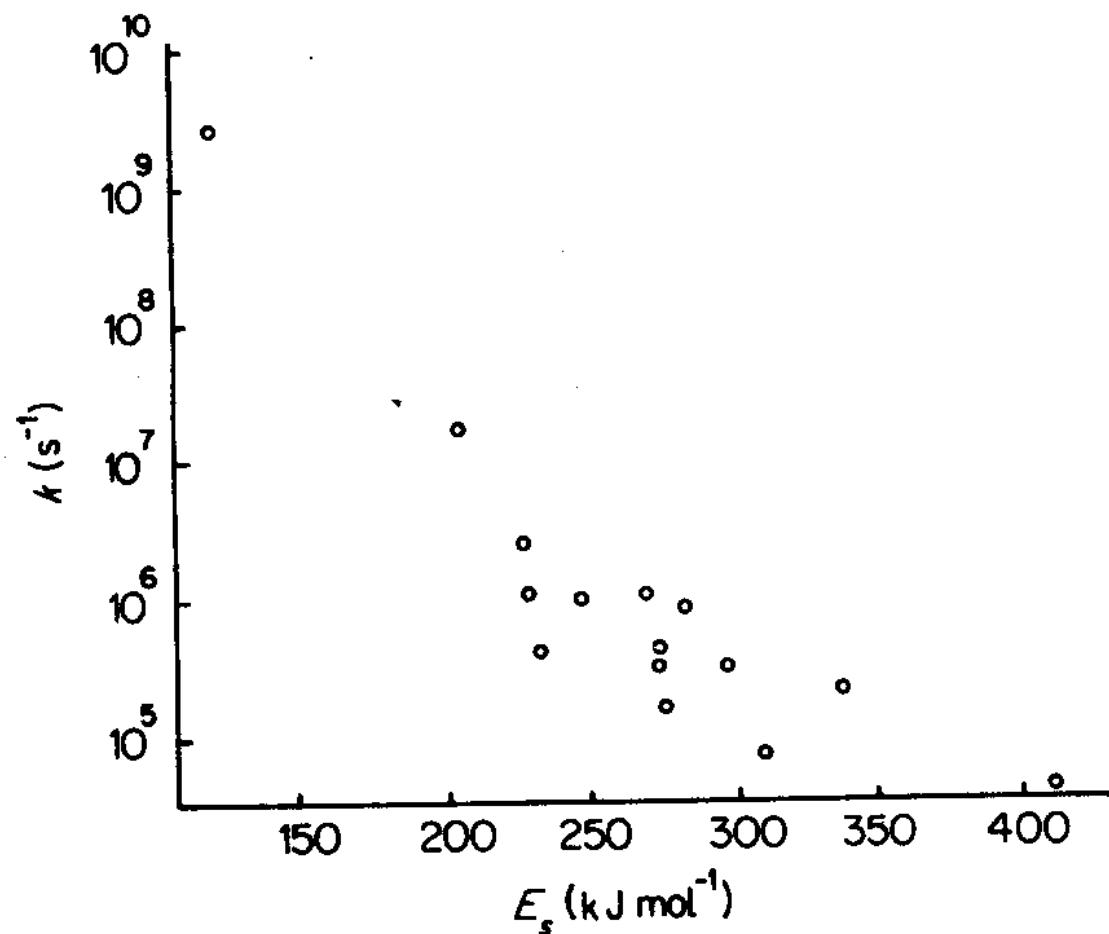


Figure 3.25. Singlet decay rate constants (k) of aromatic hydrocarbons plotted against the singlet energy (E_s). (From data in J. B. Birks, *Photophysics of Aromatic Molecules*, (1970), Wiley)

Dependence of rate of $k_{ISC} T_1$ to S_0 on energy gap

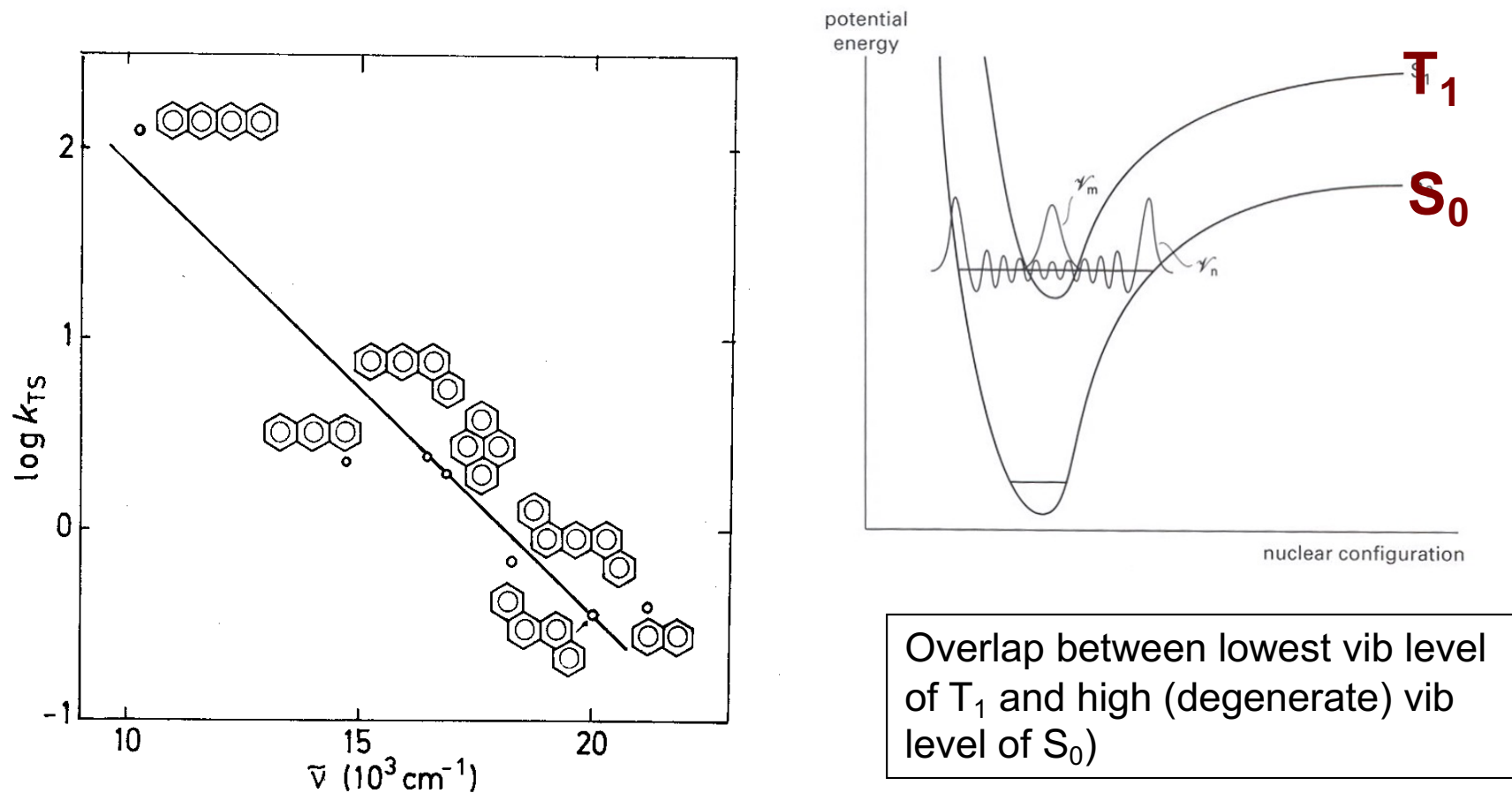
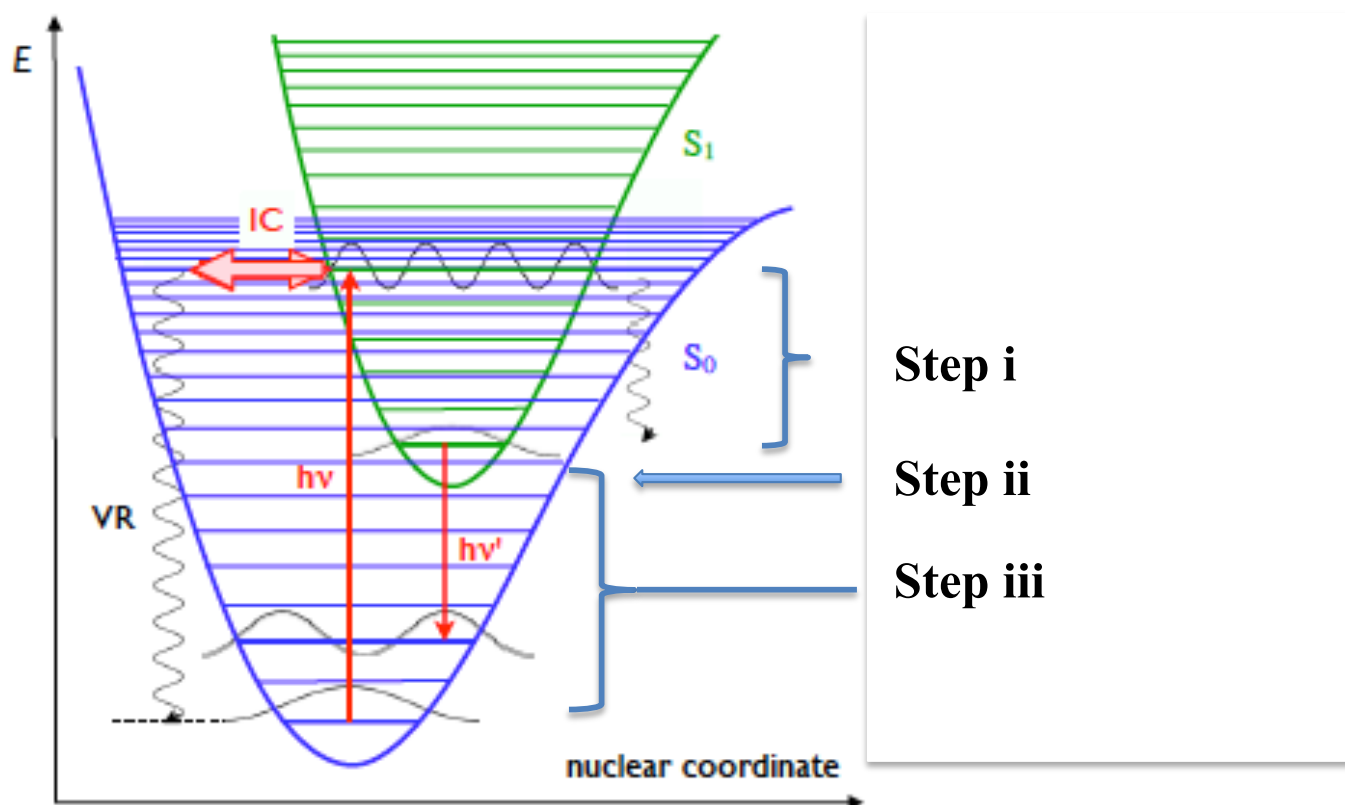


Figure 5.5. Relationship between the energy gap $\Delta E(T_1 - S_0)$ and the logarithm of the rate constant k_{TS} of intersystem crossing in aromatic hydrocarbons (data from Birks, 1970).

Conversion of electronic to vibrational energy

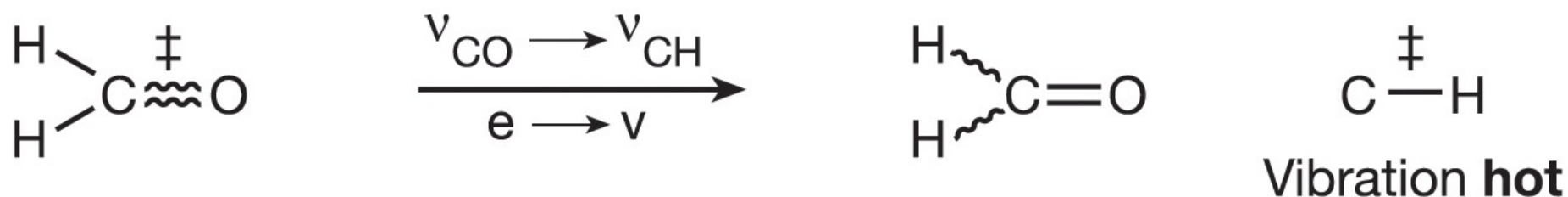
Non-radiative deactivation processes



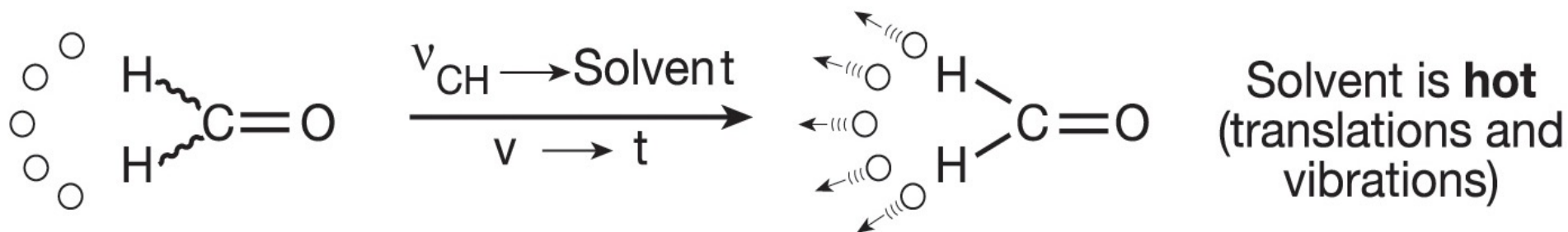
- Three step process:
- (i) upper vibrational to lower vibrational level in excited state
 - (ii) lower vibrational level to upper vibrational of the lower state
 - (iii) upper vibrational of the lower state to lowest vibrational level

Visualization of Electronic Energy to Vibrational Energy Transfer

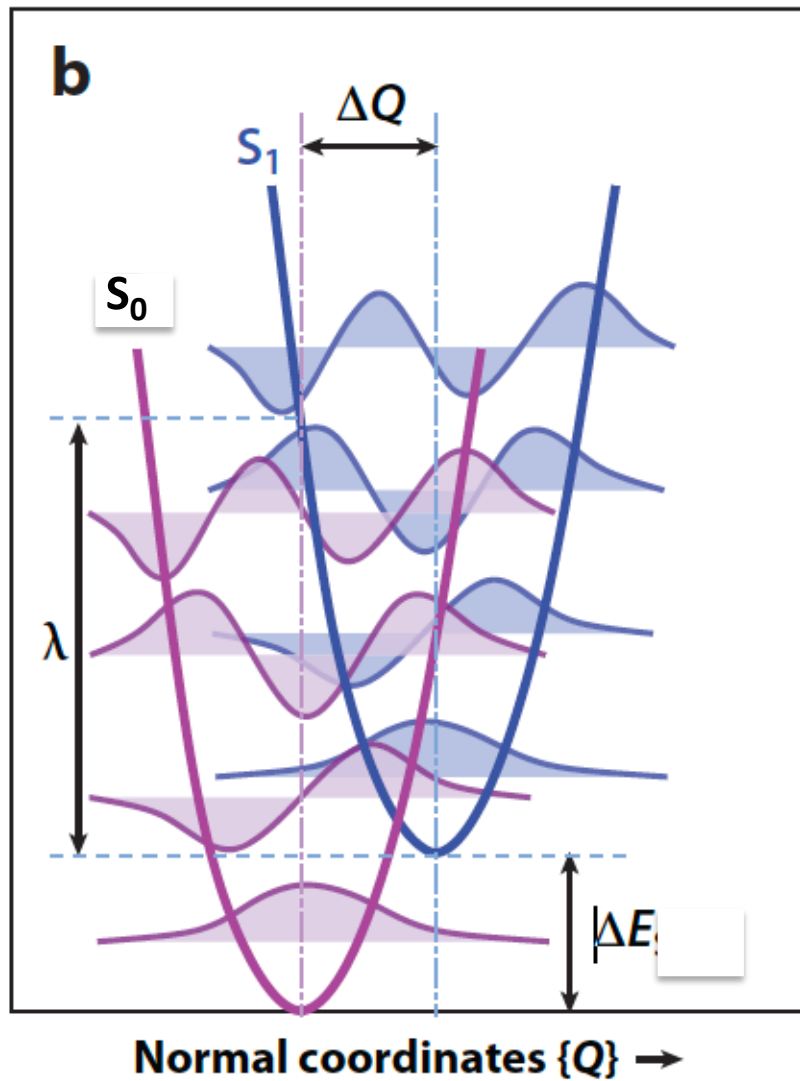
Intramolecular vibrational relaxation (IVR) occurs within 10 to 0.1 ps



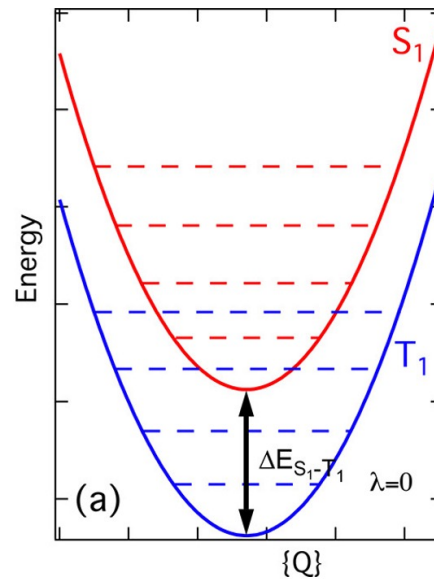
Intermolecular vibrational energy transfer (VET) from the molecule to the solvent occurs in the time range 100 to 10 ps



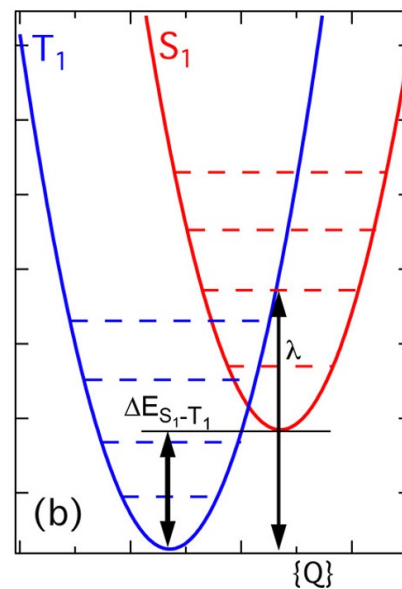
Crossing surfaces



Equilibrium geometries dissimilar

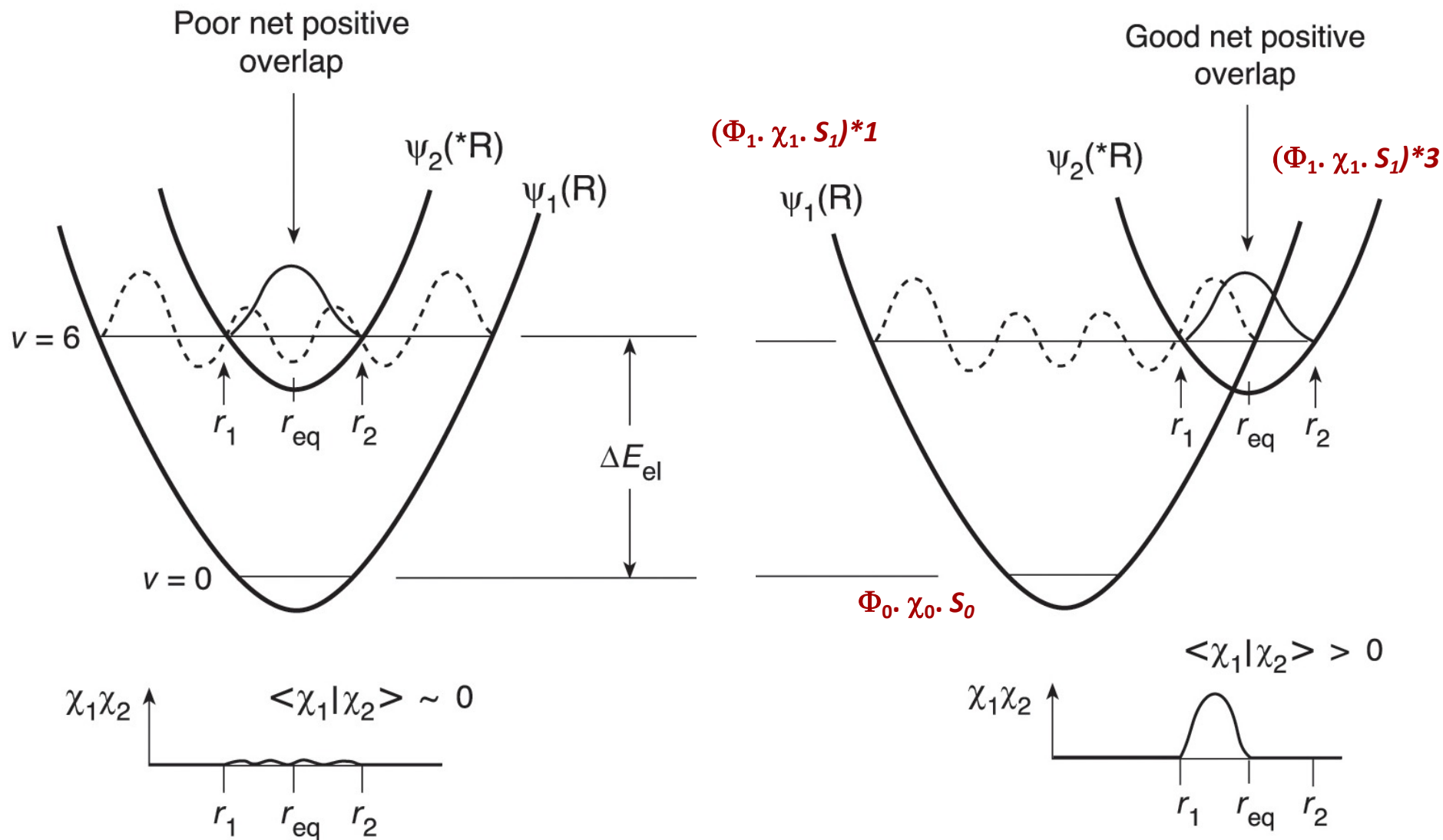


Weak Coupling



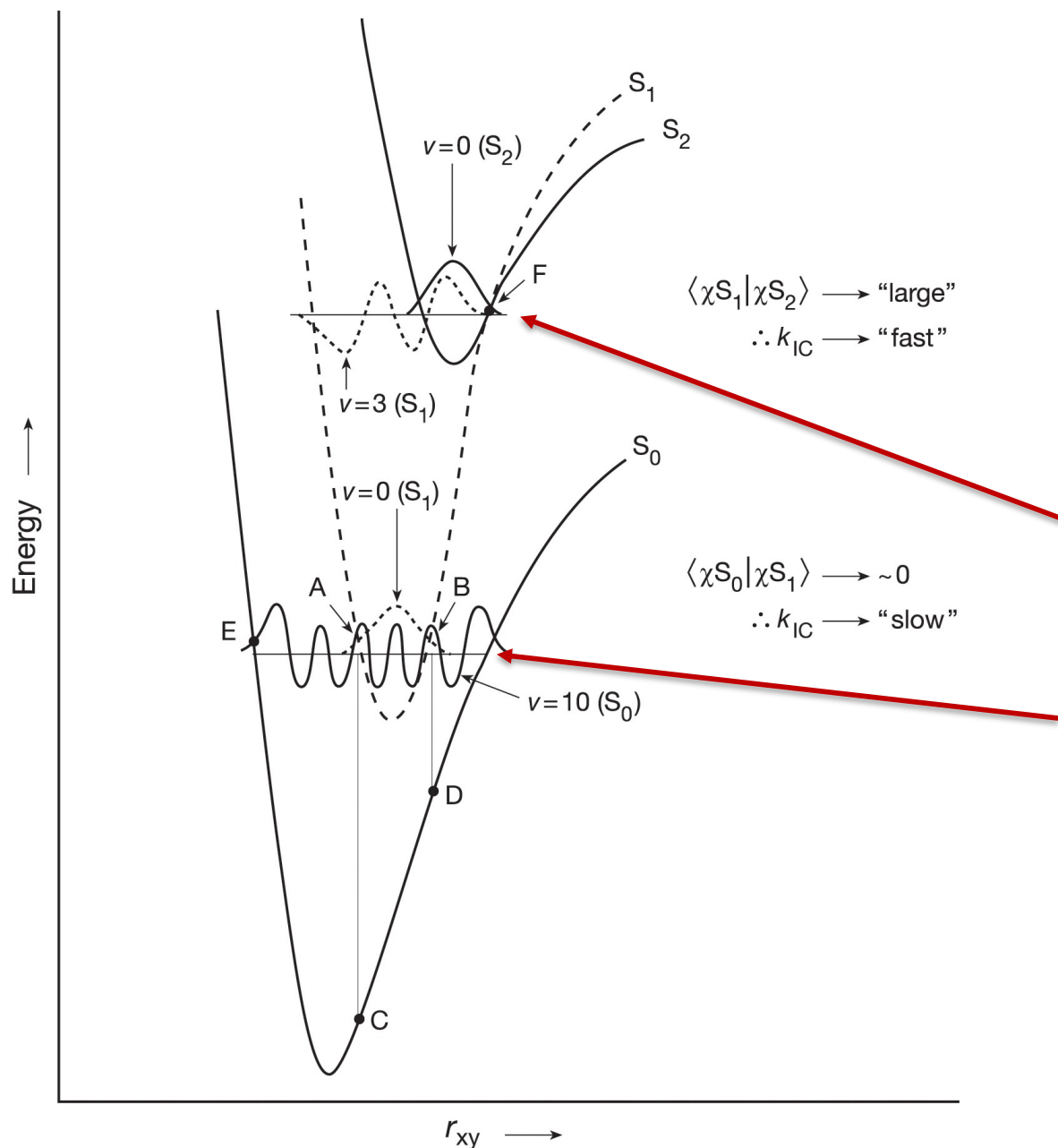
Strong coupling

Matching vs. Crossing Surfaces



For the same energy gap the rates are different for the two types of surfaces

Basis of Kasha's Rule



Kasha's Rule

All photophysical and photochemical processes usually start in S_1 or T_1 , irrespective of which excited state or vibrational level is initially produced.

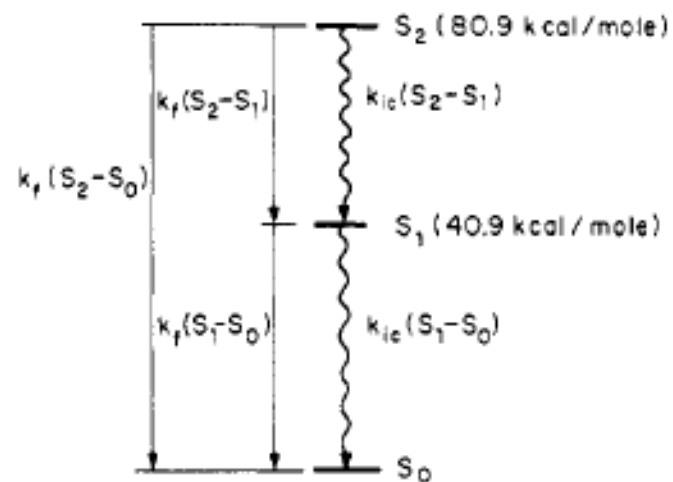
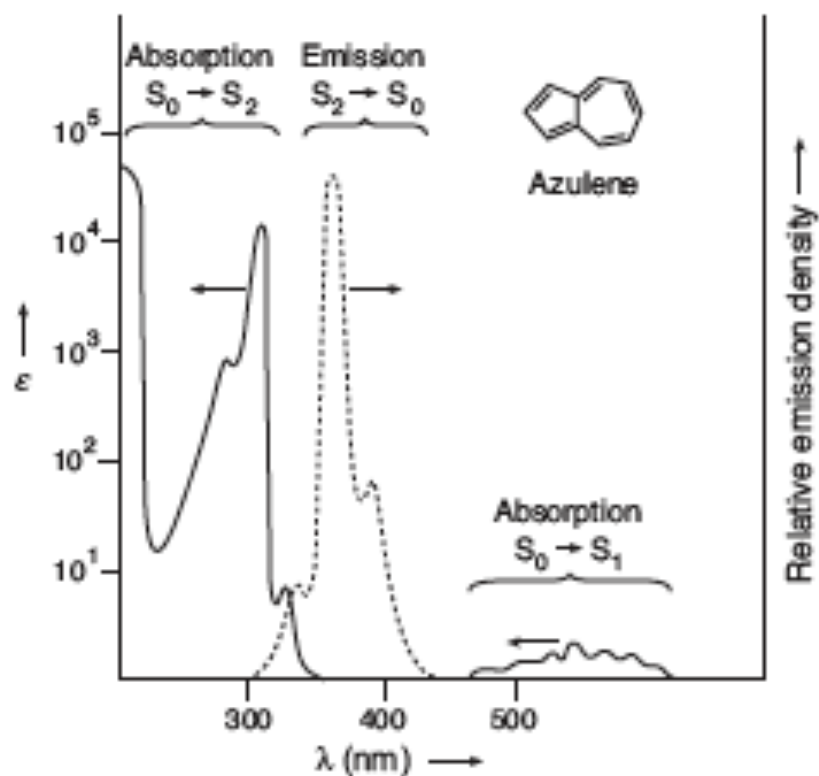
S_2 to S_1 IC is fast due to possible surface crossing and smaller gap

S_1 to S_0 IC is slow due to matching surface and larger gap

S_2 to S_1 IC can be slow if gap is larger and the surfaces don't cross

Energy Gap Law and Azulene Anomaly

Fluorescence occurs only from S_1 to S_0 ; phosphorescence occurs only from T_1 to S_0 ; S_n and T_n emissions are extremely rare (Kasha's rule).



$$k_f(S_2-S_0) = 1.4 \times 10^7$$

$$k_f(S_2-S_1) \approx 1.4 \times 10^4$$

$$k_f(S_1-S_0) = 1.3 \times 10^6$$

$$k_{ic}(S_2-S_1) = 7 \times 10^8$$

$$k_{ic}(S_1-S_0) = 1.2 \times 10^{11}$$

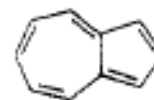
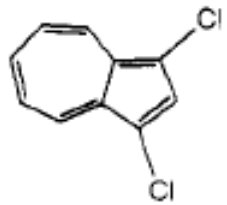
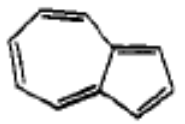
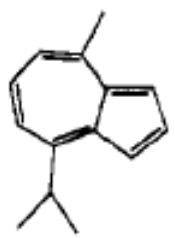
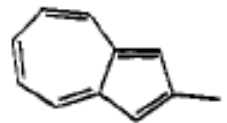
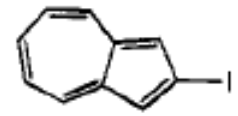
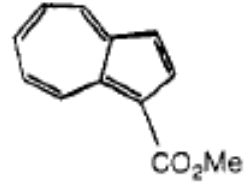


TABLE I. Fluorescence Quantum Yields and the Energies of the First Two Excited Singlet States of Substituted Azulenes^a

	Φ_{fl}	E_{S_1} , kcal/mol	E_{S_2} , kcal/mol	ΔE , kcal/mol
	0.058	36.3	77.0	40.9
	0.031	40.9	80.9	40.0
	0.014	39.5	77.8	38.3
	0.0081	42.6	79.5	36.9
	0.0034	42.9	77.5	34.6
	$\sim 10^{-4}$	44.3	77.2	32.9
	↑			↑

S_2 to S_1 rate vs Energy Gap

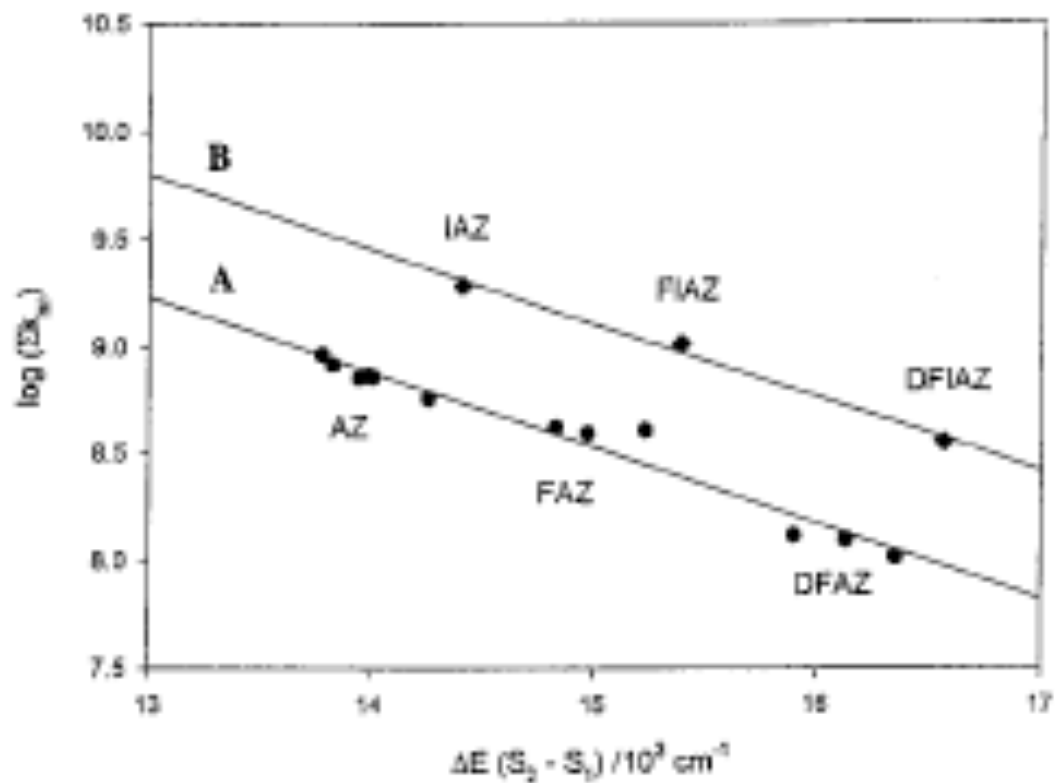
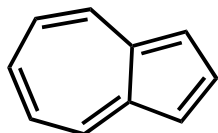
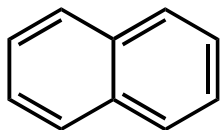
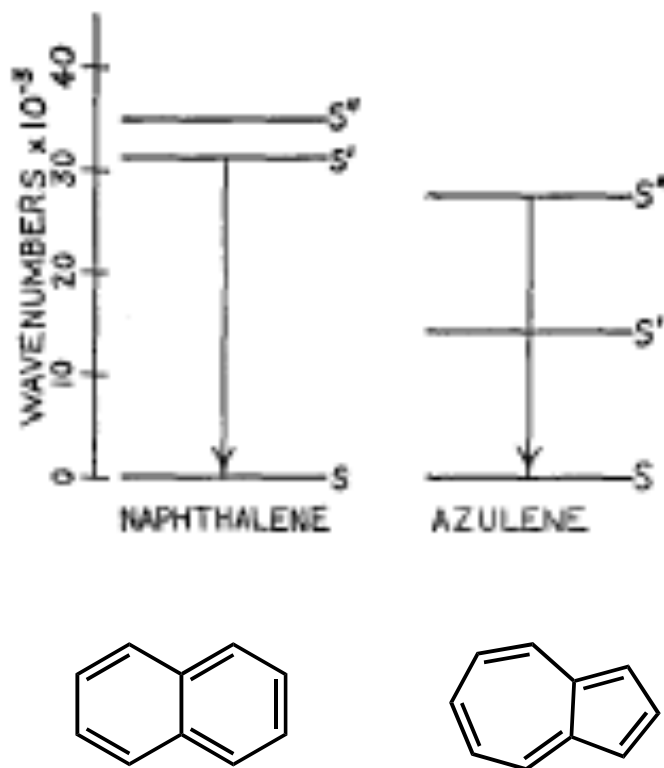
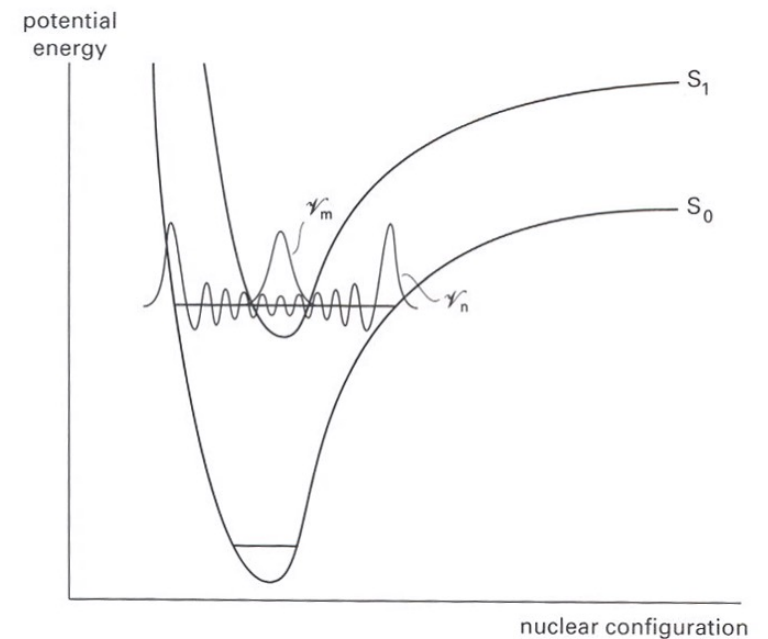
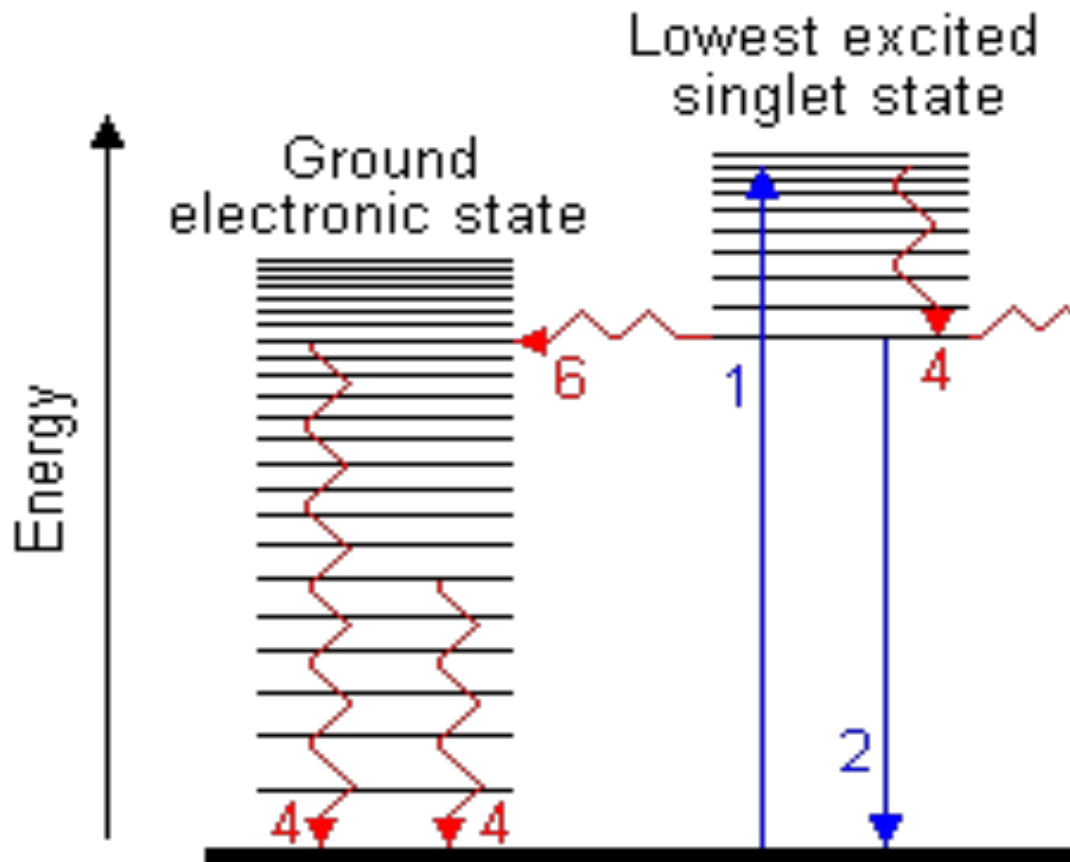


Figure 3. Log-linear energy gap law plots (see text) for azulene (AZ), 1-fluoroazulene (FAZ), and 1,3-difluoroazulene (DFAZ) in several solvents (line A), and for 6-isopropylazulene (IAZ), 1-fluoro-6-isopropylazulene (FLAZ), and 1,3-difluoro-6-isopropylazulene in *n*-hexane (line B). The data for AZ in several solvents are taken from ref 11.

Role of vibrational level (v_n) on radiationless process



Electronic to Vibrational Energy Transfer

Bond Type	Vibrational Type	Frequency
C=C	stretch	2200 cm ⁻¹
C=O	stretch	1700 cm ⁻¹
C=C	stretch	1600 cm ⁻¹
N=N	stretch	1500 cm ⁻¹
C-H	bend	1000 cm ⁻¹
C-C	stretch	1000 cm ⁻¹
C-C	bend	500 cm ⁻¹
C-H	stretch	3000 cm⁻¹ ←
C-D	stretch	2100 cm⁻¹

High frequency vibrations are important in radiationless transitions.

Vibrational level to match the gap is of lower # with high frequency vibrations.

Table 5.4 Some Representative Values of Triplet Energies, Phosphorescence Radiative Rates, Intersystem Crossing Rates, and Phosphorescence Yields^a

Molecule	E_T	k_P	k_{TS}	Φ_P
Benzene- h_6	85	~ 0.03	0.03	0.20
Benzene- d_6	85	~ 0.03	< 0.001	~ 0.80
Naphthalene- h_8	60	~ 0.03	0.4	0.05
Naphthalene- d_8	60	~ 0.03	< 0.01	~ 0.80
$(CH_3)_2C=O$	78	~ 50	1.8×10^3	0.043
$(CD_3)_2C=O$	78	~ 50	0.6×10^3	0.10

a. In organic solvents at 77 K. E_T in kcal mol⁻¹, k , in s⁻¹.

C-H stretch

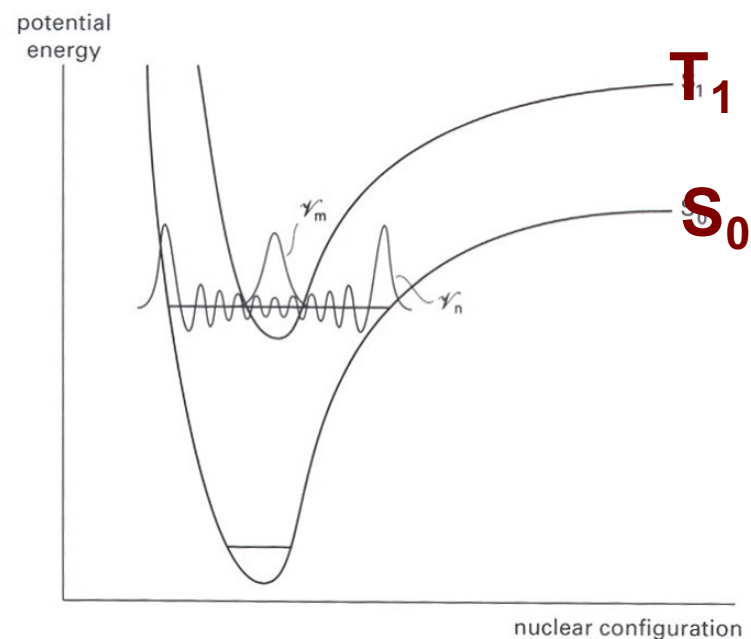
3000 cm⁻¹

C-D stretch

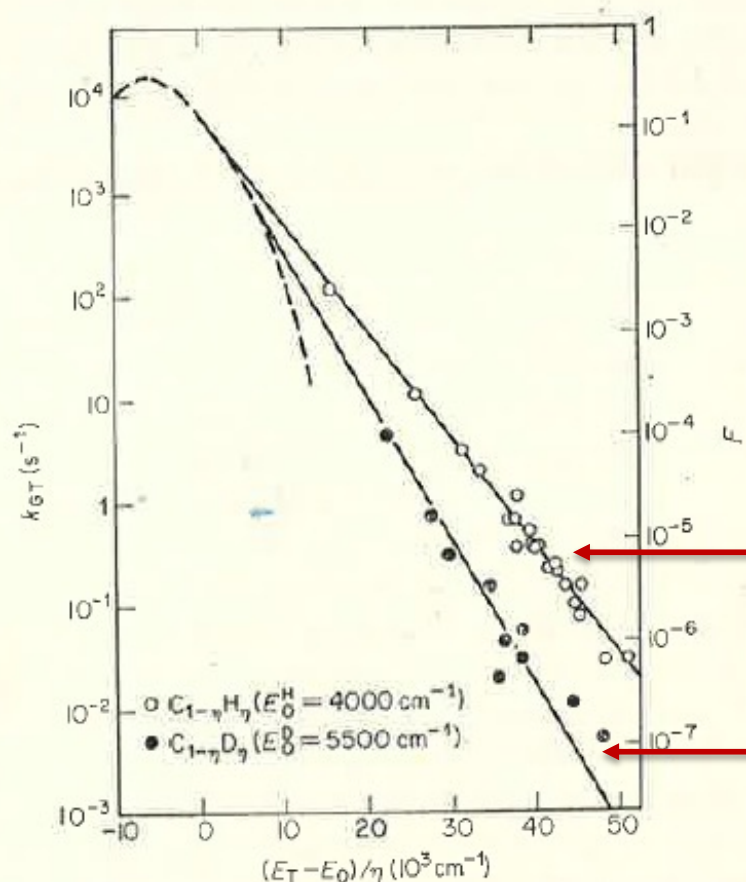
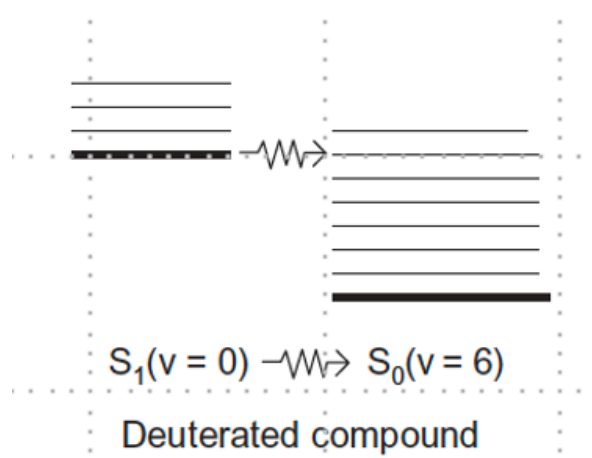
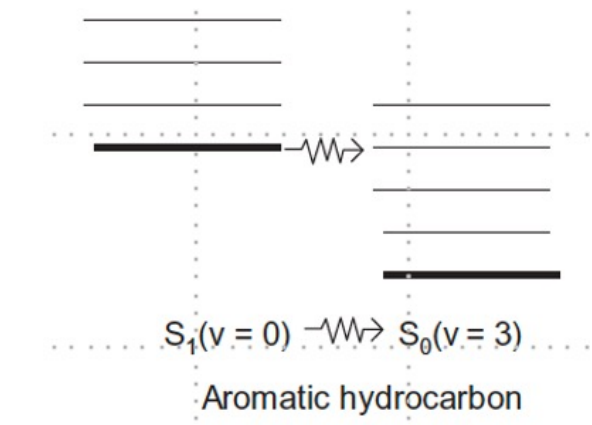
2100 cm⁻¹

Higher vibrational level needed to match; poor overlap, slow decay, large Φ_P

Isotope Effect on Rate of T_1 to S_0



Effect of deuteration on radiationless process (T_1 to S_0)

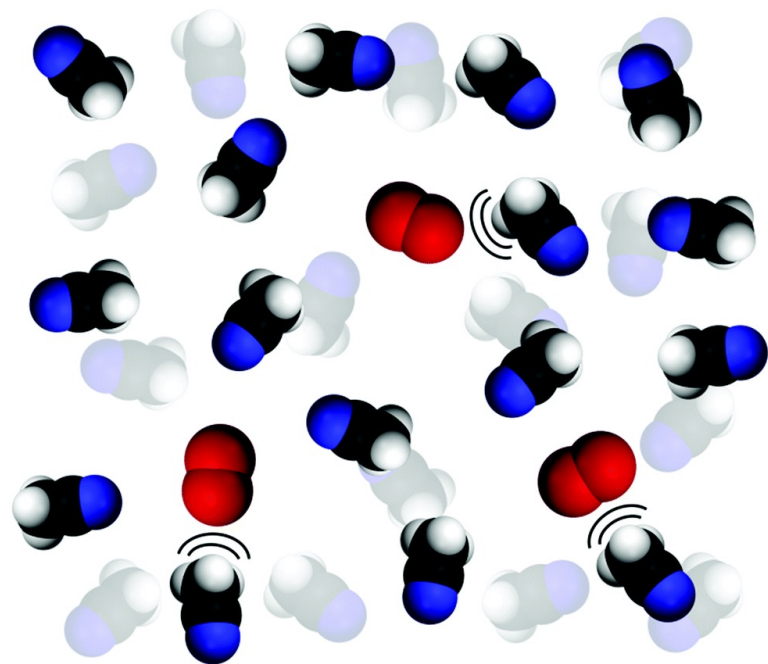


← perprotonated

□ perdeuterated

Figure 5.2 $T_1 - S_0$ intersystem crossing rate $k_{GT} (s^{-1})$ and Franck-Condon factor F against normalized triplet state energy $(E_T - E_0)/\eta$ for unsubstituted perprotonated and perdeuterated aromatic hydrocarbons. The broken line represents F as derived from phosphorescence spectra. The F -scale is normalized by drawing the two solid lines as tangents to this function (after Siebrand⁶)

Decay of singlet oxygen depends on solvent and deuteration



Mikkel Bregnh.j, Michael Westberg, Frank Jensen and Peter R. Ogilby, *Phys. Chem. Chem. Phys.*, **2016**, *18*, 22946

Solvent	$\tau_{\Delta}/\mu\text{s}$	
	Averaged published data ^a	Current data ^b
Benzene- <i>h</i> ₆	30.6 ± 0.9	30.4
Benzene- <i>d</i> ₆	640 ± 150	747
Toluene- <i>h</i> ₈	28.6 ± 0.7	30.5
Toluene- <i>d</i> ₈	303 ± 17	314
α,α,α -Trifluorotoluene	62.5	61.7
<i>o</i> -Xylene	21.0 ± 2.0	23.4
Mesitylene	15.5 ± 0.5	16.9
Chlorobenzene	45 ± 3	43.6
Iodobenzene	37 ± 2	38.9
1,2-Dichlorobenzene	—	57.0
1,2,4-Trichlorobenzene	—	93.8
Cyclohexane- <i>h</i> ₁₂	23.3 ± 0.5	24.0
Cyclohexane- <i>d</i> ₁₂	450	483
<i>n</i> -Pentane	34.8 ± 0.2	34.8
<i>n</i> -Hexane- <i>h</i> ₁₄	30.8 ± 0.6	32.2
<i>n</i> -Hexane- <i>d</i> ₁₄	—	586
<i>n</i> -Heptane	28.9 ± 0.5	30.1
<i>n</i> -Octane	—	28.6
<i>n</i> -Decane	27.6	26.5
Methanol- <i>h</i> ₄	9.8 ± 0.6	9.4
Methanol-OD	31 ± 5	31.4
Methanol- <i>d</i> ₄	246 ± 16	276
1-Propanol	17.2 ± 0.9	15.9
1-Octanol	18.5	17.8
Benzyl alcohol	—	14.4
Acetone- <i>h</i> ₆	48 ± 4	45.6
Acetone- <i>d</i> ₆	770 ± 140	1039
Acetonitrile- <i>h</i> ₃	77 ± 4	81.0
Acetonitrile- <i>d</i> ₃	890 ± 330	1610
Benzonitrile	36 ± 4	40.0
H ₂ O	3.7 ± 0.4	3.5 ^e
D ₂ O	68 ± 1 ^f	68.9 ^e

Vibrational effects on singlet oxygen lifetime

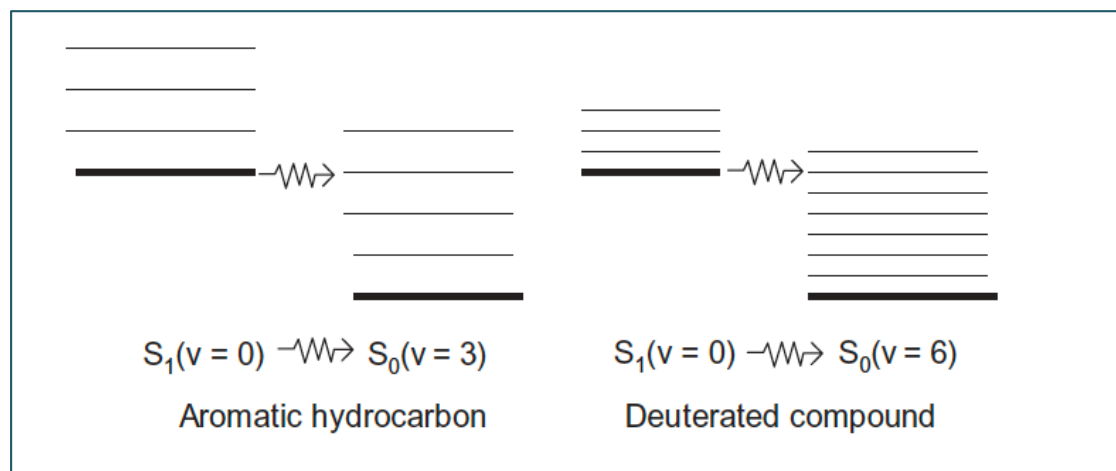
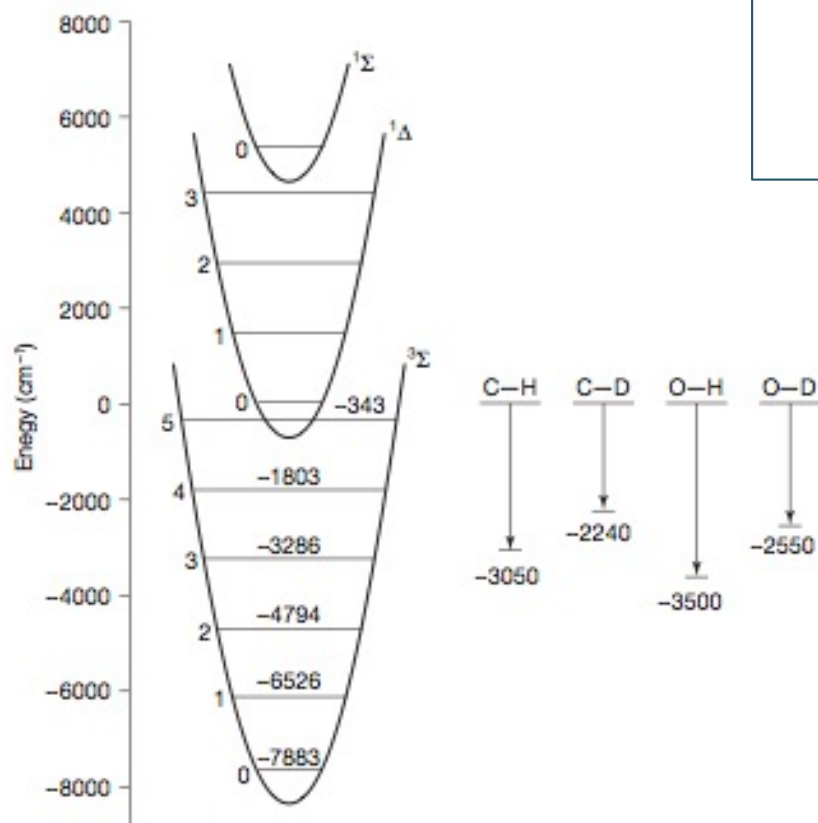


Table 14.3 Approximate Rate Constants^a for the Deactivation of $^1\Delta$ by Various Kinds of X—Y Bonds in Organic Solvents^b

Bond Type	k_d ($M^{-1} s^{-1}$)	Vibrational Energy (cm^{-1})
O—H	2900	~ 3600
C—H (aromatic)	1500	~ 3000
C—H (aliphatic)	300	~ 2900
O—D	100	~ 2600
C—D (aromatic)	20	~ 2200
C—D (aliphatic)	10	~ 2100
C—F (aromatic)	0.6	~ 1200
C—F (aliphatic)	0.05	~ 1200

a. Reference 9.

b. The energies of X—D vibrations are typically at 0.73 times the energy of a X—H vibration.

Figure 14.3 Comparison of the energy levels of $^1\Delta$ to common high frequency X—H and X—D vibrations of solvents. Energies in cm^{-1} .

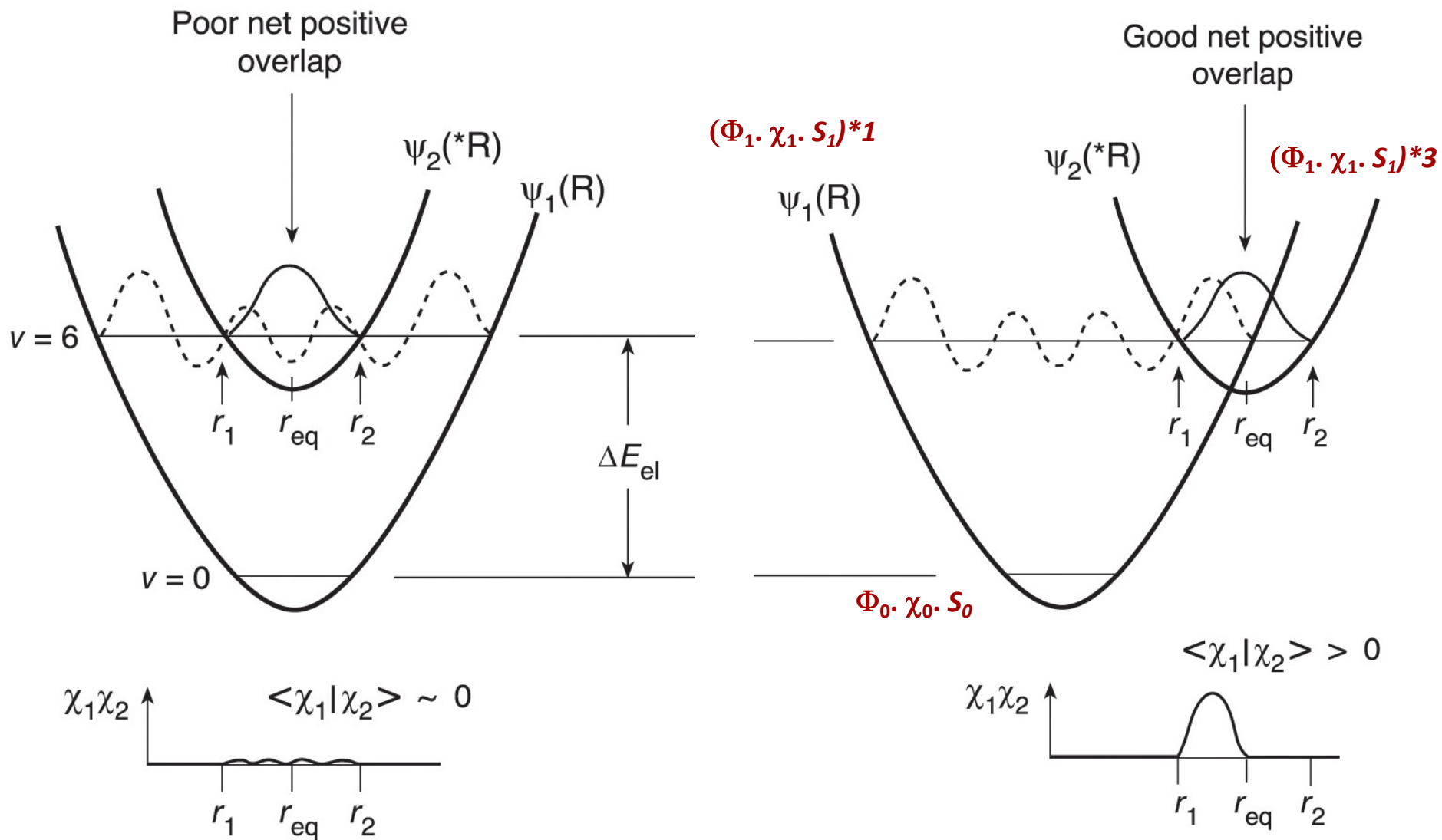
In aromatics because of the large S_1 to S_0 energy gap internal conversion does not compete with k_{ISC} and k_F

Table 4.2 Quantum yields for fluorescence ($S_1 \rightarrow S_0 + h\nu$) and intersystem crossing ($S_1 \rightsquigarrow T_1$) for some aromatic hydrocarbons in ethanol solution (Data from Birks, J. B. (ed.) (1975). Organic molecular photophysics, Vol. 2, Tables 2.6 and 3.4. Wiley, London)

Compound	ϕ_f	ϕ_{ISC}	$\phi_f + \phi_{ISC}$
Benzene	0.04	0.15	0.19 (exception)
Naphthalene	0.80	0.21	1.01
Fluorene	0.32	0.68	1.00
Anthracene	0.72	0.32	1.02
Tetracene	0.66	0.16	0.82
Phenanthrene	0.85	0.13	0.98
Pyrene	0.38	0.65	1.03
Chrysene	0.85	0.17	1.03

For large aromatic molecules the sum of the quantum yields of fluorescence and ISC is one i.e., rate of internal conversion is very slow with respect to the other two (Ermolaev's rule).

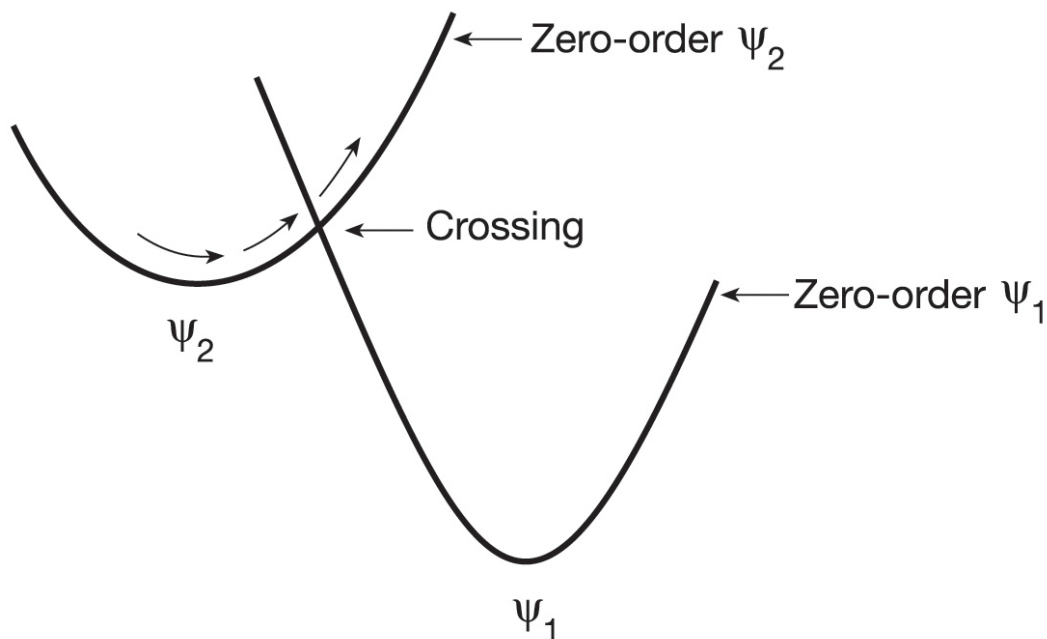
Internal conversion in matching vs. crossing surfaces



For the same energy gap the rates are different for the two types of surfaces

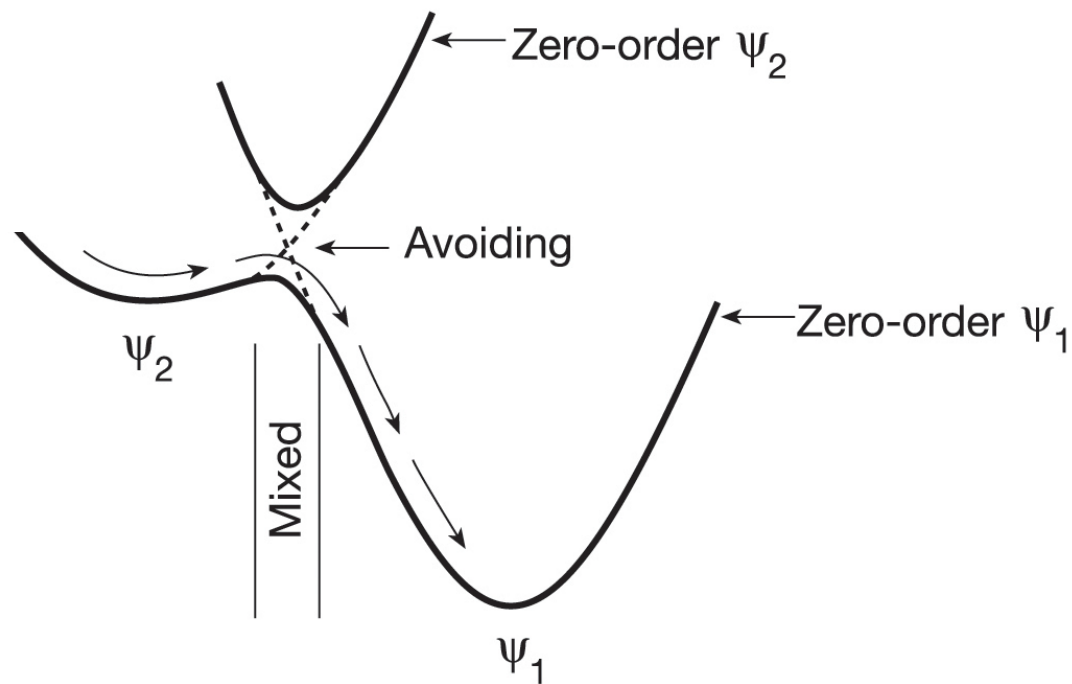
Breakdown of Born-Oppenheimer Approximation

Mixing of surfaces



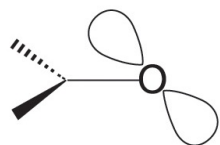
Two surfaces with different electronic or spin configurations

For the same nuclear configuration there are two electronic configurations with identical energies. Under favorable conditions this would lead to mixing resulting in avoided crossing.



Breakdown of Born-Oppenheimer Approximation

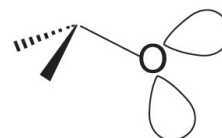
Vibronic mixing enables surface mixing



Strictly planar

$$n_0 = p_0$$

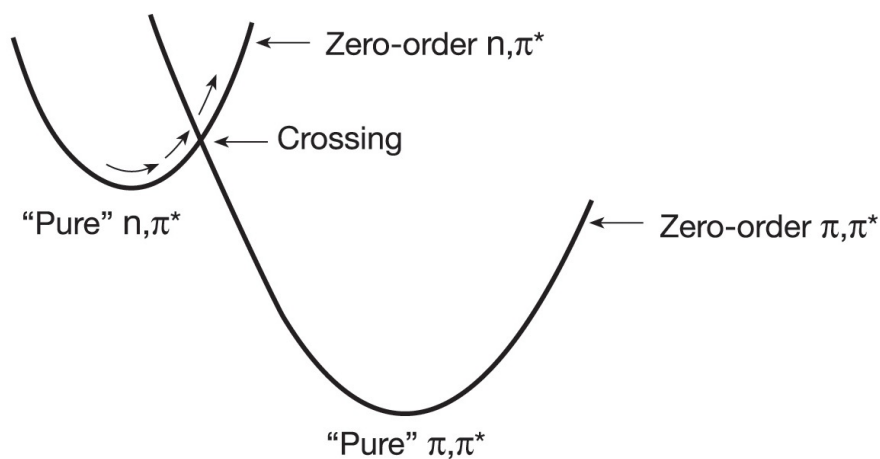
$$\langle n_0 | \pi \rangle = 0$$



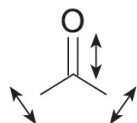
Nonplanar

$$n_0 = sp^n$$

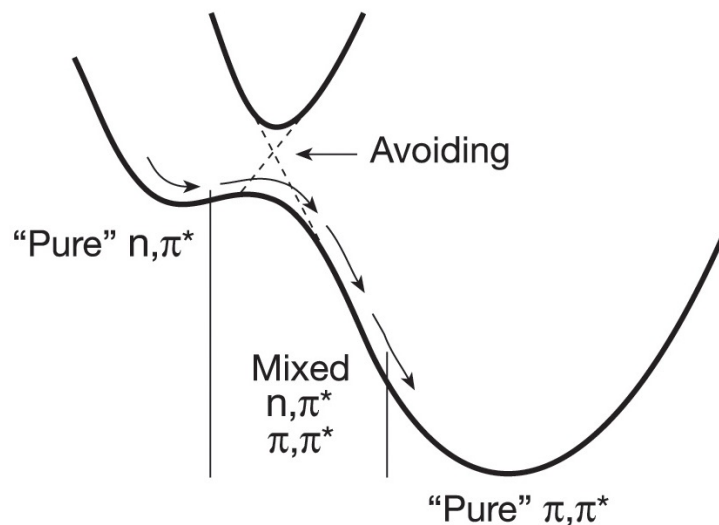
$$\langle n_0 | \pi \rangle \neq 0$$



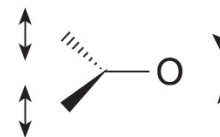
→



Planar vibrations



→



Nonplanar vibrations

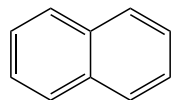
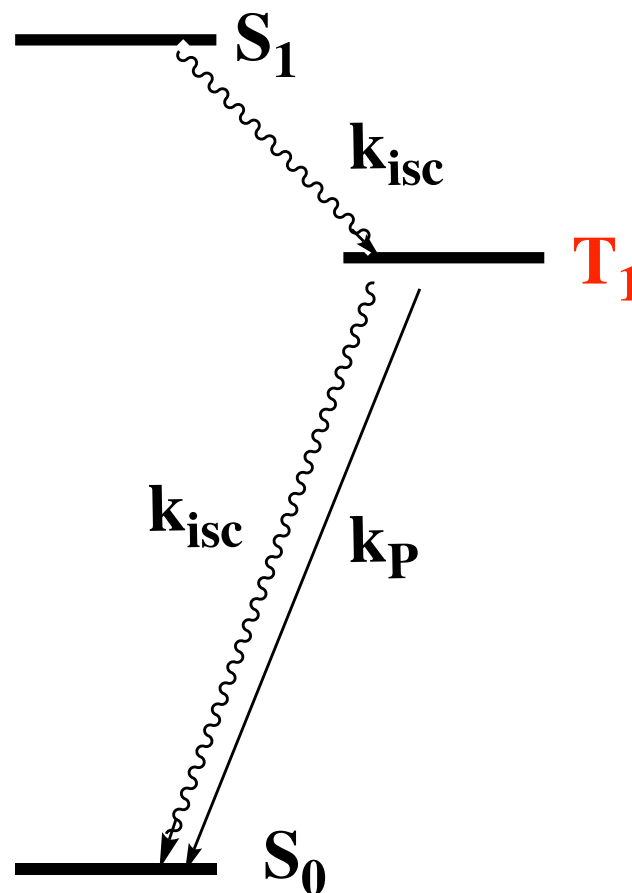
Energy is fine, but
orbitals don't overlap

**Intersystem crossing in aromatic molecules ($\pi\pi^*$)
and olefins ($\pi\pi^*$)**

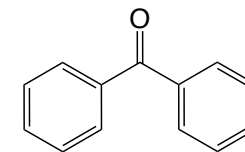
**Intersystem crossing in
carbonyl compounds ($n\pi^*$)**

**Intersystem Crossing in
Diradicals and Radical Pairs**

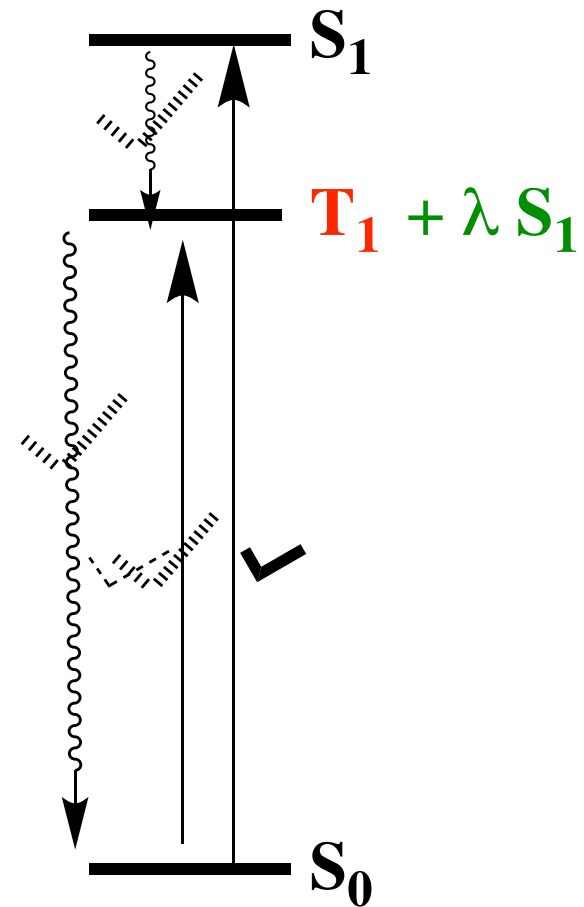
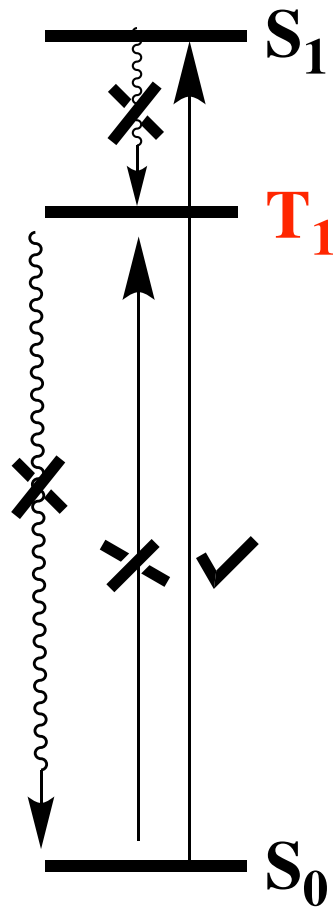
Spin forbidden transitions



Intersystem crossing in molecules with $n\pi^*$ and $\pi\pi^*$ states



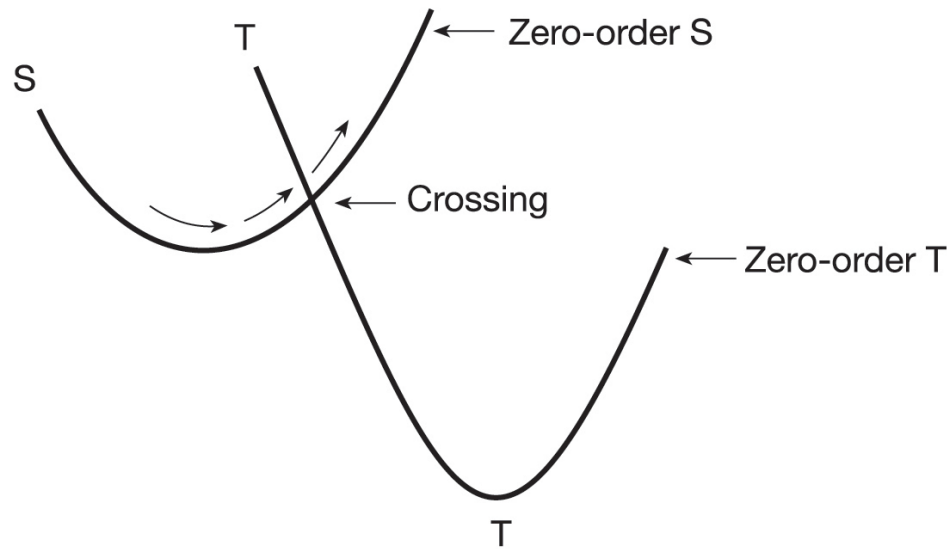
Singlet-Triplet Transitions Role of Spin-Orbit Coupling



Spin-Orbit coupling mixes the states,
no longer pure states

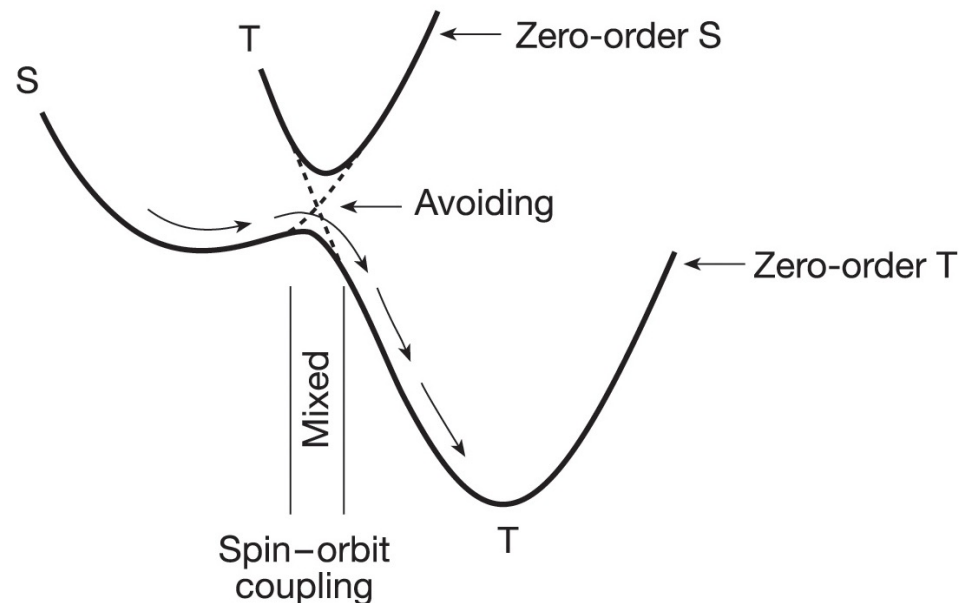
Breakdown of Born-Oppenheimer Approximation

Spin-Orbit coupling enables surface mixing



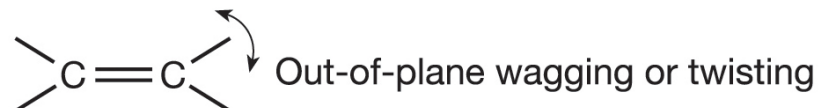
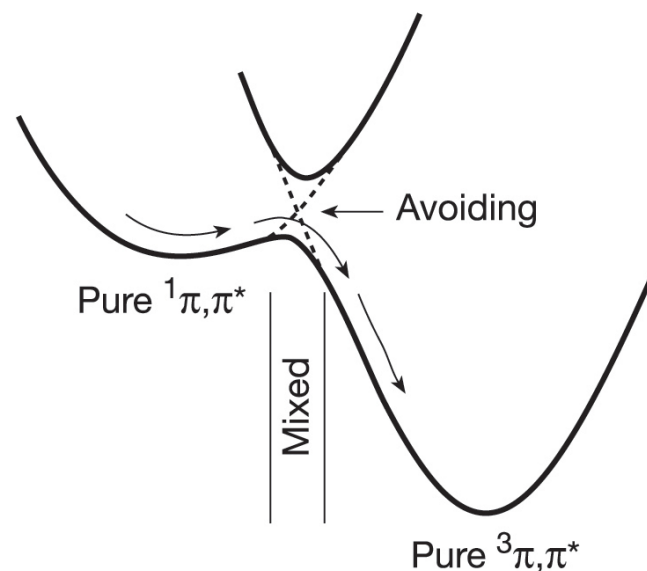
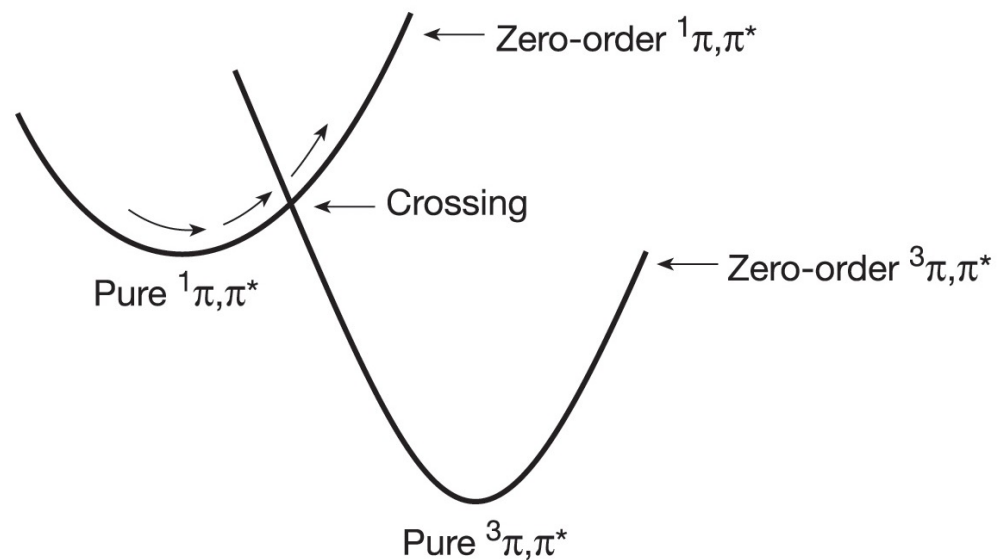
Two surfaces with different spin configurations.

For the same nuclear configuration there are two spin configurations. Coupling between the two surfaces could lead to mixing and result in avoided crossing.

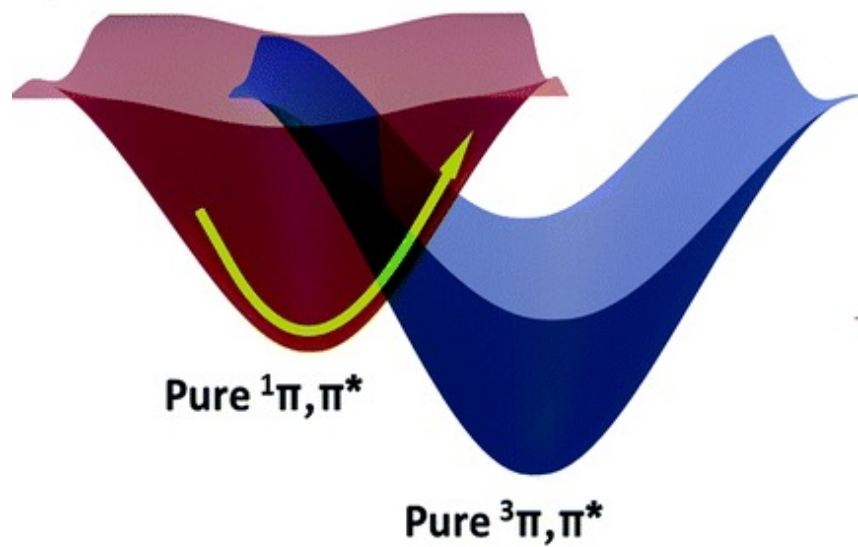


Breakdown of Born-Oppenheimer Approximation

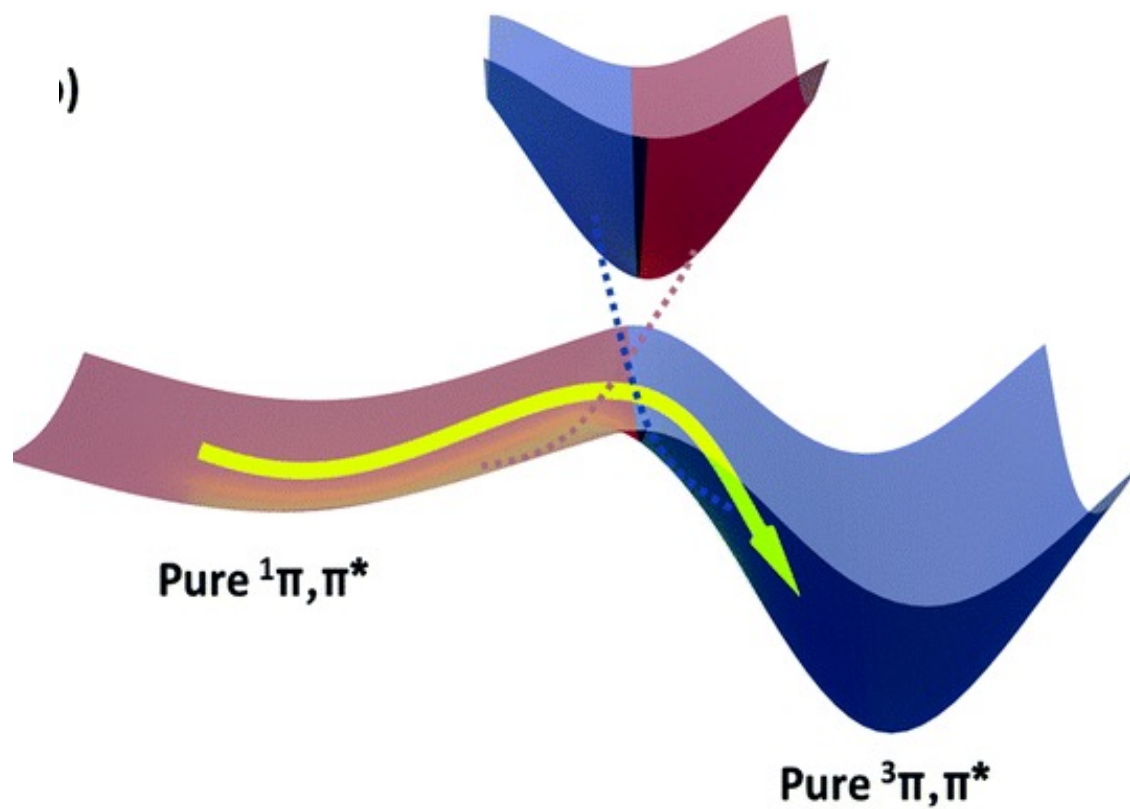
Spin-orbit coupling facilitated by vibronic mixing enables surface mixing



a)

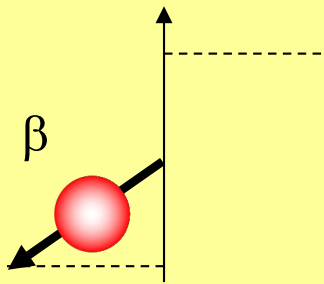
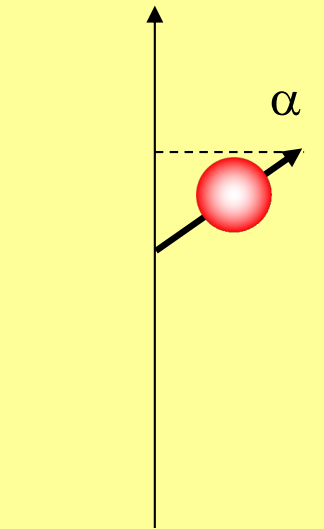


b)



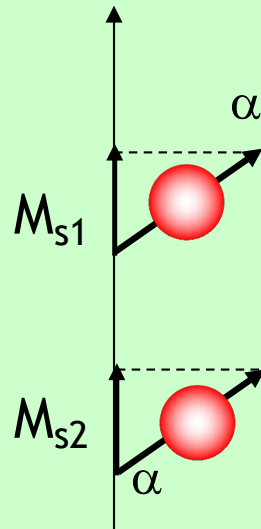
Two spins of $\frac{1}{2}$: $S = 0$
 Spin multiplicity = $2S+1 = 1$

Two spins of $\frac{1}{2}$: $S = 1$



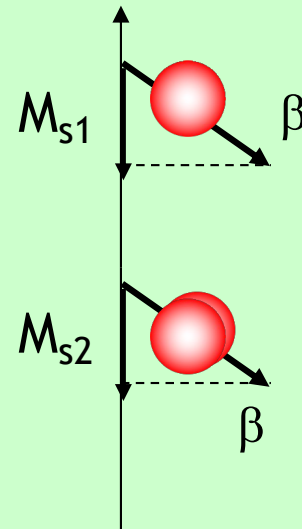
$M_S = 0$

$\alpha\beta - \beta\alpha$



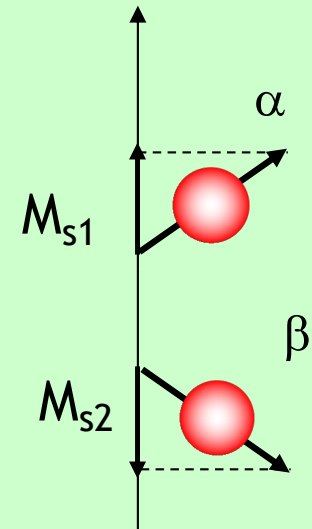
$M_S = 1$

$\alpha\alpha$



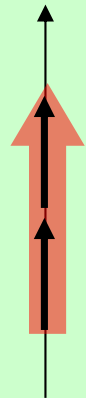
$M_S = -1$

$\beta\beta$

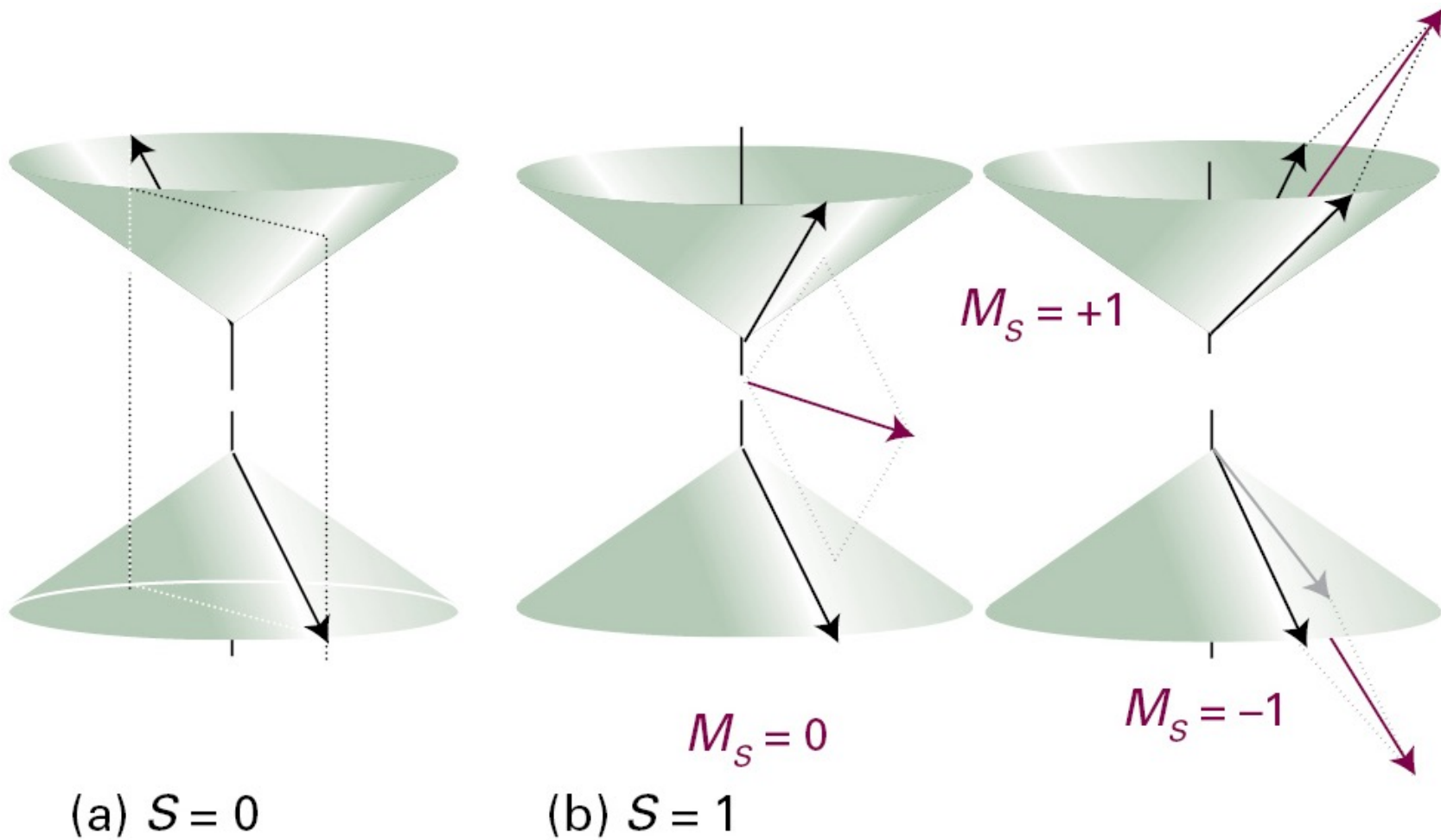


$M_S = 0$

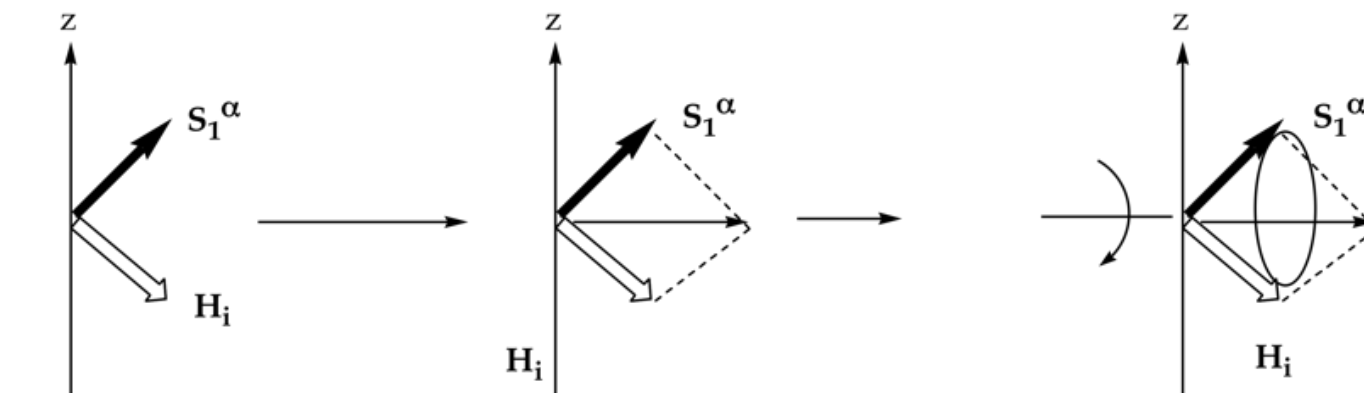
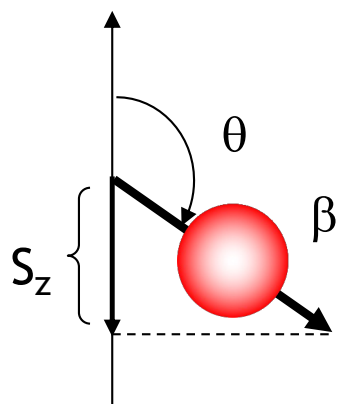
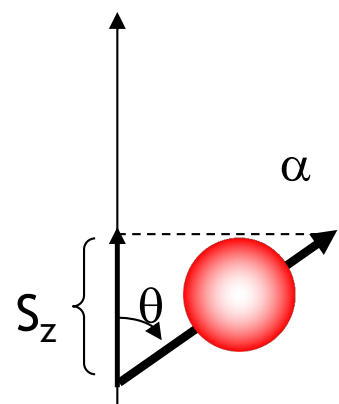
$\alpha\beta + \beta\alpha$



Angular momentum vector representations of two electron system: Singlet and Triplet



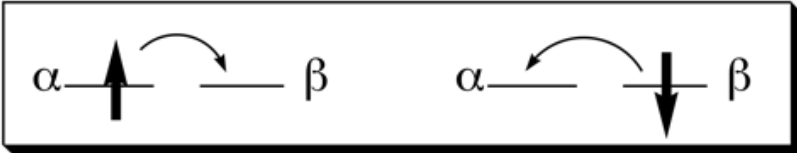
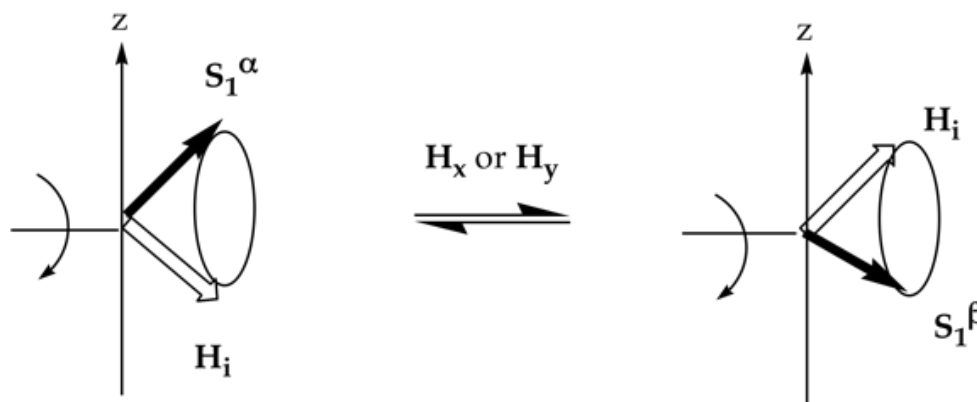
Spin interconversion in one spin system



S_1 and H_i
uncoupled

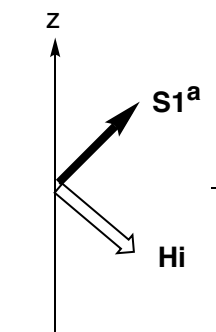
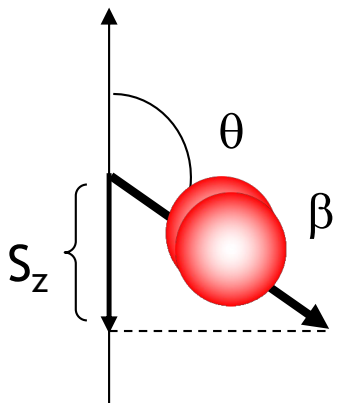
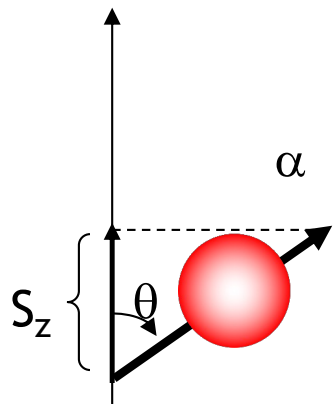
S_1 and H_i coupled to
yield the resultant $S_1 + H_i$

S_1 and H_i precess about
resultant

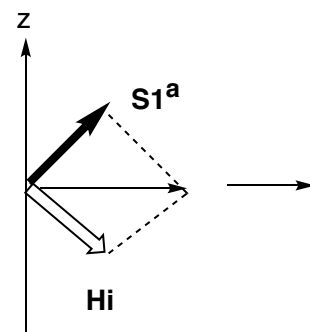


Zero Field

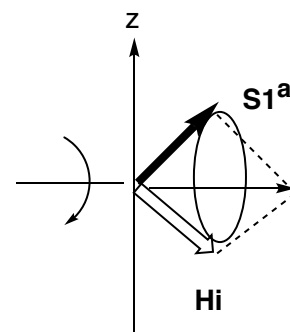
Spin interconversion in one spin system in zero and high magnetic field



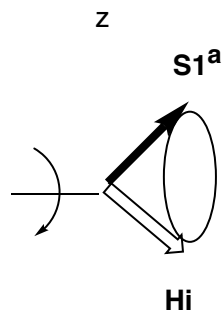
S₁ and H_i uncoupled



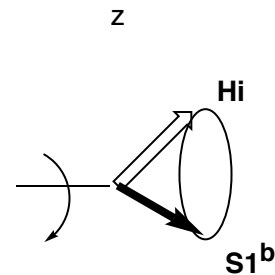
S₁ and H_i coupled to yield the resultant S₁ + H_i



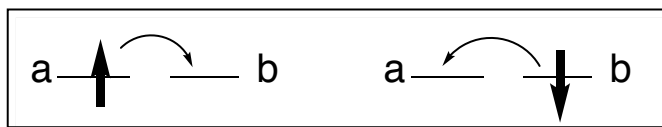
S₁ and H_i precess about resultant



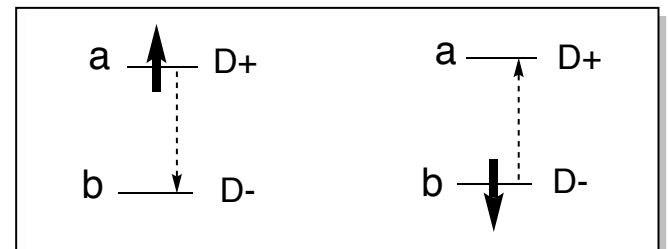
H_x or H_y



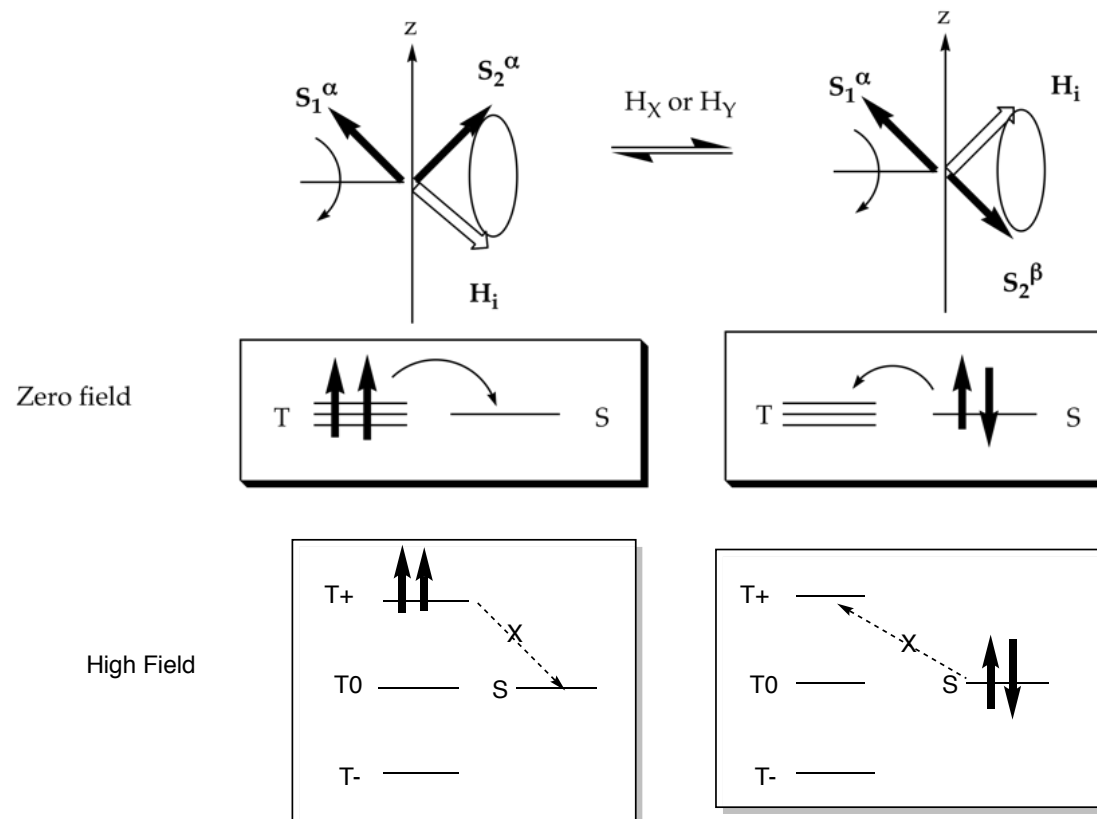
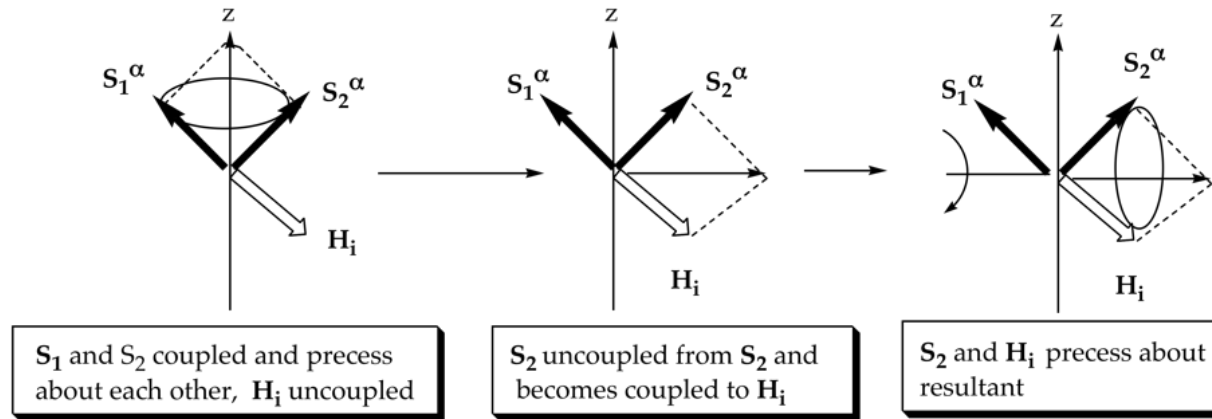
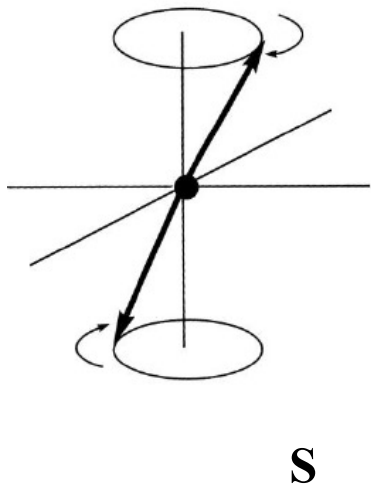
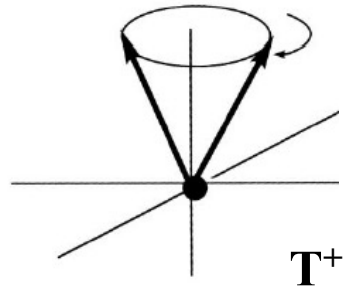
Zero Field



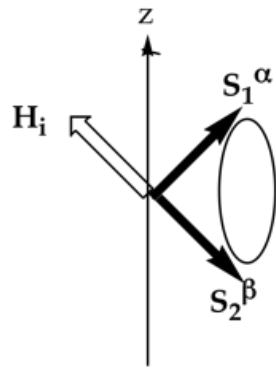
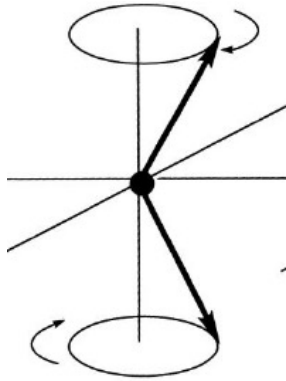
High Field



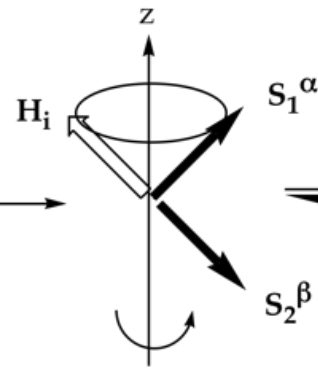
Spin interconversion in two spin system



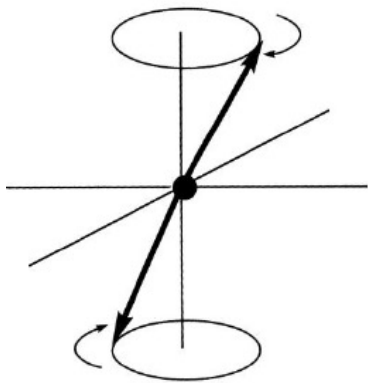
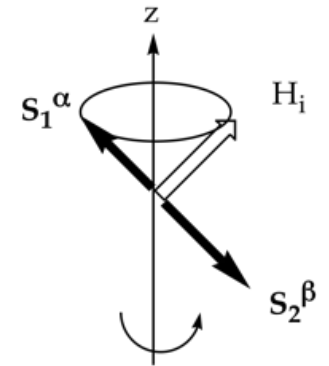
Spin interconversion in two spin system



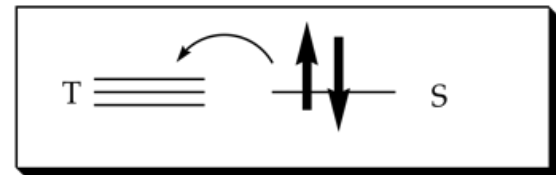
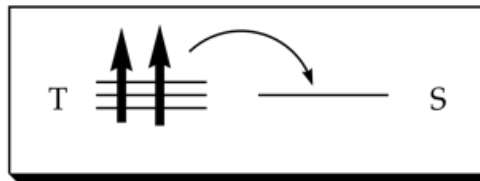
S_1 and S_2
coupled, H_i
uncoupled



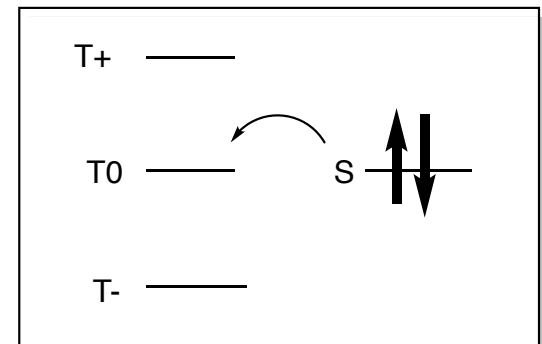
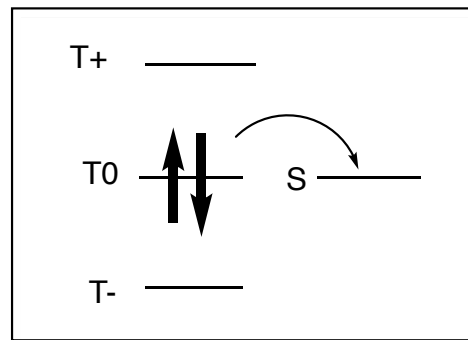
S_2 becomes
uncoupled from S_1
and becomes coupled to H_i



Zero field



High Field



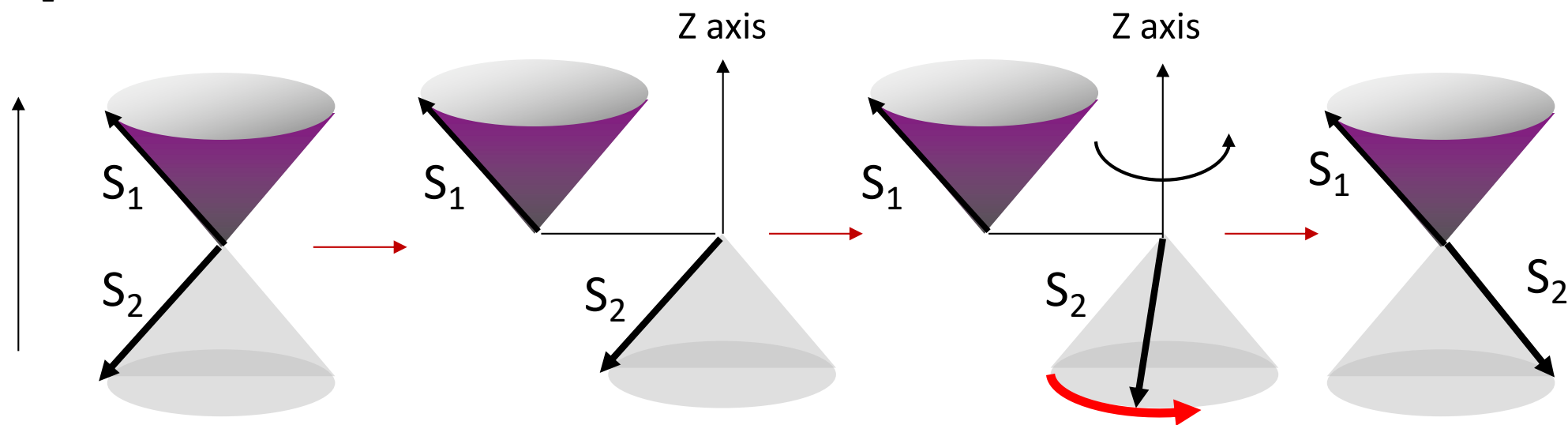
Spin interconversion in two spin system (Spin rephasing)

tightly coupled

loosely coupled

tightly coupled

H_z

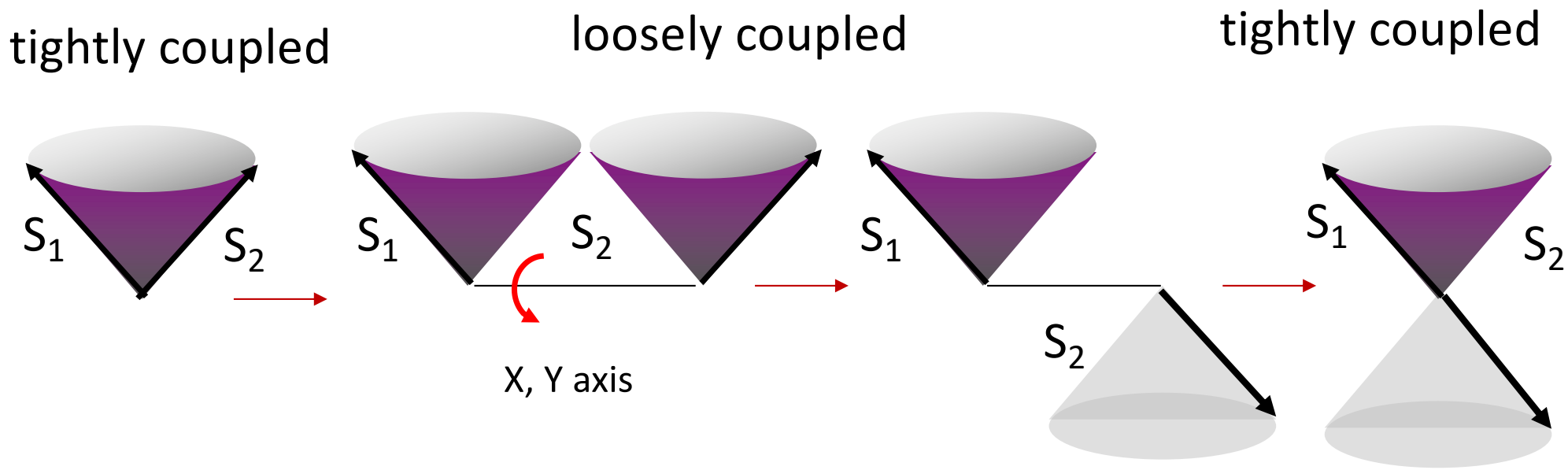


triplet, T_0

torques producing
a **rotation** of S_2 about z

singlet

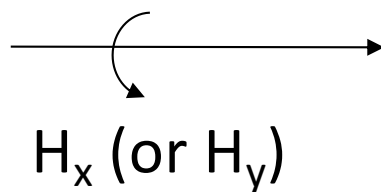
Spin interconversion in two spin system: Spin flipping



triplet, T_+

torques producing a rotation of S_2 about x or y

singlet, S



External and Internal Magnetic Fields

An **external magnetic fields** cannot be responsible for the singlet-triplet transition, because it would act equally on both spins.

Available Internal Magnetic Fields

ORBITAL
COUPLING

ELECTRON OR
NUCLEAR
SPIN COUPLING

ZEEMAN
COUPLING

LATTICE
COUPLING

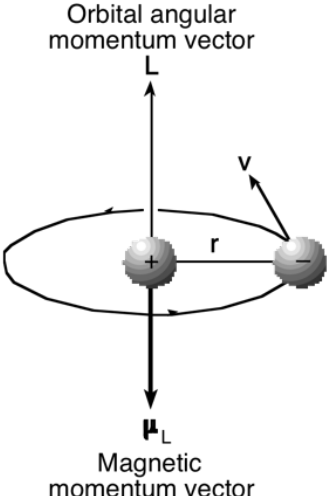
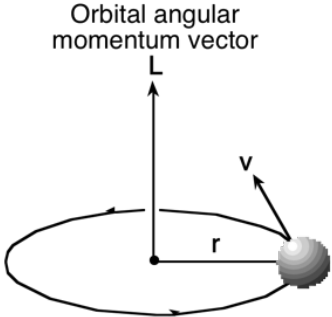
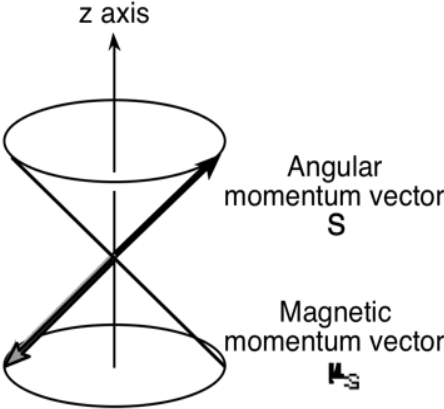
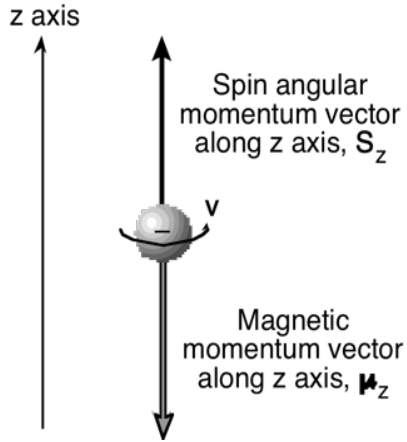
PHOTON
COUPLING

Angular momentum

Magnetic moment

spin

orbital



Precession and Spin-Orbit coupling

Besides an external magnetic field another source of coupling is the **spin-orbit coupling**: if L is coupled to S , they both precess around their resultant. The rate of precession about an axis is proportional to the strength of the coupling of the spin to the new magnetic field.

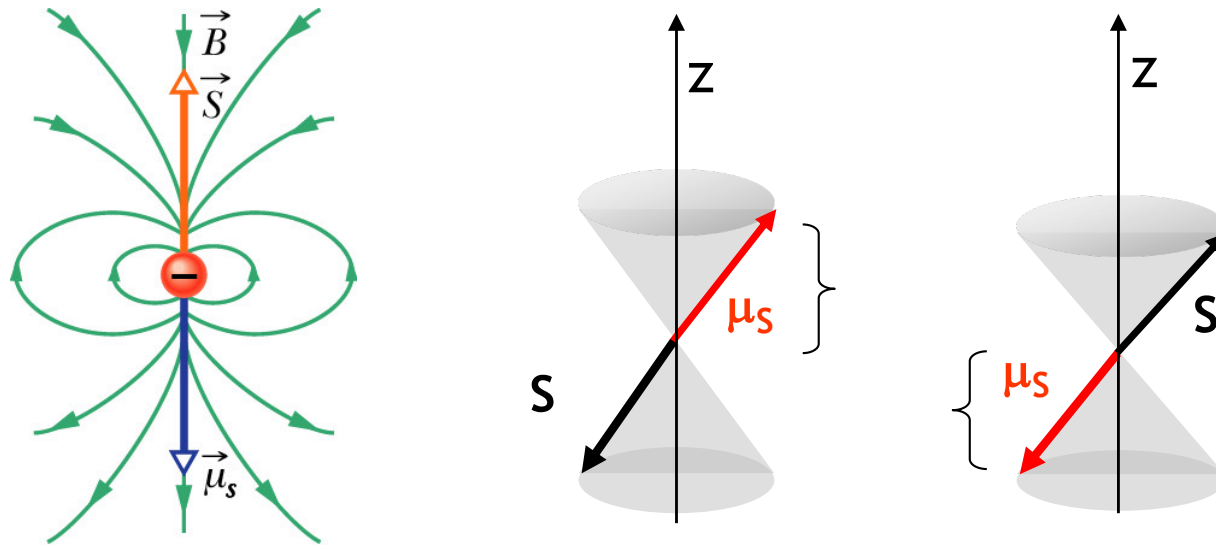
When L and S are strongly coupled it is difficult for other forces to break the coupling

The power of the magnetic field generated is proportional to the rate of precession.

More on Spin-Orbit Coupling

- The strength or energy (E_{SO}) of spin-orbit coupling is directly proportional to the magnitude of the magnetic moment due to electron orbital motion, μ_L (a variable quantity depending on the orbit), and the electron spin, μ_S (a fixed quantity).
- Spin-orbit coupling in organic molecules will be effective in inducing transitions between different spin states if one (or both) of the electrons involved approaches a “heavy” atom nucleus that is capable of causing the electron to accelerate and thereby create a strong magnetic moment as the result of its orbital motion for a one electron atom, $\zeta_{SO} \sim Z^4$).
- For maximum effect of the nuclear charge, the electron must be in an orbital that approaches the nucleus closely, i.e., an orbital with some s-character, since s-orbitals have a finite probability of being located near or even in the nucleus!

Magnetic moment due to spin

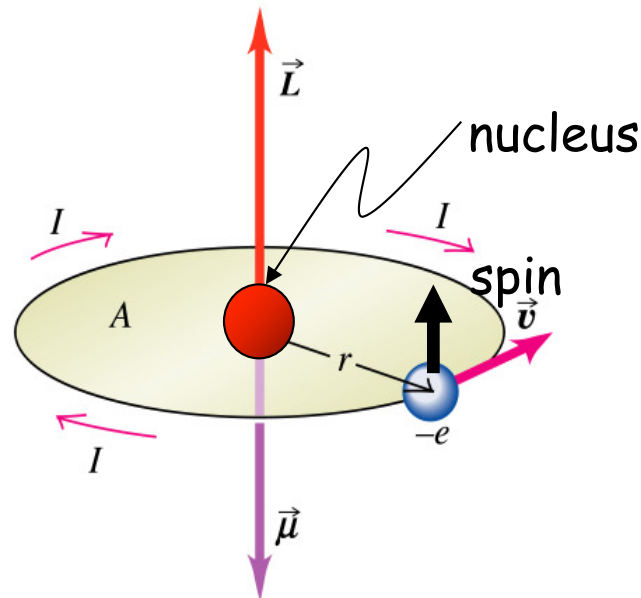


The electron possesses a **spin magnetic** moment due to its charge and spin. The magnetic moment μ_s is quantized in magnitude and orientation as the angular momentum \mathbf{S} from which it arises

Magnetic moment of an orbiting electron

An electron in a Bohr atom is modeled as a point charge rotating about a fixed axis centered in the nucleus. Then it possesses an **orbital** magnetic moment:

$$\mu_L = -(e/2m) \mathbf{L}$$



Spin-Orbit Coupling and Heavy Atom Effect

Field at a molecular level is generated from the *orbital motion* of the electron around the nucleus.

$$\hat{H}_{SO} = \zeta \mathbf{l} \cdot \mathbf{s}$$

$$\zeta_{n,l} \propto \frac{Z^4}{n^3 l(l + 1/2)(l + 1)}$$

The Spin-Orbit coupling constant depends on the fourth power of the atomic number and its effect is very large for heavy atoms.

Spin-orbit coupling energies for selected atoms

Table 4.7 Spin-Orbit Coupling in Atoms^{a,b}

Atom	Atomic number	ζ (kcal mol ⁻¹)	Atom	Atomic number	ζ (kcal mol ⁻¹)
C ^c	6	0.1	I	53	14.0
N ^c	7	0.2	Kr	36	15
O ^c	8	0.4	Xe	54	28
F ^c	9	0.7	Pb	82	21
Si ^c	14	0.4	Hg	80	18
P ^c	15	0.7	Na	11	0.1
S ^c	16	1.0	K	19	0.2
Cl ^c	17	1.7	Rb	37	1.0
Br	35	7.0	Cs	55	2.4

Spin-orbit coupling parameter is related to atomic number

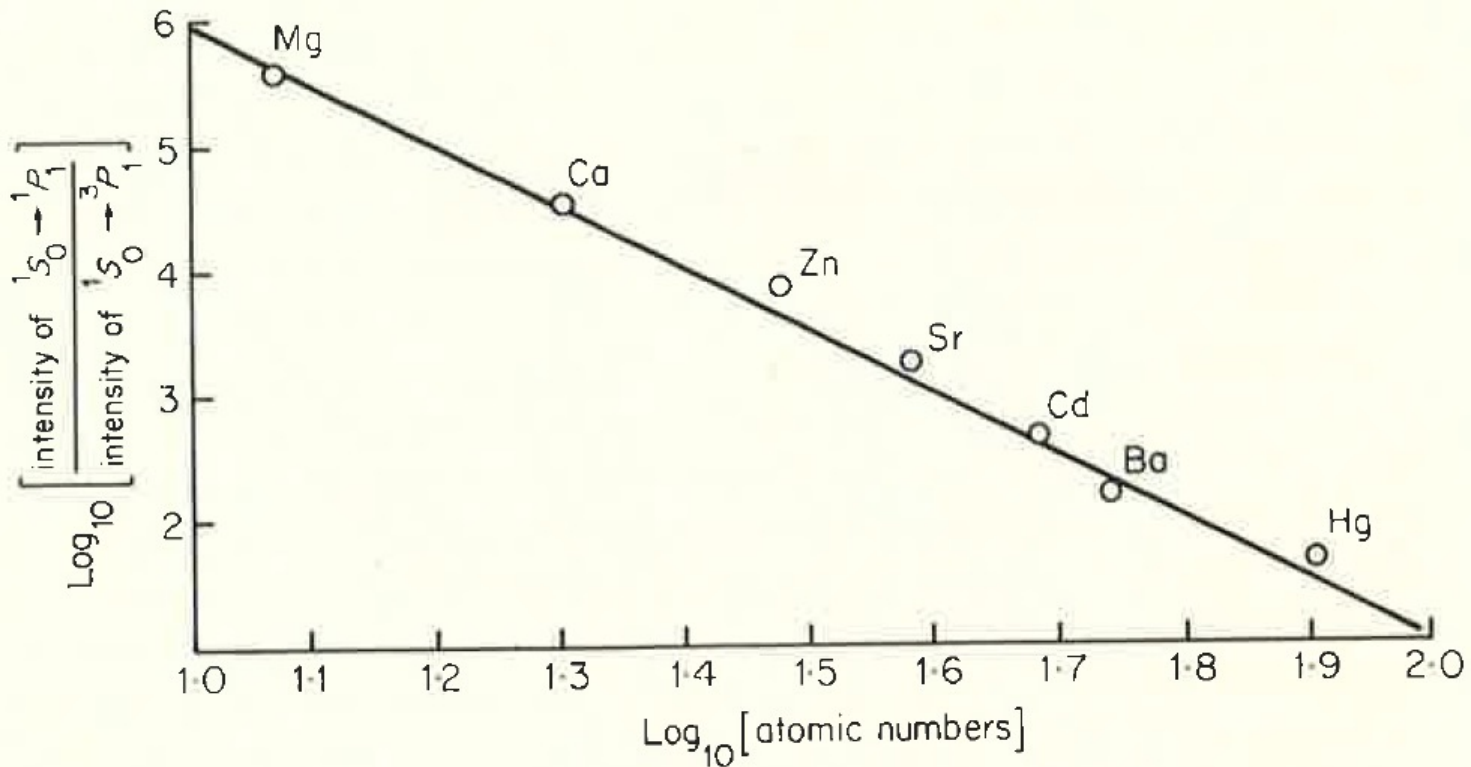


Figure 2.3 A log-log plot illustrating the effect of atomic number on the intensity of a spin-forbidden transition. (From R. M. Hochstrasser, *Behaviour of Electrons in Atoms*, W. A. Benjamin, N.Y., 1964, p. 103.)

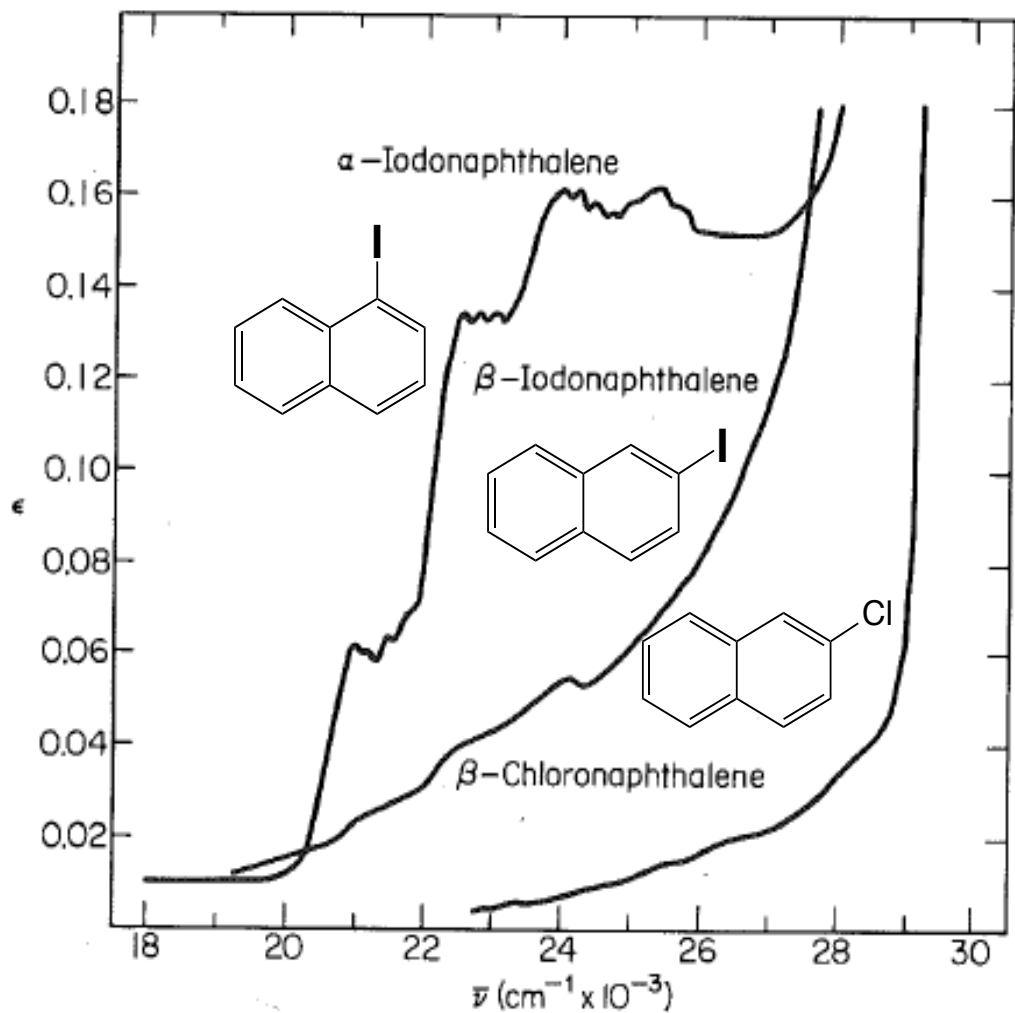
The heavy atom effect on spin transitions

The “heavy atom” effect is an “atomic number” effect that is related to the coupling of the electron spin and electron orbital motions (spin-orbit coupling, SOC).

Most commonly, the HAE refers to the rate enhancement of a spin forbidden photophysical radiative or radiationless transition that is due to the presence of an atom of high atomic number, Z .

The heavy atom may be either internal to a molecule (molecular) or external (supramolecular).

Internal Heavy Atom Effect: Spin forbidden absorption



THE JOURNAL OF CHEMICAL PHYSICS VOLUME 17, NUMBER 10 OCTOBER, 1949

Triplet-Singlet Transitions in Organic Molecules. Lifetime Measurements of the Triplet State*

DONALD S. McCLURE
Department of Chemistry, University of California, Berkeley, California
(Received December 20, 1948)

THE JOURNAL OF CHEMICAL PHYSICS VOLUME 17, NUMBER 12 DECEMBER, 1949

Effects of Perturbations on Phosphorescence: Luminescence of Metal Organic Complexes

PHILIP YUSTER* AND S. I. WEISSMAN
Department of Chemistry, Washington University, Saint Louis, Missouri
(Received February 16, 1949)

THE JOURNAL OF CHEMICAL PHYSICS VOLUME 20, NUMBER 1 JANUARY, 1952

Collisional Perturbation of Spin-Orbital Coupling and the Mechanism of Fluorescence Quenching. A Visual Demonstration of the Perturbation*

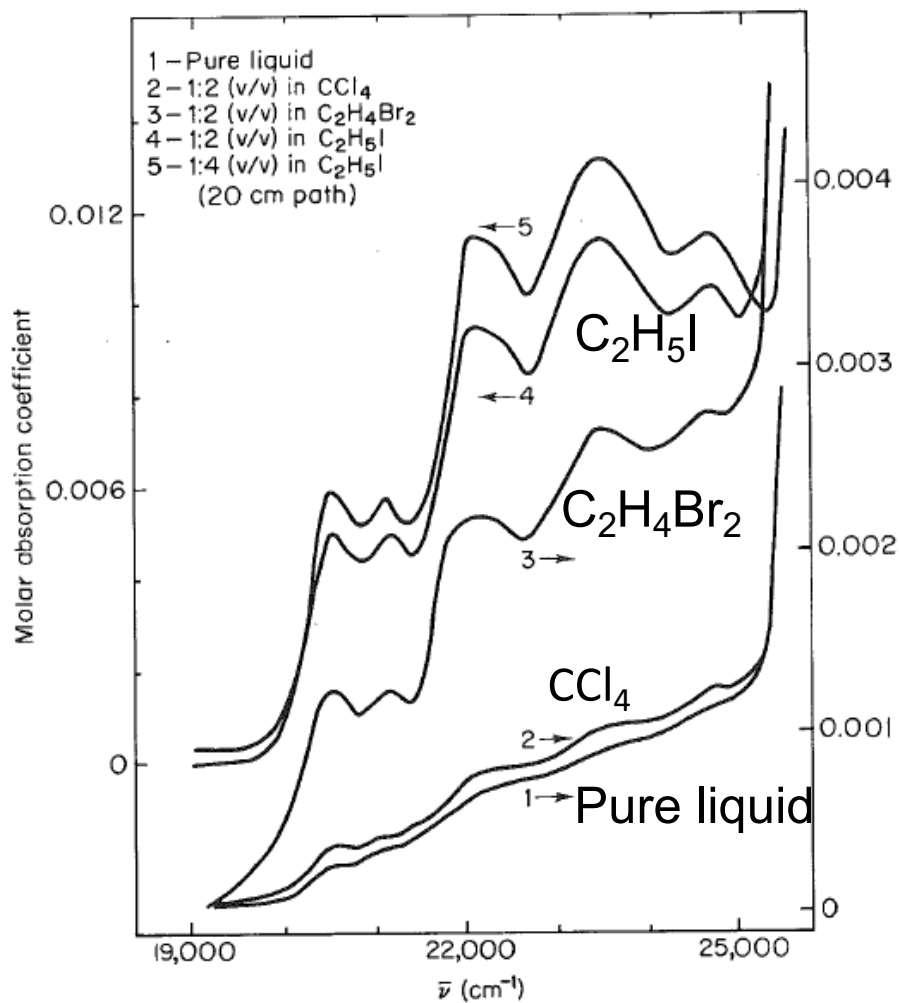
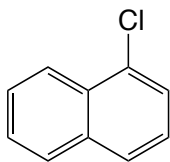
MICHAEL KASHA†
Department of Chemistry, University of Manchester, England
(Received August 13, 1951)

THE JOURNAL OF CHEMICAL PHYSICS VOLUME 22, NUMBER 2 FEBRUARY, 1954

Singlet-Triplet Absorption Bands in Some Halogen Substituted Aromatic Compounds*†

DONALD S. McCLURE, NORMAN W. BLAKE,‡ AND PHILIP L. HANST§
Department of Chemistry and Chemical Engineering, University of California, Berkeley, California
(Received August 13, 1953)

External Heavy Atom Effect: Spin forbidden absorption



THE JOURNAL OF CHEMICAL PHYSICS VOLUME 37, NUMBER 8 OCTOBER 15, 1962

External Heavy-Atom Spin-Orbital Coupling Effect. I. The Nature of the Interaction*

S. P. McGLYNN, R. SUNSERI, AND N. CHRISTODOULEAS

Coates Chemical Laboratories, Louisiana State University, Baton Rouge 3, Louisiana

THE JOURNAL OF CHEMICAL PHYSICS VOLUME 40, NUMBER 2 15 JANUARY 1964

External Heavy-Atom Spin-Orbital Coupling Effect. V. Absorption Studies of Triplet States*

S. P. McGLYNN AND T. AZUMI

Coates Chemical Laboratories, Louisiana State University, Baton Rouge, Louisiana 70803

AND

M. KASHA

Department of Chemistry and Institute of Molecular Biophysics, The Florida State University, Tallahassee, Florida 32301

(Received 16 September 1963)

Heavy-Atom-Induced Phosphorescence of Aromatics and Olefins Included within Zeolites

V. Ramamurthy,* J. V. Caspar, D. F. Eaton, Erica W. Kuo, and D. R. Corbin

Contribution No. 6068 from Central Research and Development, Experimental Station, The Du Pont Company, Wilmington, Delaware 19880-0328. Received December 2, 1991

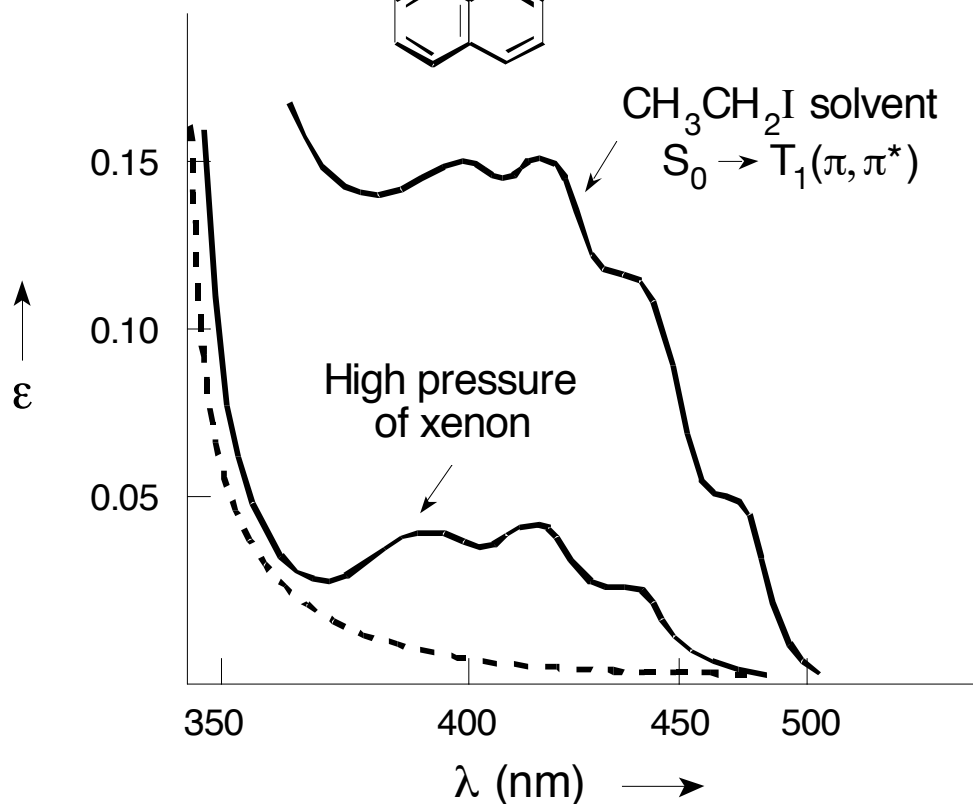
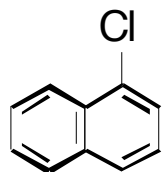
J. Am. Chem. Soc. **1992**, *114*, 3882-3892

External Heavy Atom Effect: Spin forbidden absorption

THE JOURNAL OF CHEMICAL PHYSICS VOLUME 20, NUMBER 1 JANUARY, 1952

Collisional Perturbation of Spin-Orbital Coupling and the Mechanism of Fluorescence Quenching. A Visual Demonstration of the Perturbation*

MICHAEL KASHA†
Department of Chemistry, University of Manchester, England
(Received August 13, 1951)



Phosphorescence Lifetime of Benzene. An Intermolecular Heavy-Atom Effect, a Deuterium Effect, and a Temperature Effect*

M. R. WRIGHT, R. P. FROSC, AND G. W. ROBINSON

Gates and Crellin Laboratories of Chemistry,†
California Institute of Technology, Pasadena, California

(Received June 20, 1960)

J. Chem. Phys. **33**, 934 (1960);

Enhancement of the singlet-triplet absorption band of α -chloronaphthalene in the presence of xenon under high pressure

ANNA GRABOWSKA

Institute of Physical Chemistry, Polish Academy of Sciences,
ul. Pasteura 1, Warszawa 22, Poland

Spectrochimica Acta, 1963, Vol. 19, pp. 307 to 313.

J. Am. Chem. Soc. **1994**, 116, 1345-1351

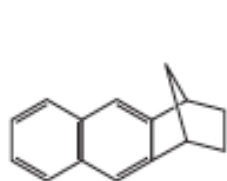
Organic Guests within Zeolites: Xenon as a Photophysical Probe†

V. Ramamurthy

Influence of Heavy Atom Effect on ISC and phosphorescence

Molecule	k_F^0	k_{ST}	k_P^0	k_{TS}	Φ_F	Φ_P
Naphthalene	10^6	10^6	10^{-1}	10^{-1}	0.55	0.05
1-Fluoronaphthalene	10^6	10^6	10^{-1}	10^{-1}	0.84	0.06
1-Chloronaphthalene	10^6	10^8	10	10	0.06	0.54
1-Bromonaphthalene	10^6	10^9	50	50	0.002	0.55
1-Iodonaphthalene	10^6	10^{10}	500	100	0.000	0.70

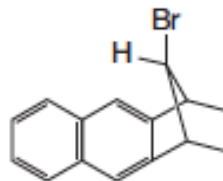
F. Wilkinson in Organic molecular physics, J. B. Birks (ed.), Wiley, 1975. p. 126



10

$$k_{ST} = 2 \times 10^6 \text{ s}^{-1}$$

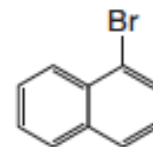
$$k_{TS} = 2 \times 10^{-1} \text{ s}^{-1}$$



11

$$k_{ST} = 300 \times 10^6 \text{ s}^{-1}$$

$$k_{TS} = 40 \times 10^{-1} \text{ s}^{-1}$$



12

$$k_{ST} = 500 \times 10^6 \text{ s}^{-1}$$

$$k_{TS} = 600 \times 10^{-1} \text{ s}^{-1}$$

TABLE 7.2
Spectroscopic Data on Group IV Tetraphenyls^a

Molecule	Fluorescence band maximum (Å)	Phosphorescence band maxima (Å)	Φ_P/Φ_F	τ_P (sec) ^b	τ_P (sec) ^c	ζ_{np}^2 (cm ⁻¹) ² ^d	$\sum_K \zeta_K^2$ (cm ⁻¹) ² ^e	τ_P (sec) ^f	k_{ISC} (sec ⁻¹) ^g
C(C ₆ H ₅) ₄	3200	4500, 4700, 5100	≤ 0.1	2.9	—	7.84 × 10 ²	5.49 × 10 ³	≡ 2.9	10 ⁶ –10 ⁷
Si(C ₆ H ₅) ₄	3100	4300, 4600	0.1	1.1	—	2.02 × 10 ⁴	2.49 × 10 ⁴	0.66	10 ⁸
Ge(C ₆ H ₅) ₄	3200	4500, 4700, 5100	1	0.055	0.003	7.74 × 10 ⁵	7.79 × 10 ⁵	0.021	10 ⁹
Sn(C ₆ H ₅) ₄	3200	4500, 4700	10	0.003	0.0006	4.39 × 10 ⁵	4.39 × 10 ⁶	0.0038	10 ¹¹
Pb(C ₆ H ₅) ₄	—	4250, 4550	≫ 10	(0.0008)	0.00008	5.32 × 10 ⁷	5.32 × 10 ⁷	0.00031	—

^a All data refer to glassy solutions at 77°K; the experimental data are taken from LaPaglia (11).

^b Phosphorescence emission data.

^c Calculated from $T_1 \leftarrow S_0$ absorption data.

^d Spinorbit coupling factors squared for the np^2 configurations of C(I), Si(I), Ge(I), Sn(I), and Pb(I), respectively.

^e Sum of squares of spinorbit coupling factors, ζ_{np}^2 , over all atoms in the molecule.

^f Calculated from the equation $\tau_P^0 = \tau_P^0[\text{C}(\text{C}_6\text{H}_5)_4] \zeta_C^2 / \zeta_K^2$, with $\tau_P^0[\text{C}(\text{C}_6\text{H}_5)_4] \equiv 2.9$ sec (K here refers to C, Si, Ge, Sn, and Pb).

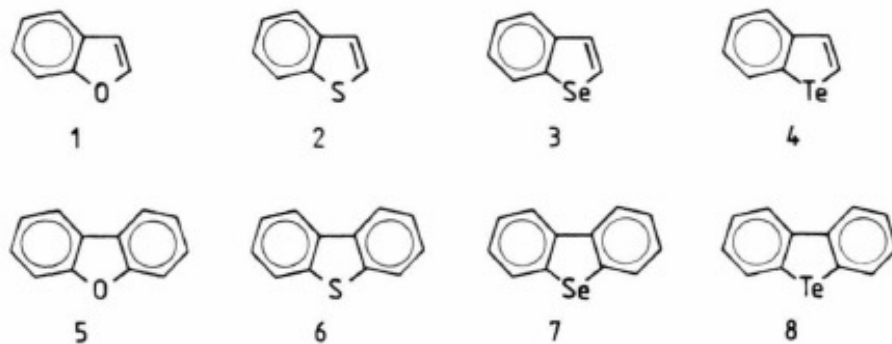
^g Obtained using Eq. 7.15 and the approximation $k_{QP} \sim 0$ (which is known to be wrong).

TABLE 7.3

Spectroscopic Data on Naphthalene Derivatives^a

Molecule	$F_{0,0}$ (cm^{-1})	$P_{0,0}$ (cm^{-1})	Φ_F	Φ_P	Φ_P/Φ_F (approx.)	τ_P (sec)	k_{ISC} (sec^{-1})	k_F (sec^{-1})
Naphthalene	31750	21250	0.55	0.051 ± 0.003	0.093	2.3 ± 0.1	$\sim 10^5$	$\sim 10^6$
1-Methylnaphthalene	31450	21000	0.85 ± 0.19	0.044 ± 0.013	0.053	2.1 ± 0.1	$\sim 2 \times 10^5$	$\sim 3 \times 10^6$
1-Hydroxynaphthalene	30775	20600	0.76 ± 0.04	0.036 ± 0.004	0.047	1.9	$\sim 2 \times 10^5$	$\sim 3 \times 10^6$
1-Fluoronaphthalene	31600	21150	0.84 ± 0.08	0.056 ± 0.009	0.068	1.5	$\sim 2 \times 10^5$	$\sim 3 \times 10^6$
1-Chloronaphthalene	31360	20700	0.058 ± 0.005	0.30 ± 0.06	5.2	0.29 ± 0.01	$\sim 1.5 \times 10^7$	$\sim 3 \times 10^6$
1-Bromonaphthalene	31280	20650	0.0016 ± 0.0005	0.27 ± 0.04	164	2.0×10^{-2}	$\sim 5 \times 10^8$	$\sim 3 \times 10^6$
1-Iodonaphthalene	—	20500	<0.0005	0.38 ± 0.06	>1000	2.0×10^{-3}	$>3 \times 10^9$	$\sim 3 \times 10^6$

^a All data refer to glassy solutions at 77°K; these data are taken from Ermolaev and Svitashv (22, 23) and Ermolaev, Kotlyar, and Svitashv (24).



Non-Radiative decay from T₁

Radiative decay from T₁

Table 1. Fluorescence 0–0 band ($\tilde{\nu}_f$), phosphorescence 0–0 band ($\tilde{\nu}_p$), fluorescence quantum yield (Φ_f), phosphorescence quantum yield (Φ_p), phosphorescence lifetime (τ_p), quantum yield (Φ_T) of triplet formation, rate constant of the radiative (k_{pT}) and non-radiative (k_{GT}) T₁ → S₀ transition (ethanol, 77 K).

Compound		$\tilde{\nu}_f$ [cm ⁻¹]	$\tilde{\nu}_p^a$ [cm ⁻¹]	Φ_f	Φ_p	τ_p [sec]	Φ_T	k_{pT} [sec ⁻¹]	k_{GT} [sec ⁻¹]
Benzo[b]furan	(1)	33 110	25 130 (25 157)	0.63	0.24	2.35	0.37	0.28	0.15
Benzo[b]thiophene	(2)	32 895	24 040 (24 010)	0.02	0.42	0.32	0.98	1.34	1.79
Benzo[b]selenophene	(3)	32 360	23 585 (23 585)	$5 \cdot 10^{-4}$	0.27	$7 \cdot 10^{-3}$	≈ 1	38.6	104
Benzo[b]tellurophene	(4)	–	22 730 (22 573)	$< 5 \cdot 10^{-4}$	0.18	$6 \cdot 10^{-4}$	≈ 1	300	1370
Dibenzo[b, d]furan	(5)	33 110	24 450 (24 510)	0.40	0.29	5.6	0.60	0.086	0.092
Dibenzo[b, d]thiophene	(6)	30 395	24 330 (24 272)	0.025	0.47	1.5	0.97	0.32	0.35
Dibenzo[b, d]selenophene	(7)	29 670	23 980 (23 866)	$1 \cdot 10^{-3}$	0.74	0.04	≈ 1	18.5	6.5
Dibenzo[b, d]tellurophene	(8)	–	23 530 (23 585)	$< 5 \cdot 10^{-4}$	0.79	$2.5 \cdot 10^{-3}$	≈ 1	316	84

^a Figures in brackets: phosphorescence 0–0 band in n-pentane, 77 K.

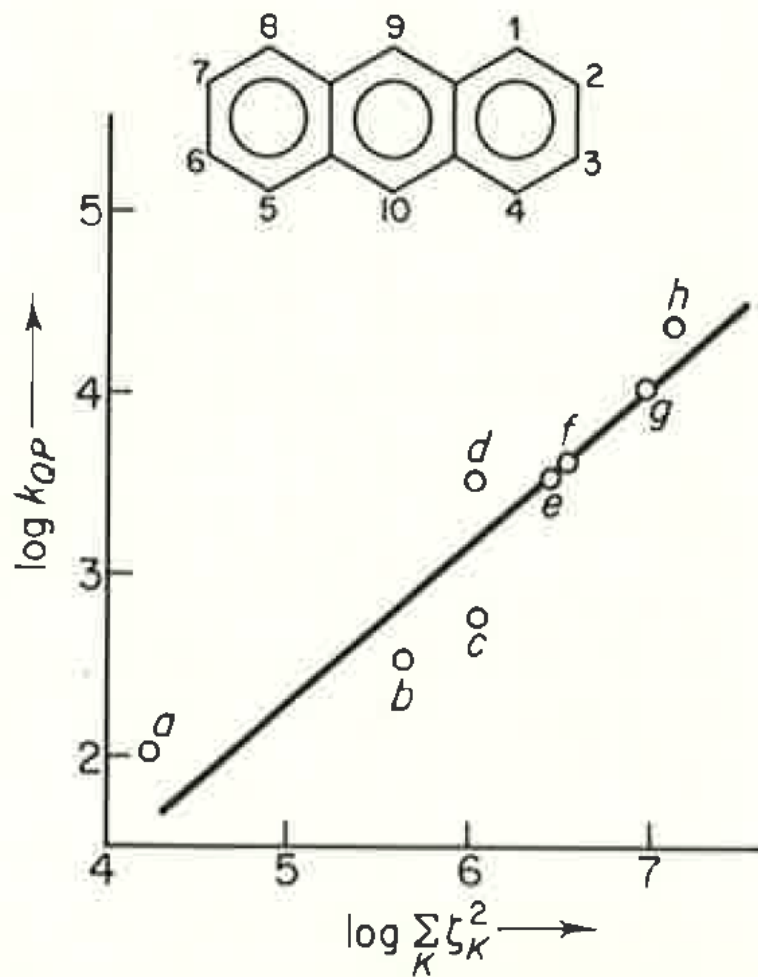


Fig. 7.2 Plot of k_{QP} (in sec^{-1}) versus $\sum_K \zeta_K^2$ (in cm^{-2}), the summation being over all halogen centers. The data plotted are for the following molecules: (a) anthracene; (b) 1-chloroanthracene; (c) 1,5-dichloroanthracene; (d) 9,10-dichloroanthracene; (e) 2,9,10-trichloroanthracene; (f) 1,5,9,10-tetrachloroanthracene; (g) 9-bromoanthracene; (h) 9,10-dibromoanthracene. The slope of the log-log plot is approximately 45° .

Intersystem crossing
in carbonyl compounds and others with $n\pi^*$)

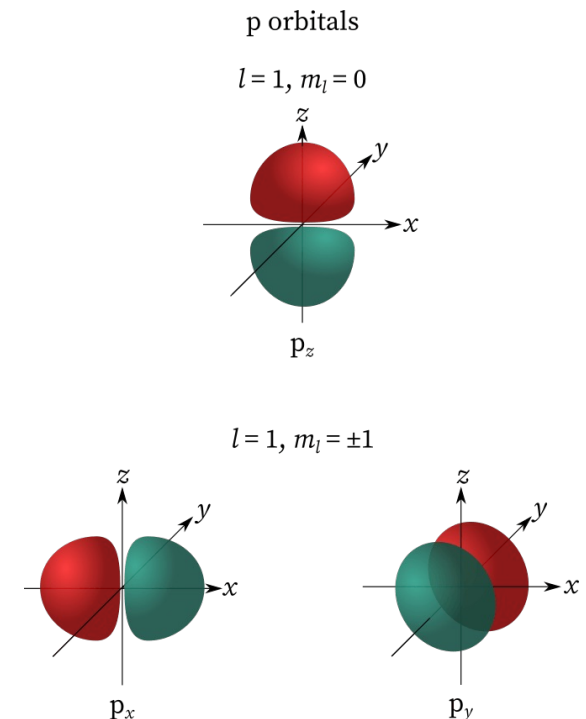
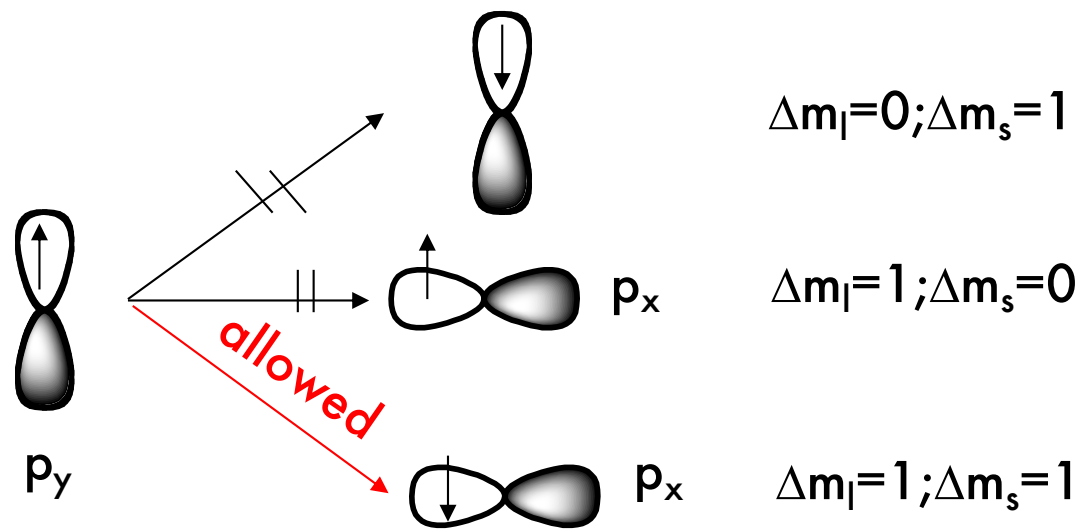
Conservation of energy and angular momentum (spin & orbit coupling)

Spin change will occur at a place where the energies of singlet and triplet are identical. Occurs at curve crossing.

Spin-orbit coupling in organic molecules will be effective in inducing transitions between states of different spin if a “ $p_x \rightarrow p_y$ ” orbital transition *on a single (the same) atom* is involved in the electronic transition. This orbital transition provides both a means of conserving total angular momentum during the transition and also a means of generating orbital angular momentum that can be employed in spin-orbit coupling. This works in the case of $n\pi^*$ state.

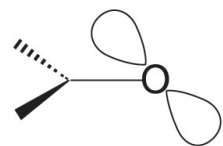
Energy and angular momentum conservation

- The electron spin must either remain unchanged or *change by one unit of angular momentum*, \hbar (say, $+1/2 \hbar \rightarrow -1/2 \hbar$).
- A spin change is exactly compensated by an equal and opposite change of angular momentum which occurs from some other (coupled) interaction with another source of angular momentum.
- In a spin-flip, induced by the spin-orbit interaction, the conservation of angular momentum is guaranteed from the magnetic orbital quantum number m_l .



Breakdown of Born-Oppenheimer Approximation

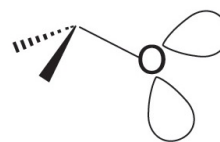
Vibronic mixing enables surface mixing



Strictly planar

$$n_0 = p_0$$

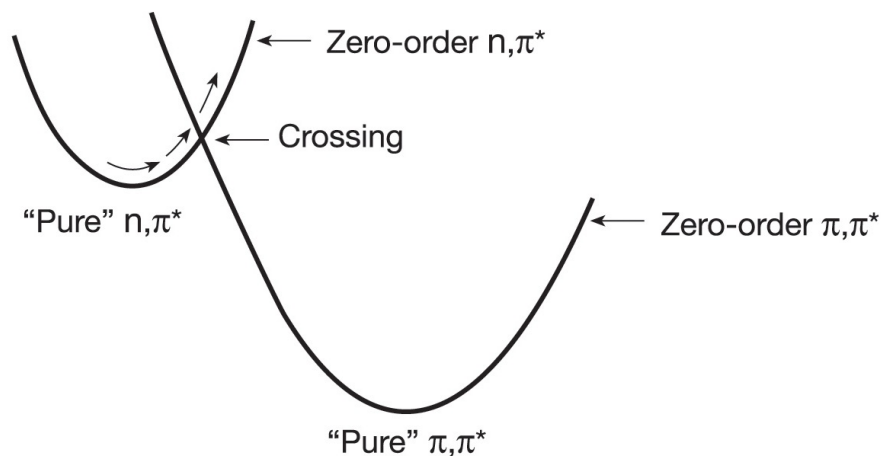
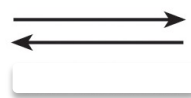
$$\langle n_0 | \pi \rangle = 0$$



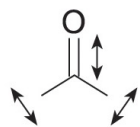
Nonplanar

$$n_0 = sp^n$$

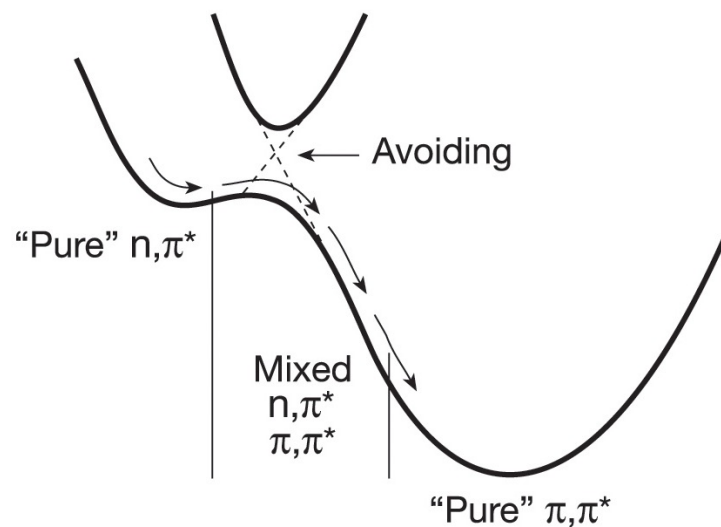
$$\langle n_0 | \pi \rangle \neq 0$$



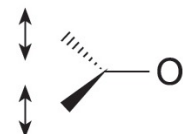
Planar vibrations



Energy is fine, but orbitals don't overlap, remain perpendicular

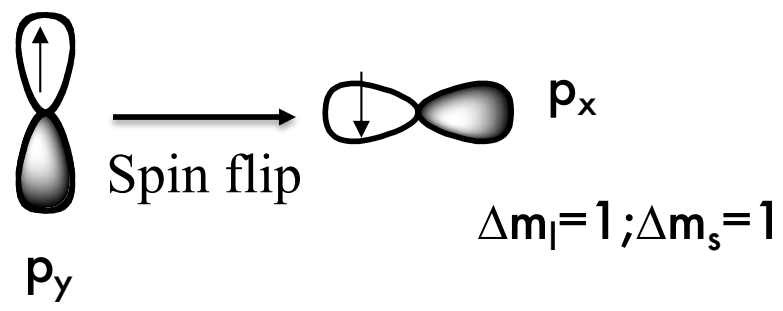
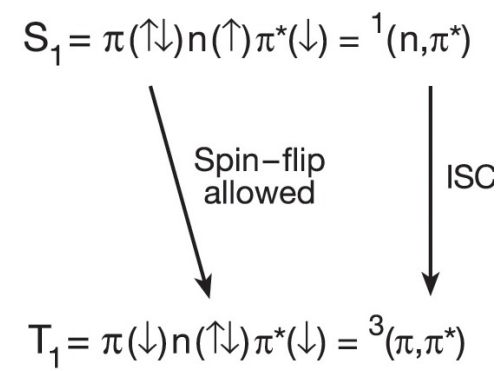
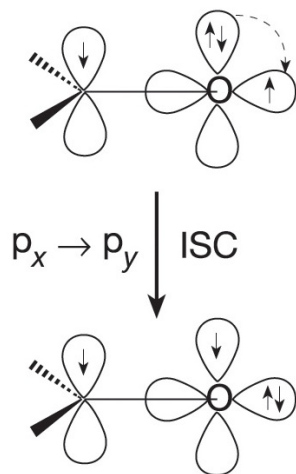
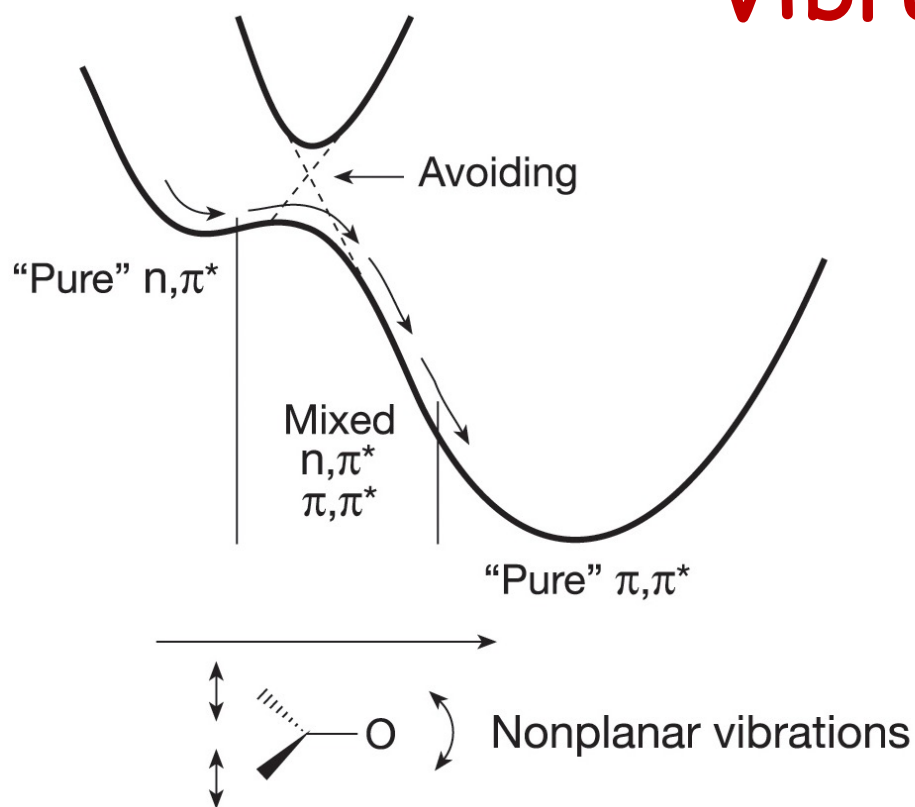


Nonplanar vibrations



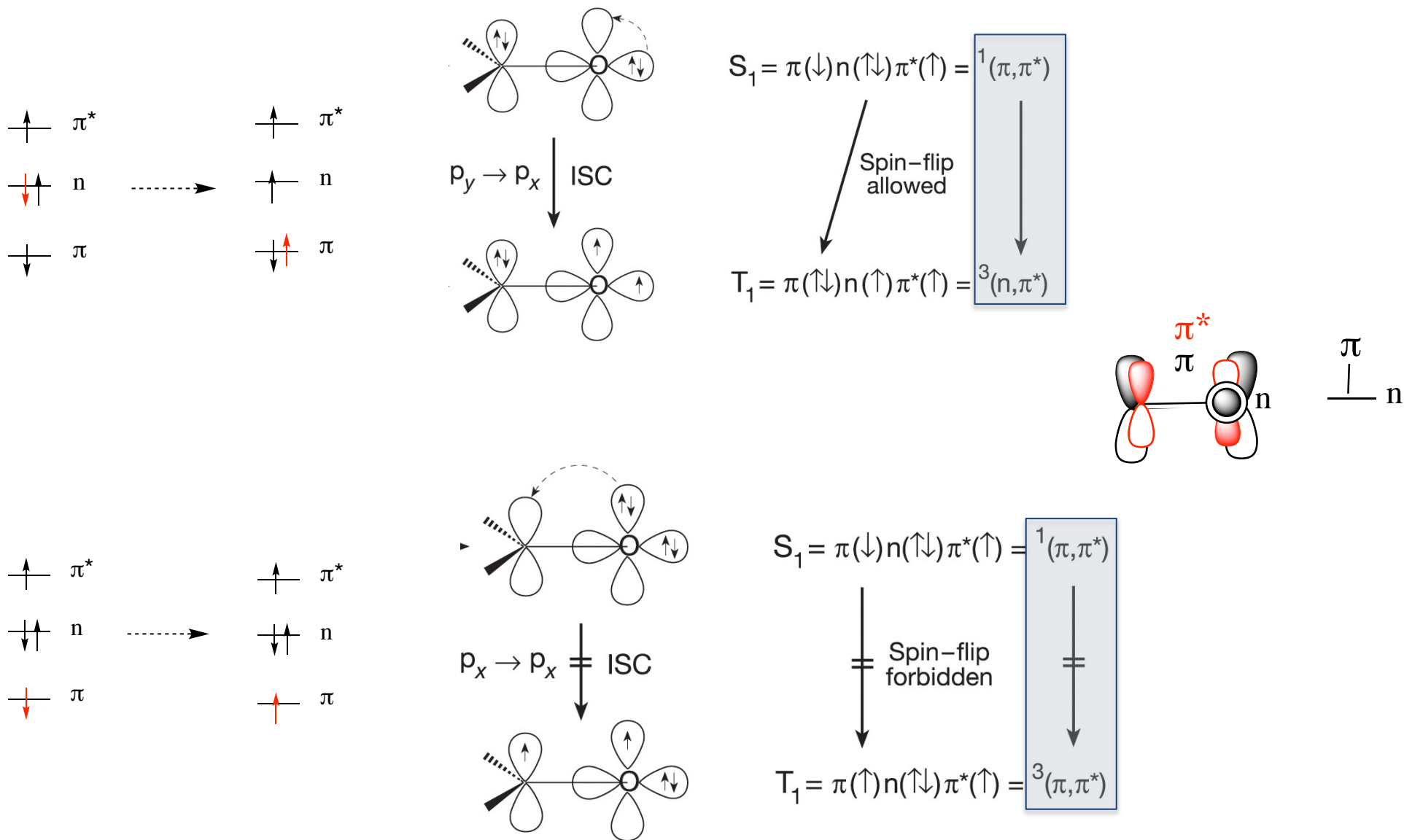
Vibronic mixing enables overlap of n and pi orbitals

Vibration and SO helps ISC

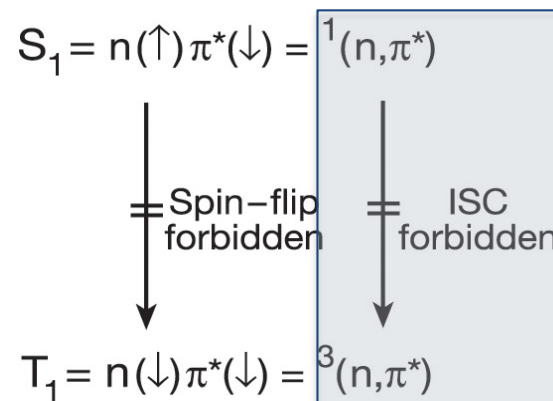
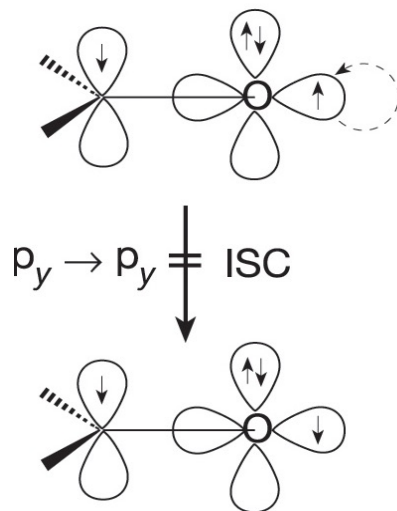
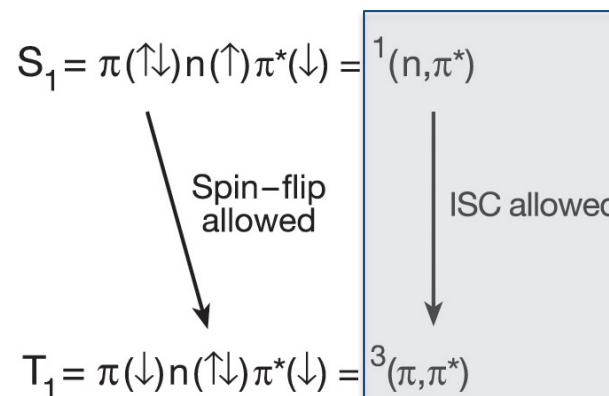
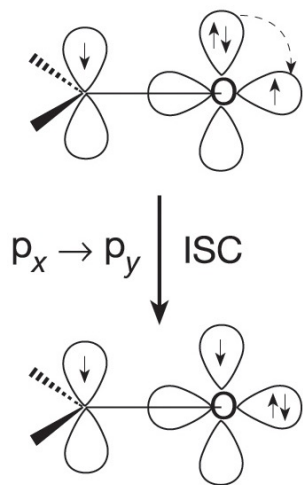
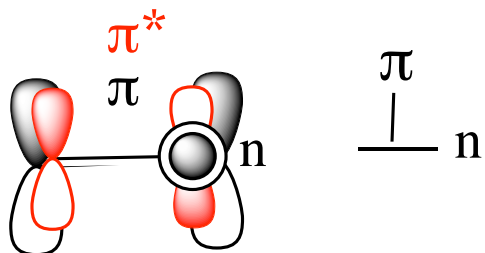


Conservation of spin and orbital angular momentum favors ISC

The Effect of Spin-Orbit Coupling on Intersystem Crossing from $S_1(\pi\pi^*)$ to T_1 in carbonyls



The Effect of Spin-Orbit Coupling on Intersystem Crossing from $S_1(n\pi^*)$ to T_1



El-Sayed's Rule



Intersystem crossing is likely to be very slow unless it involves a change of orbital configuration.

$S_1(n, \pi^*) \rightarrow T_1(n, \pi^*)$ Forbidden

$S_1(n, \pi^*) \rightarrow T_1(\pi, \pi^*)$ Allowed

$S_1(\pi, \pi^*) \rightarrow T_1(n, \pi^*)$ Allowed

$S_1(\pi, \pi^*) \rightarrow T_1(\pi, \pi^*)$ Forbidden

$T_1 \rightarrow S_0$ $T_1(n, \pi^*) \rightarrow S_0(n^2)$ Allowed

Transitions

$T_1(\pi, \pi^*) \rightarrow S_0(\pi^2)$ Forbidden

THE TRIPLET STATE AND MOLECULAR ELECTRONIC PROCESSES
IN ORGANIC MOLECULES

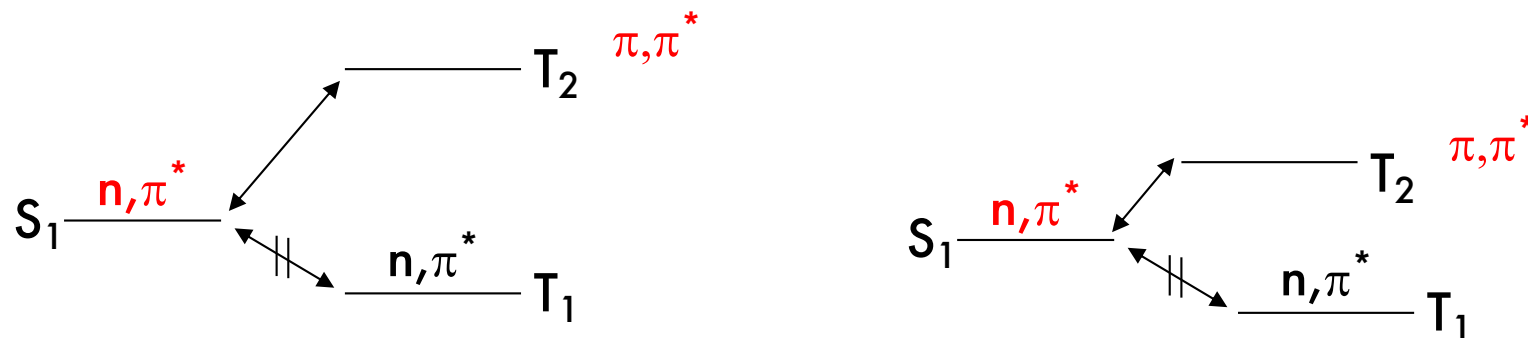
S. K. LOWER¹ AND M. A. EL-SAYED*

Department of Chemistry,² University of California, Los Angeles, California 90024

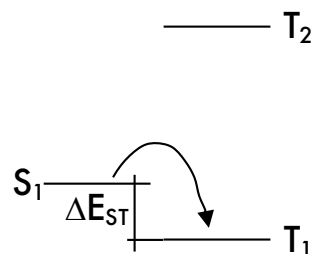
Received June 25, 1965

Chem. Rev., 1966, 66, 199-241

Thus, for ketones with T_1 (n, π^*), the only mechanism to undergo a Singlet-Triplet ISC is going through a T_2 (π, π^*) followed by internal conversion to T_1 (n, π^*)

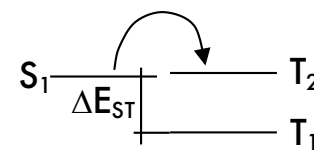
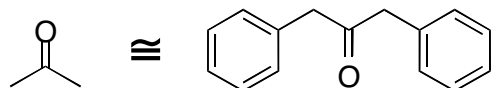


Thus, the ISC crossing rate depends whether or not it is allowed and on the energy gaps involved.



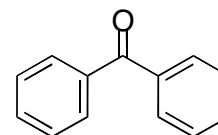
$$k_{ST} = 10^8 \text{ s}^{-1}$$

$$\Delta E_{ST} = 5 \text{ Kcal/mol}$$



$$k_{ST} = 10^{11} \text{ s}^{-1}$$

$$\Delta E_{ST} = 5 \text{ Kcal/mol}$$



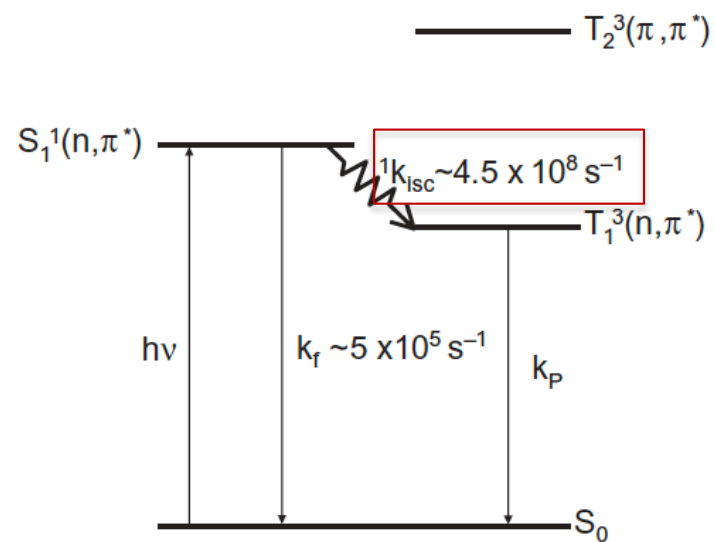


Figure 5.5 State diagram for acetone. Notice that intersystem crossing occurs between (n, π^*) states

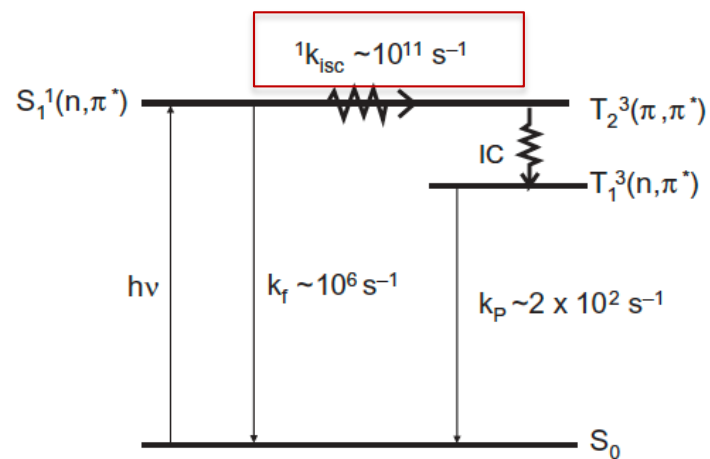
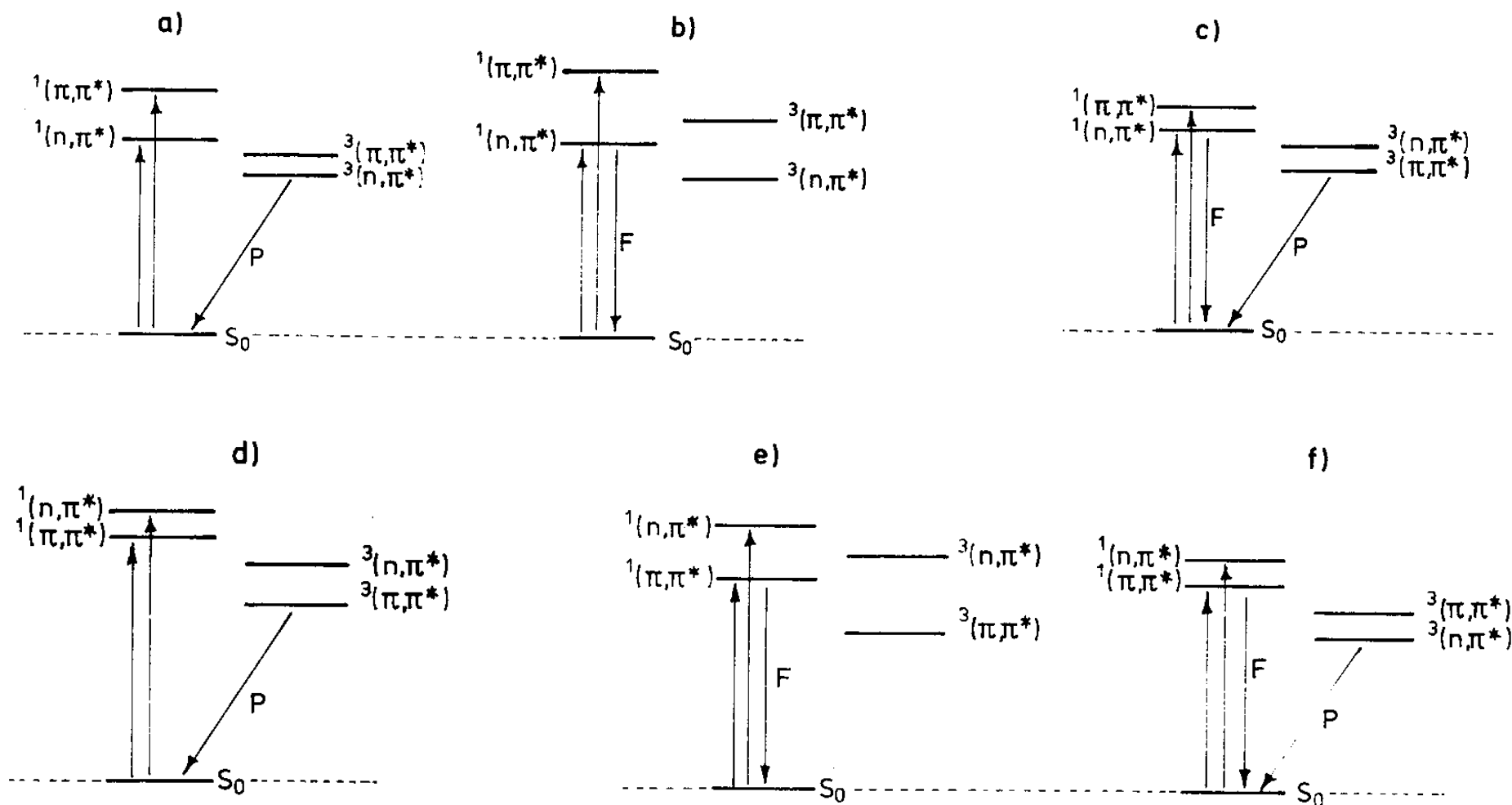


Figure 5.6 State diagram for benzophenone. Here intersystem crossing involves a change in orbital type

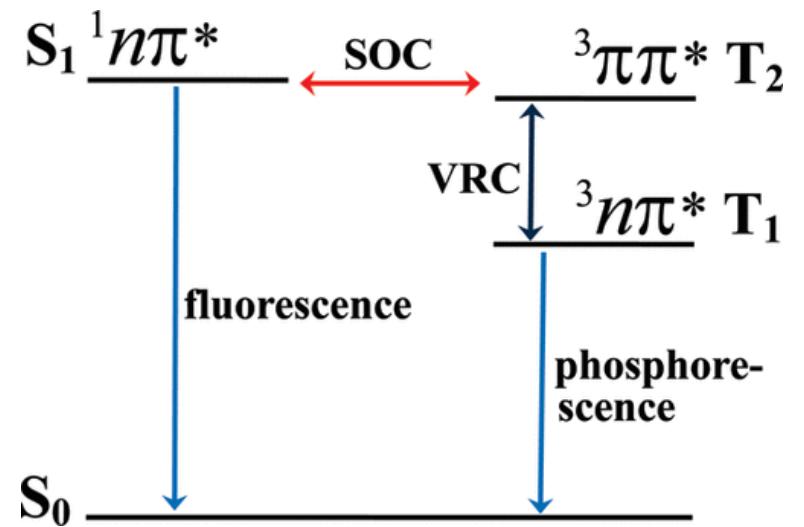
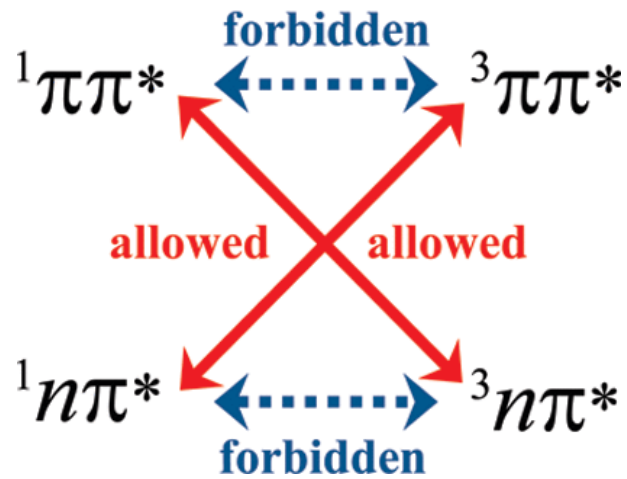
El-Sayed's Rule

Intersystem crossing is likely to be slow unless it involves a change of orbital configuration.

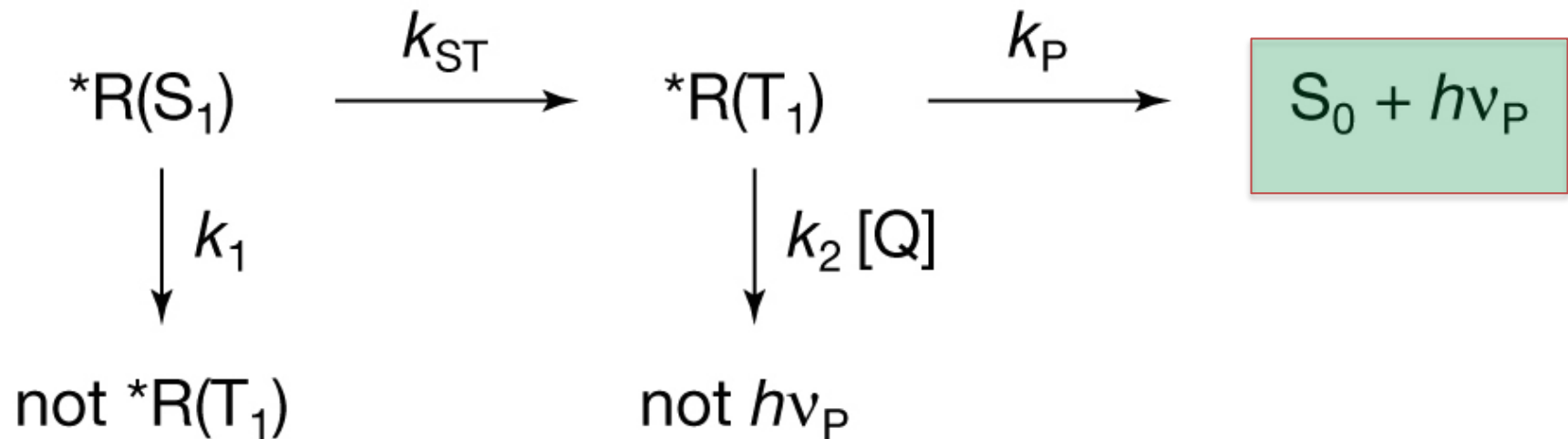
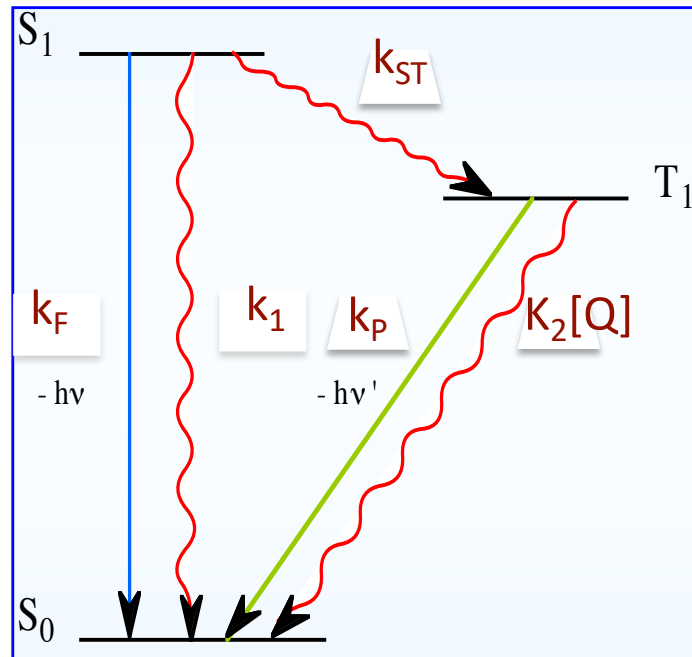


Summary

spin-orbit coupling



Room Temperature Phosphorescence



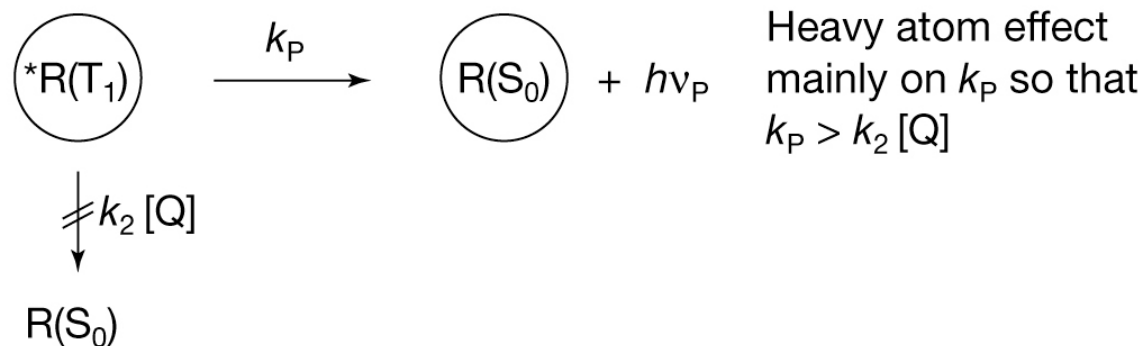
Strategy to record phosphorescence at room temperature through supramolecular approach

Stage 1



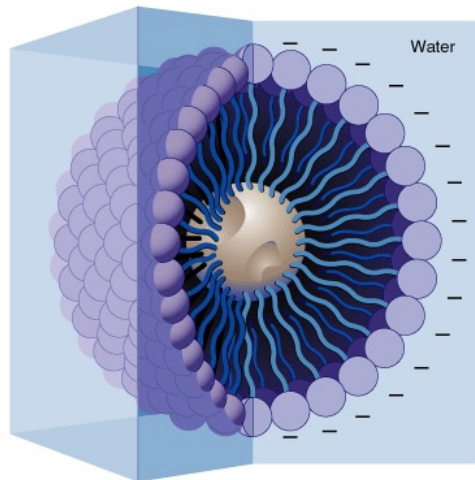
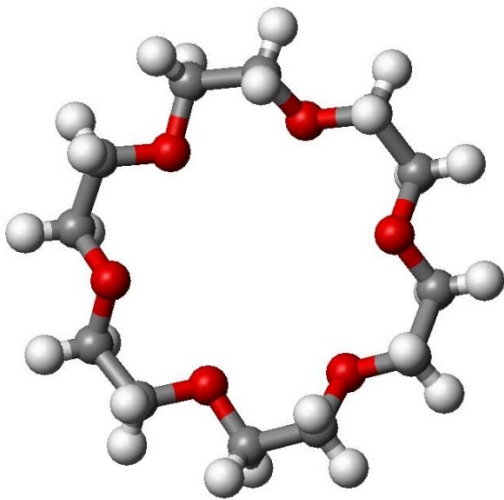
Make more triplets through the heavy atom effect

Stage 2

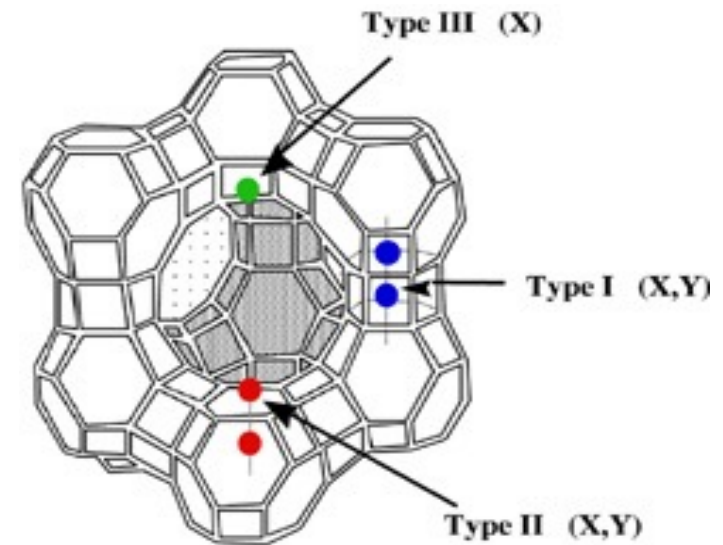


Make triplets emit faster in competition with quenching processes

Crown ethers, micelles and zeolites contain cations

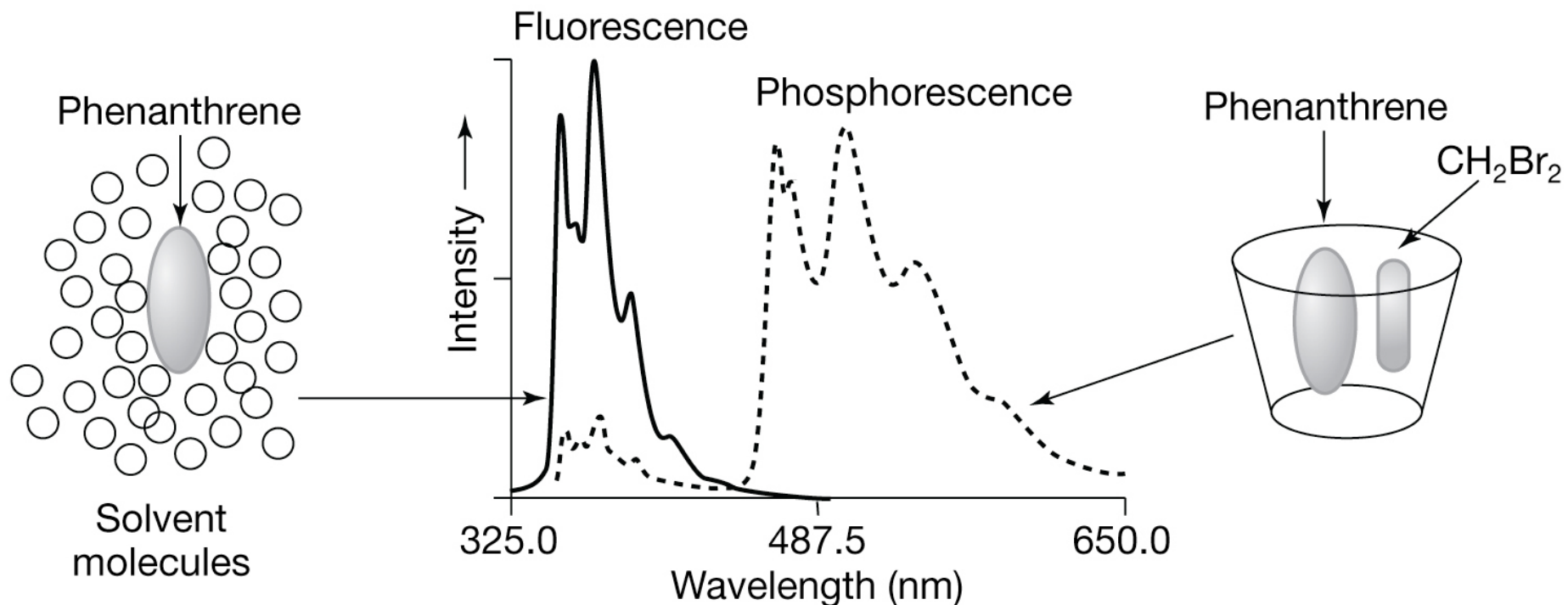


Copyright 1999 John Wiley and Sons, Inc. All rights reserved.



Cyclodextrins as hosts

Phenanthrene@Cyclodextrin: effect of CH_2Br_2 as co-guest



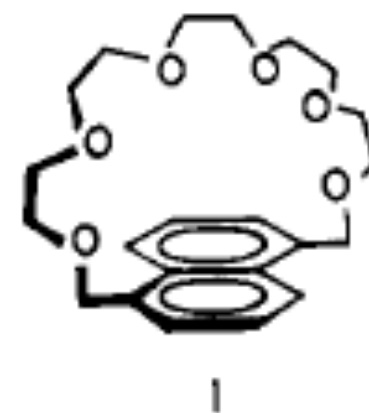
Induced Intersystem Crossing Depends on the SOC: Cations as the heavy atom perturber

Atom	Ionic Radius of the Cation (Å)	Spin-Orbit Coupling ζ cm⁻¹
Li	0.86 (+)	0.23
Na	1.12	11.5
K	1.44	38
Rb	1.58	160
Cs	1.84	370
Tl	1.40	3410
Pb	1.33 (2+)	5089

External heavy atom effect: Crown ether approach

Table II. Estimates^{a,b} of Rate Constants for Excited-State Processes of 1,5-Naphtho-22-crown-6 (**1**) in Alcohol Glass^c at 77 K with Alkali Metal Chloride Salts Added in 5:1 Molar Excess (Crown at $1.00 \times 10^{-4} F$)

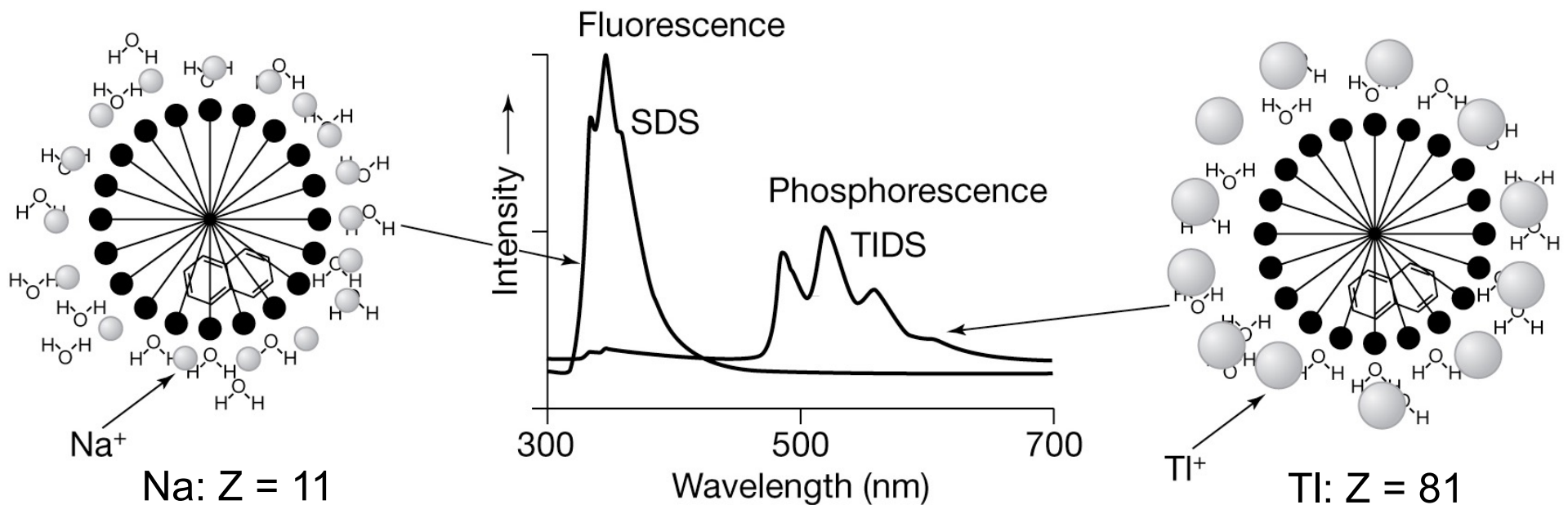
Salt added	$10^{-6}k_f$	$10^{-6}k_{nr}$	$10^2k_p^d$	k_{dt}^d
None	3.1	25	8.7	0.37
NaCl	2.6	32	6.7	0.41
KCl	2.3	35	5.8	0.39
RbCl	1 ^e	52	12.	0.50
CsCl	1 ^e	670	81.	1.57



^a All rate constants in s^{-1} . ^b $k_f = \phi_f \tau_f^{-1}$; $k_{nr} = (1 - \phi_f) \tau_f^{-1}$; $k_p = \phi_p (1 - \phi_f)^{-1} \tau_p^{-1}$; $k_{dt} = \tau_p^{-1} - k_p$. ^c See note 4. ^d With $\phi_f + \phi_{isc} = 1.0$ assumed. ^e Estimated from 77 K UV absorption spectra.

Micelles as hosts

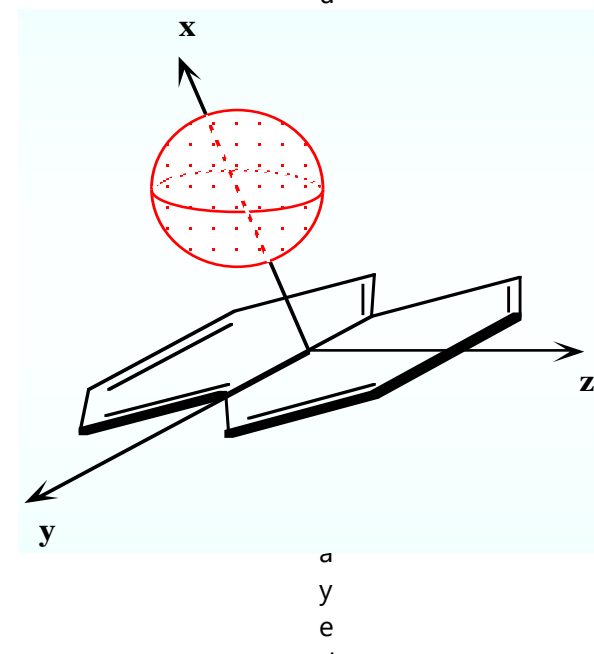
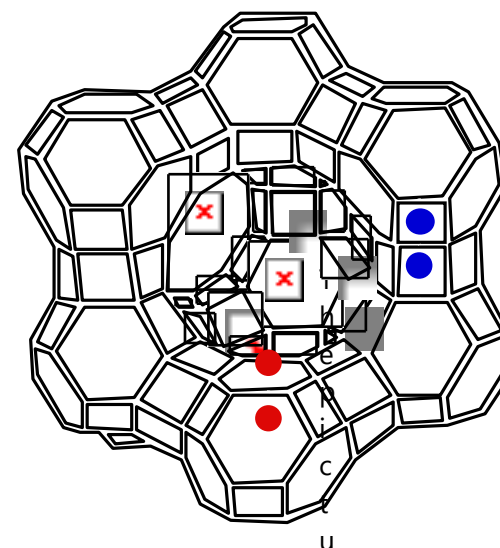
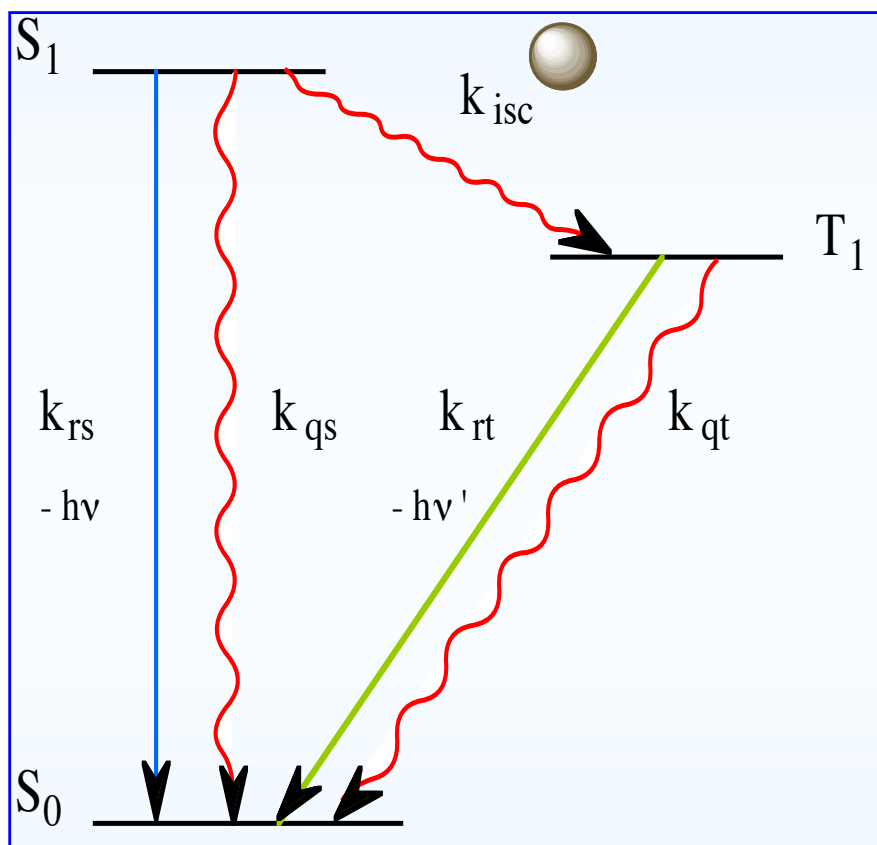
Naphthalene@SDS micelle: effect of heavy atom counterions



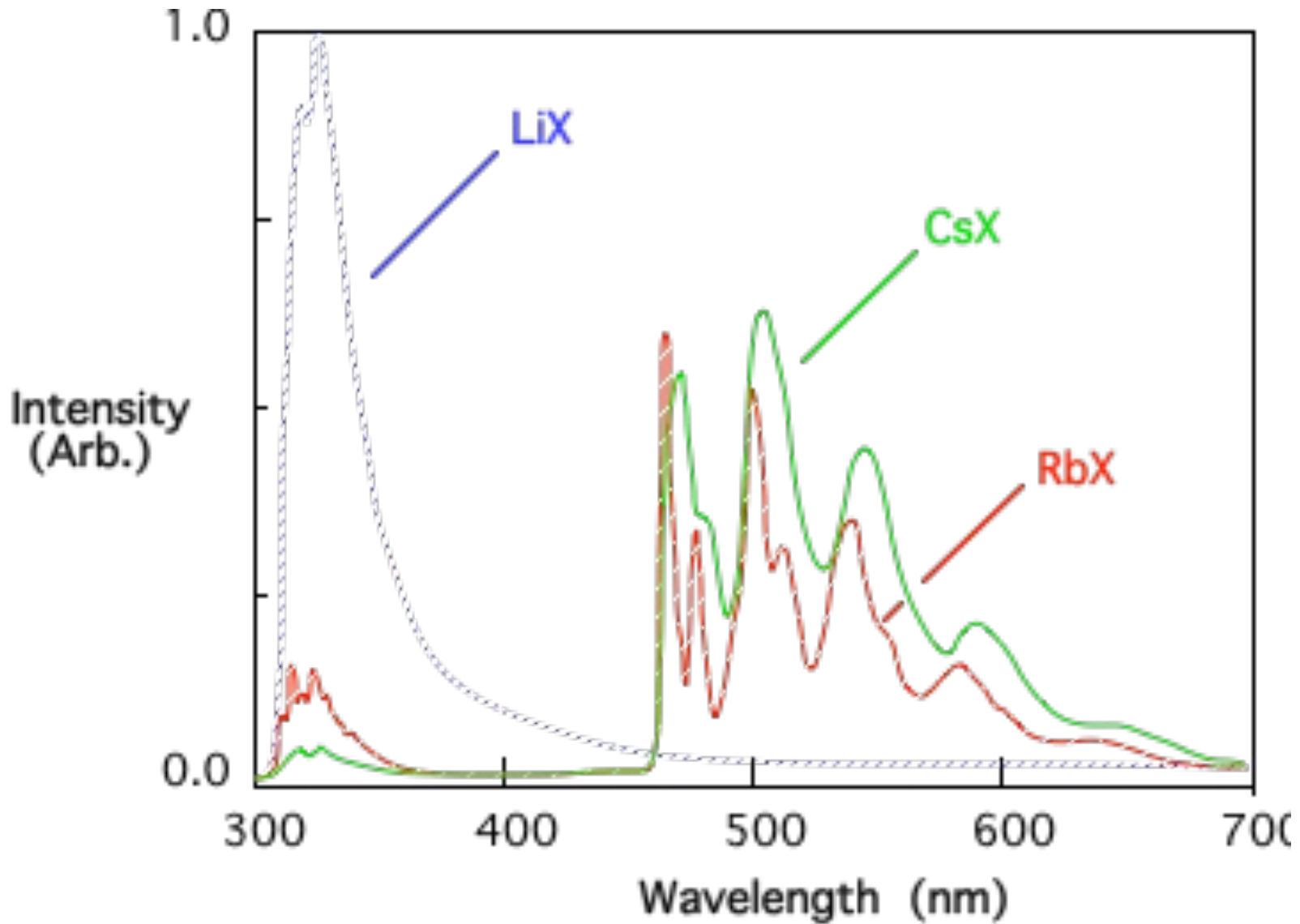
Heavy atom produces more triplets and the triplets produced phosphoresce at a faster rate

Cation Effect

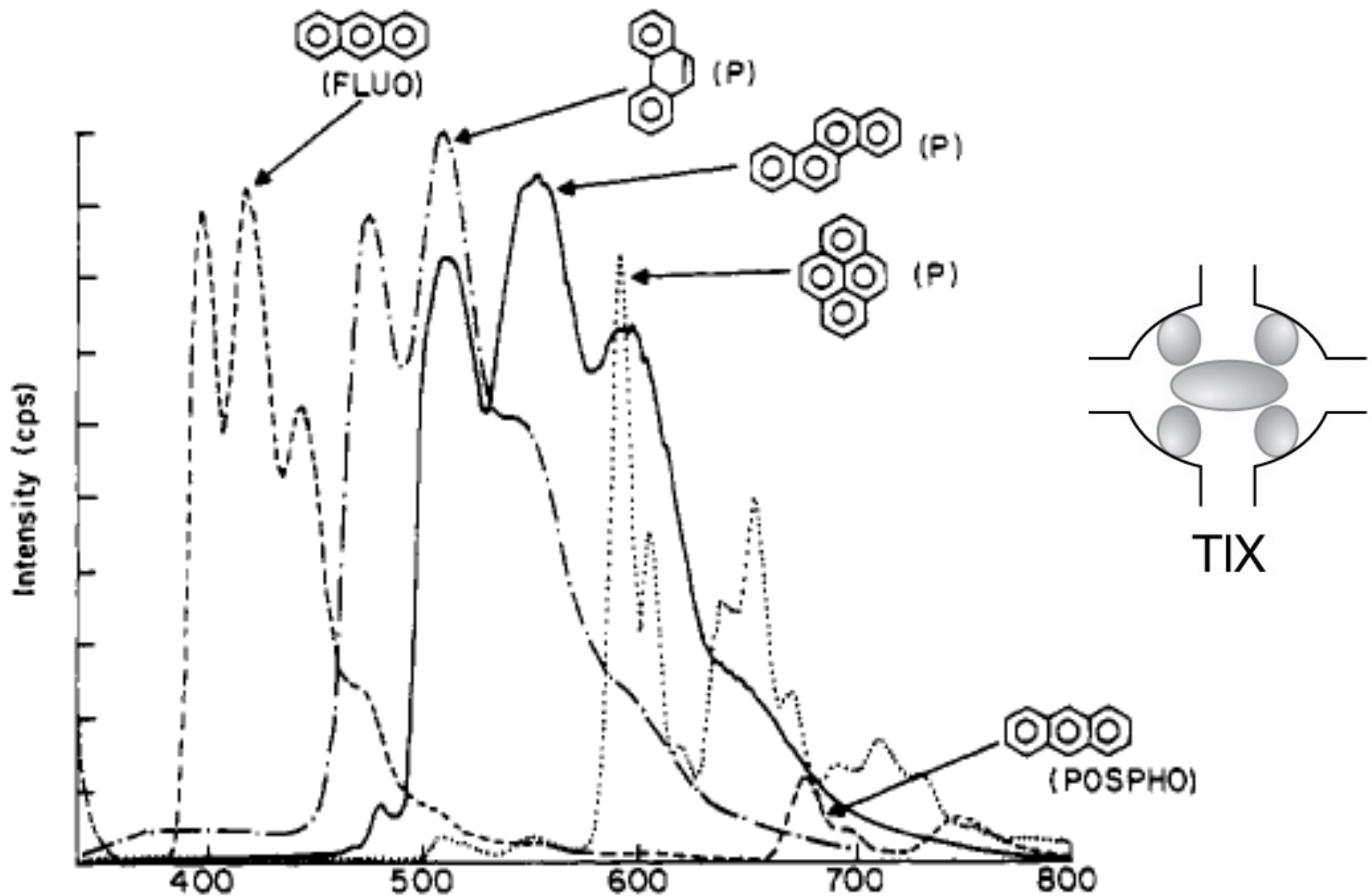
Heavy Cations Enhance the S_1 to T_1 Crossing



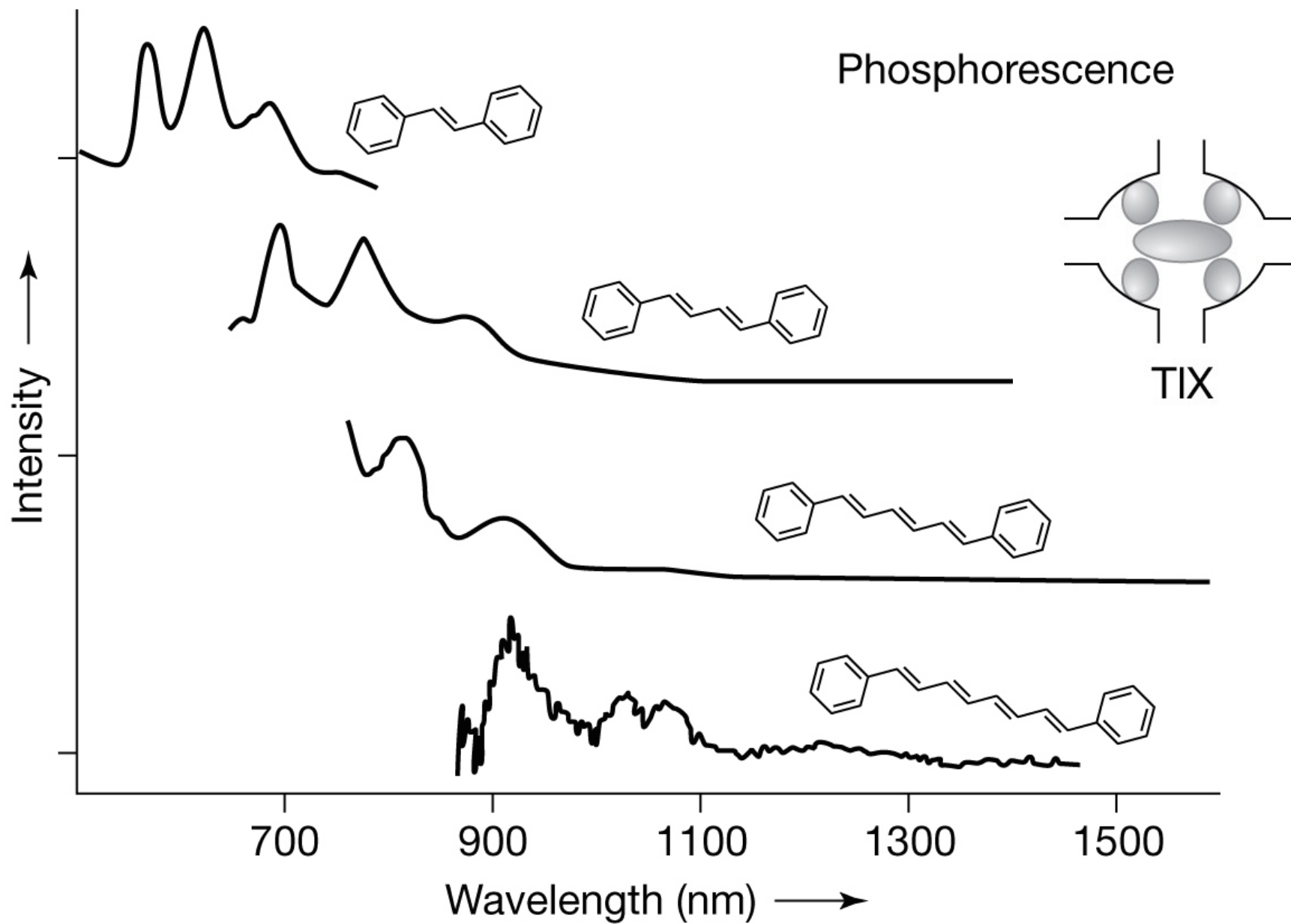
Emission Spectra of Naphthalene Included in MY Zeolites



Room temperature phosphorescence



Phosphorescence from Diphenyl Polyenes



Phosphorescence from Azo Compounds in TIY at 77 K $n\pi^*$ – $n\pi^*$ crossing

